

The treatment of oil sands process-affected water by submerged ceramic
membrane microfiltration system

by

Shimiao Dong

A thesis submitted in partial fulfillment of the requirements for the degree of

Master of Science

In

Environmental Engineering

Department Civil and Environmental Engineering
University of Alberta

©Shimiao Dong, 2014

ABSTRACT

With the rapid expansion of the oil sands exploitation in Northern Alberta over the past decade, oil sands process-affected water (OSPW) management has become a significant issue. In this study, the use of a submerged microfiltration was proposed as a potential process for pretreating OSPW. Suspended solids in OSPW were removed by unmodified ceramic membrane and SiO₂ and TiO₂ modified ceramic membranes. The direct coagulation-flocculation (CF) and increasing feed water pH successfully reduced fouling of unmodified ceramic membrane. Further studies conducted on surface modified membranes demonstrated that membrane surface charge was the main factor to ceramic membrane fouling behavior. In addition, membrane surface roughness has also shown a significant impact on fouling accumulation. However, the removals of components in OSPW (with more than 93% removal of total suspended solids and less than 15% removal of organics) remained the same in all filtration runs regardless of CF, pH or membrane materials.

Preface

Some of the research conducted for this thesis forms part of research collaboration, led by Dr. Eun-Sik Kim, who was a postdoctoral fellow at the University of Alberta. The reverse osmosis membrane filtration experiments referred to in section 4.2.3 and membrane surface characterization experiments referred to in section 4.2.4 were performed by Dr. Eun-Sik Kim. The data analysis in chapter 4 and concluding analysis in chapter 5 are my original work, as well as the literature review in chapter 2.

Acknowledgement

I would like to express my sincere gratitude to my two advisors: Dr. Mohamed Gamal El-Din and Dr. Yang Liu for their invaluable guidance and support throughout my research. Their experience and knowledge was essential to accomplish this work. I am privileged to have worked with you both.

My sincere gratitude goes to the post-doctoral fellows of Dr. Gamal El-Din research group, Dr. Eun-Sik Kim and Dr. Alla Alpatova for their support, comments, and recommendations during my research and thesis editing; I am deeply grateful of their valuable help.

I would also like to acknowledge the financial support from Meidensha Corporation. I would like to thank, in particular, to Dr. Noguchi Hiroshi, his expertise in membrane filtration was crucial to my experiment analyses.

I extend my appreciation to the technicians of Dr. Gamal El-Din research group: Maria Demeter and Nian Sun. Their patience, advice, suggestions and technical support assisted the success of my research studies.

Finally, special thanks to my good friends and family for their unwavering encouragement throughout this process.

Table of Contents

CHAPTER 1:	INTRODUCTION.....	1
1.1	Oil Sands and Oil Sands Process-affected Water	1
1.2	Objectives.....	4
CHAPTER 2:	LITERATURE REVIEW	6
2.1	Oil Sands and OSPW Challenges	6
2.2	Treatment Technologies for OSPW	7
2.2.1	Coagulation-flocculation	7
2.2.2	Membrane Filtration.....	11
2.2.3	Adsorption	21
2.2.4	Advanced Oxidation.....	24
2.2.5	Biological Treatment	25
2.2.6	Integrated Treatment Process	27
2.3	Research Request for OSPW Remediation.....	28
CHAPTER 3:	EXPIRIMENTAL PROCEDURE AND METHODS .	30
3.1	Experimental Materials and Apparatus	30
3.1.1	OSPW and Chemicals	30
3.1.2	Microfiltration and Reverse Osmosis Membranes	32
3.1.3	Microfiltration and Reverse Osmosis Membrane Treatment System....	33
3.2	Experimental Procedure.....	37
3.2.1	Coagulation-Flocculation Experiment.....	37
3.2.2	Microfiltration Experiment	38
3.3	Sample Analysis Techniques	42
3.3.1	pH.....	42
3.3.2	Conductivity.....	42
3.3.3	Turbidity	43
3.3.4	Total Organic Carbon.....	43
3.3.5	Chemical Oxygen Demand.....	43
3.3.6	Total Suspended Solids	44
3.3.7	Total Dissolved Solids.....	44
3.3.8	Ion Chromatography.....	45
3.3.9	Inductively Coupled Plasma-Mass Spectrometry	45

3.3.10	Naphthenic Acids	45
3.3.11	Acid Extractable Fraction	46
3.3.12	Silt Density Index	46
3.3.13	Scanning Electron Microscopy and Energy-dispersive X-ray Spectroscopy	47
3.3.14	Atomic Force Microscopy	47
CHAPTER 4:	RESULTS AND DISSCUSSION	48
4.1	Optimization of alum and PAC Dose for MF Process	48
4.1.1	CF Test for Selecting Optimal Doses Of alum and PAC	48
4.1.2	CFS Test for Selecting Optimal Doses of alum and PAC	51
4.2	Unmodified Ceramic Membrane Filtration Performance	53
4.2.1	Unmodified Membrane Filtration Performance	53
4.2.2	Permeate Quality after Unmodified ceramic MF Treatment	62
4.2.3	Permeate Quality Analysis after RO Treatment	66
4.2.4	Unmodified Ceramic Membrane Surface Characterization	68
4.3	Surface Modified Ceramic Membrane Filtration Performance	72
4.3.1	Modified Membrane Filtration Performance	72
4.3.2	Surface Roughness of Unmodified and Modified Membranes	77
4.3.3	Permeate Quality after Modified Membrane Filtration	80
4.3.4	Modified Membrane Surface Characterizations	82
CHAPTER 5:	CONCLUSIONS AND RECOMMENDATIONS.....	86
REFERENCES	89	
APPENDIX A	104	
APPENDIX B	113	

List of Tables

Table 1-1 Operational conditions of submerged MF ceramic membrane system. .	5
Table 2-1 Advantages and disadvantages of inorganic coagulants	9
Table 2-2 Degradation of NAs using AOPs	25
Table 3-1 Characterization of the Suncor Energy Inc. Pond 7’s OSPW.	31
Table 3-2 Physico-chemical properties of membranes.	33
Table 3-3 Detailed descriptions of OSPW filtration runs.	40
Table 4-1 MF permeate quality and removal of selected components after first stage of 6 runs (all water quality parameters tested for raw OSPW, permeate after first, second and during second stage in 6 membrane filtration runs are shown in Appendix B).	64
Table 4-2 MF permeate quality and removal of selected components after second stage of 6 runs (all water quality parameters tested for raw OSPW, permeate after first, second and during second stage in 6 membrane filtration runs are shown in Appendix B).	65
Table 4-3 The removal of organic and inorganic compounds after RO treatment.	67
Table 4-4 Roughness of unmodified and modified ceramic membranes.....	80
Table 4-5 MF permeate quality and removal of selected components after first stage of filtrations through two modified membranes (all water quality parameters tested for raw OSPW, permeate after first, second and during second stage in all membrane filtration runs are shown in Appendix B). ...	81
Table 4-6 MF permeate quality and removal of selected components after second stage of filtrations through two modified membranes (all water quality parameters tested for raw OSPW, permeate after first, second and during second stage in all membrane filtration runs are shown in Appendix B). ...	81
Table B 1 Physico-chemical properties of OSPW in Run 1.....	114
Table B 2 Physico-chemical properties of OSPW in Run 2.....	115

Table B 3 Physico-chemical properties of OSPW in Run 3.....	116
Table B 4 Physico-chemical properties of OSPW in Run 4.....	117
Table B 5 Physico-chemical properties of OSPW in Run 5.....	118
Table B 6 Physico-chemical properties of OSPW in Run 6.....	119
Table B 7 Physico-chemical properties of OSPW in Run 7.....	120
Table B 8 Physico-chemical properties of OSPW in Run 8.....	121

List of Figures

Figure 2-1 Properties of pressure driven membrane processes.....	13
Figure 2-2 Membrane module configurations (a) Dead-end configuration; (b) cross flow configuration; (c) submerged configuration.....	15
Figure 2-3 pH changes in zeta potential of Al ₂ O ₃ and Al ₂ O ₃ – TiO ₂ membranes	17
Figure 2-4 Normalized environmental impacts of MF, DAF-ABS and HYDRO-ABS technologies	21
Figure 2-5 NAs concentration at different petroleum coke doses.....	23
Figure 3-1 Cross-section of ceramic membrane.....	32
Figure 3-2 (a) Images of MF ceramic membrane treatment system (1) transportable membrane test unit panel, water pumps, air pumps and flow meters; (2) feed tank and a mechanical stirrer; (3) membrane and permeate tanks; (4) data recorder; (5) membrane test unit and feed tank. (b) Schematic diagram of MF filtration process.....	35
Figure 3-3 (a) Images of RO polymeric membrane treatment system: (1) RO filtration system; (2) RO membrane module and mechanical pump; (3) feed tank, overhead stirrer and electrical scale; and (4) RO membrane and membrane module. (b) Schematic of RO filtration system.	36
Figure 3-4 Jar test unit with coagulated OSPW.	38
Figure 3-5 Membrane filtration processes.	39
Figure 4-1 (a) Average particle size and (b) zeta potential after coagulation with different doses of PAC and alum at neutral pH.	49
Figure 4-2 Zeta potential of unmodified ceramic membrane at different pHs.....	51
Figure 4-3 (a) Turbidity versus PAC concentrations after CF and CFS pretreatments; and (b) turbidity versus alum concentrations after CF and CFS pretreatments.	52
Figure 4-4 Simplified TMP data at (a) first stage and (b) second stage of Run 1. The original TMP data are shown in Figure A1 in Appendix A.....	54
Figure 4-5 Simplified TMP data at (a) first stage and (b) second stage of Run 2. The original TMP data are shown in Figure A2 in Appendix A.....	55

Figure 4-6 Simplified TMP data at (a) first stage and (b) second stage of Run 3. The original TMP data are shown in Figure A3 in Appendix A.....	57
Figure 4-7 Simplified TMP data at (a) first stage and (b) second stage of Run 4. The original TMP data are shown in Figure A4 in Appendix A.....	58
Figure 4-8 Effect of pH on (a) the zeta potential of alum-coagulated OSPW; (b) the average particle size of alum-coagulated OSPW; (c) zeta potential of PAC-coagulated OSPW; (d) average particle size of PAC-coagulated OSPW.....	60
Figure 4-9 Simplified TMP data (a) first stage and (b) second stage of Run 5. The original TMP data are shown in Figure A5 in Appendix A.....	61
Figure 4-10 Simplified TMP data (a) first stage and (b) second stage of Run 6. The original TMP data are shown in Figure A6 in Appendix A.....	62
Figure 4-11 SEM images of (a) bare membrane; (b) membrane treated with 10 mg/L alum-coagulated OSPW; TMP at end of filtration was -12 kPa (Run 3); (c) membrane treated with 30 mg/L alum-coagulated OSPW; TMP at end of filtration was -12 kPa (Run 4); and (d) membrane treated with 10 mg/L alum-coagulated OSPW at pH 10; TMP at end of filtration was -16 kPa (Run 6).....	69
Figure 4-12 EDX spectrums of (a) bare membrane; (b) membrane treated with 10 mg/L alum-coagulated OSPW; TMP at end of filtration was -12 kPa (Run 3); (c) membrane treated with 30 mg/L alum-coagulated OSPW; TMP at end of filtration was -12 kPa (Run 4); and (d) membrane treated with 10 mg/L alum-coagulated OSPW at pH 10; TMP at end of filtration was -16 kPa (Run 6).....	72
Figure 4-13 Membrane zeta potential as a function of solution pH for tested ceramic membranes.....	74
Figure 4-14 Simplified TMP data at (a) first stage and (b) second stage of Run 7 (SiO ₂ -modified ceramic membrane). The original TMP data are shown in Figure A7 in Appendix A.....	75

Figure 4-15 Simplified TMP data at (a) first and (b) second stage of Run 8 (TiO ₂ -modified ceramic membrane). The original TMP data are shown in Figure A8 in Appendix A.	77
Figure 4-16 AFM images of (a) unmodified ceramic membrane; (b) SiO ₂ -modified ceramic membrane; (c) TiO ₂ -modified ceramic membrane.....	79
Figure 4-17 SEM images of (a) bare unmodified membrane; (b) fouled unmodified membrane, TMP at the end of filtration was -12 kPa; (c) bare SiO ₂ -modified membrane; (d) fouled SiO ₂ -modified membrane, TMP at the end of filtration was -16 kPa; (e) bare TiO ₂ -modified membrane; (f) fouled TiO ₂ -modified membrane, TMP at the end of filtration was -11kPa; All three membranes were treated with 10 mg/L alum-coagulated OSPW.....	84
Figure 4-18 EDX spectrums of (a) fouled unmodified membrane; TMP at end of filtration was -12 kPa; (b) fouled SiO ₂ -modified membrane; TMP at the end of filtration was -16 kPa; (c) fouled TiO ₂ -modified membrane; TMP at the end of filtration was -23kPa. All three membranes were treated with 10 mg/L alum-coagulated OSPW.	85
Figure A 1 TMP data of Run 1	105
Figure A 2 TMP data of Run 2	106
Figure A 3 TMP data of Run 3	107
Figure A 4 TMP data of Run 4.....	108
Figure A 5 TMP data of Run 5.....	109
Figure A 6 TMP data of Run 6.....	110
Figure A 7 TMP data of Run 7.....	111
Figure A 8 TMP data of Run 8.....	112

LIST OF SYMBOLS, NOMENCLATURE, ABBREVIATIONS

ABS	Absorbents
AEF	Acid extractable fraction
AFM	Atomic Force Microscopy
Al(OH) ₃	Aluminum Hydroxide
Alum	Aluminum Sulfate Octadecahydrate
AOP	Advanced Oxidation Process
Au	Gold
CF	Coagulation Flocculation
CFS	Coagulation Flocculation and Sedimentation
COD	Chemical Oxygen Demand
CPC	Cetylpyridinium Chloride
DAF	Dissolved Air flotation
DOC	Dissolved Organic Carbon
EDX	Energy-dispersive X-ray Spectroscopy
H ₂ O ₂	Hydrogen peroxide
HYDRO	Hydro-cyclone
IEP	Isoelectric Point
MEUF	Micellar Enhanced Ultrafiltration
MF	Microfiltration
MWCO	Molecular Weight Cut Off
NaOH	Sodium Hydroxide
NAs	Naphthenic Acids
NF	Nanofiltration
OSPW	Oil Sands Process-affected Water
PAC	Polyaluminum Chloride
R _a	Roughness Average Deviation
RMS	Root Mean Square
RO	Reverse Osmosis
SDI ₅	Silt Density Index

SEM	Scanning Electron Microscopy
SiO ₂	Silicon Oxide
TDS	Total Dissolved Solid
TiO ₂	Titanium Oxide
TMP	Transmembrane Pressure
TOC	Total Organic Carbon
TSS	Total Suspended Solid
UF	Ultrafiltration

CHAPTER 1: INTRODUCTION

1.1 Oil Sands and Oil Sands Process-affected Water

The oil sands in Northern Alberta, Canada, are the third-largest oil reserve sources in the world (Alberta Department of Energy, 2010). The Athabasca oil sands deposit is the largest deposit in Northern Alberta and is the closest to the ground's surface to cover an area of more than 100,000 square kilometers. Up to 19% of the bitumen contents is accessed by the surface mining processes (Alberta Department of Energy, 2010). Bitumen recovery through surface mining is achieved by the Clarke hot water extraction process, which mixes hot fresh water with dry oil sands after its removal from the grounds by truck and shovel (Sanders et al., 2000). This operation processes consumes a large volume of water that eventually results in a considerable amount of oil sands process-affected water (OSPW) (Tingley, 1992). OSPW is a complex mixture of suspended and dissolved solid, salts, and harmful organic compounds that are extremely toxic to the aquatic ecosystem if directly discharged into the environment (Allen, 2008a). Therefore, without treatments, OSPW needs to be stored at the mine sites in tailings ponds (Allen, 2008a). Currently, marketable oil production from Canadian oil sands is 1,617,600 barrels per day in 2011, representing 73% of the total crude bitumen production (Alberta Government, 2012). This number is projected to rise to 3.5 million barrels per day by 2020, correspondingly an increase in the need of water (Alberta Energy, 2012). Given the increasing trend of the fresh water consumption during extraction process and cumulative OSPW deposition at site, oil sands producers currently recycle OSPW within the bitumen operation processes (Allen, 2008a). However, OSPW without any treatments causes low bitumen recovery, fouling, corrosion and scaling problems at the extraction facilities (Allen, 2008a). As a result, a series of OSPW treatments are necessary before recycling or environmental release of this water.

Because of the complexity of OSPW's composition, OSPW remediation usually consists of several steps including physical, chemical and biological treatments (Gamal El-Din, 2012). The hypothetical OSPW treatment train generally starts with a physical-chemical treatment focusing on suspended solids and oil removal, followed by dissolved solids/organic removal including chemical oxidation and ultrafiltration (UF) (Oluwaseun et al., 2008). The residual organics/solids and salts are eventually dealt with in the final treatment using biological treatment and nanofiltration (NF)/reverse osmosis (RO) (Oluwaseun et al., 2008). Suspended solids are removed first, because they can cause severe membrane fouling in desalination process or can disturb the advanced oxidation treatment by scattering UV light (Pourrezaei et al., 2011; Zaidi et al., 1992; Legrini et al., 1993). Physical and physicochemical treatments of the suspended solids include gravity separation, centrifugal settling, granular media filtration, membrane filtration and coagulation-flocculation-sedimentation (CFS) (Zaidi et al., 1992). Among these treatments, low pressure membrane filtration, such as microfiltration (MF), is advantageous because of its relatively low cost and energy consumption in comparison with ultrafiltration, and its generation of high quality effluent (Singh et al., 2011). Although studies have demonstrated the effectiveness of MF for removing suspended solids in the oil field-produced water (Allen, 2008b; Ebrahimi et al., 2010), MF pretreatment has not been examined for OSPW treatment.

Traditionally, microfiltration and ultrafiltration for oil field produced water have been accomplished using polymeric materials. However, polymeric membrane can be broke down by harsh organic species in the water and membrane fouling is less effectively recovered after chemical cleaning (Benko, 2009). Ceramic membranes have high resistance to mechanical, chemical and thermal stresses and cleaning agents (Meiser, 2001; Zaidi et al., 1992). They can also operate under high pressure differentials (Zaidi et al., 1992). These advantages enable a sustainable ceramic membrane filtration under unfavorable environment and operational condition, and thereby extend the ceramic membranes' life span (Benko, 2009). But due to the limited pores size availability;

the ceramic material is most often manufactured as MF and UF membranes. In addition, ceramic membranes have a higher capital cost and lower life cycle cost compared to polymeric membranes (Benko, 2009).

Ceramic membrane sealing is a very important membrane technology for those applications of ceramic membranes constantly operating under high temperature (>900) (Basile and Nunes; 2011). For these applications, sealing process must yield a gas-tight membrane structure without significantly influencing the membranes' mechanical and chemical properties (Basile and Nunes; 2011). Inappropriate sealing may risk the fabrication of a ceramic membrane. For example, excessive radial pressure with compressive seals will cause the damage of a ceramic tube; high temperature seals may lead to a low thermal cycling capacity. These issues associated with membrane sealing point out the fact that decreasing the sealing area to membrane area will reduce the possibility of failure of membrane/seal interface (Basile and Nunes; 2011).

The fundamental limitation of MF in the oilfield-produced water treatment application is the phenomenon of flux degradation, resulting from the adsorption or accumulation of oil and suspended solids on the surface or inside the membranes' pores (Zaidi et al., 1992). OSPW contains high concentration of suspended solids that can deposit on membrane surface, increasing hydraulic resistance and thus trans-membrane pressure (TMP), but relatively low concentration of oil. As a result, operational expenses, chemical cleaning costs and maintenance costs are increased and membrane lifetime is ultimately shortened (Kim et al., 2011). Feed water chemistry modification by coagulation-flocculation (CF) process can advance the efficiency of membrane filtration through decreasing membrane fouling, as it does not only enlarge solids' sizes, but also decreases the attraction between the particles and the membrane surfaces (Mueller et al., 1997; Zhong et al., 2003). CF treatment before membrane filtration has been reported to decrease membrane fouling rate of a UF and elevate the flux rate of the crude oil wastewater (Tansel et al., 1995). It was found that colloidal particles after pre-coagulation tended to form a layer of reversible

fouling on the membrane surface rather than spreading out into membrane pores causing severe irreversible fouling (Tansel et al., 1995). The low costs and high effectiveness of aluminum sulfate octadecahydrate (alum; $\text{Al}_2(\text{SO}_4)_3 \cdot 18\text{H}_2\text{O}$) makes it the most widely used coagulant in water and wastewater treatment processes (Alfredo, 2012). In a previous OSPW treatment study, alum coagulation was applied before the high-pressure membrane filtration, and it significantly increased membrane permeability and desalination efficiencies in nanofiltration (NF) and reverse osmosis (RO) (Kim et al., 2011).

1.2 Objectives

In this study, we investigated the removal of suspended solids in OSPW which was treated by a submerged ceramic MF membrane and preliminarily examined the membrane fouling reduction with the direct CF before MF treatment. The CF-MF system operational parameters of interest were the TMP, the removal of solids and organic and inorganic compounds, as well as the membrane surface fouling characterizations. Eight membrane filtration runs were operated in this study. Different conditions of CF process and three types of ceramic membranes were investigated to optimize the membrane system and to minimize the membrane fouling. The types of membrane used were unmodified ceramic membrane and silicon oxide (SiO_2) and titanium oxide (TiO_2) modified ceramic membranes. RO treatment was performed once using MF permeate to demonstrate the applicability of the MF-RO process for the treatment OSPW. The conditions of ceramic membrane system operation are listed in Table 1-1.

Table 1-1 Operational conditions of submerged MF ceramic membrane system.

	OSPW		Pre-treatment	OSPW pH adjustment	MF treatment	Post-treatment
Run 1	Suncor Energy Pond 7	Inc.	n/a	n/a	Submerged system + unmodified ceramic membrane	n/a
Run 2	Suncor Energy Pond 7	Inc.	CF with PAC 20 mg/L	n/a	Submerged system + unmodified ceramic membrane	n/a
Run 3	Suncor Energy Pond 7	Inc.	CF with alum 10 mg/L	n/a	Submerged system + unmodified ceramic membrane	n/a
Run 4	Suncor Energy Pond 7	Inc.	CF with alum 30 mg/L	n/a	Submerged system + unmodified ceramic membrane	n/a
Run 5	Suncor Energy Pond 7	Inc.	CF with alum 10 mg/L	pH at 10	Submerged system + unmodified ceramic membrane	n/a
Run 6	Suncor Energy Pond 7	Inc.	CF with alum 10 mg/L	pH at 10	Submerged system + unmodified ceramic membrane	RO
Run 7	Suncor Energy Pond 7	Inc.	CF with alum 10 mg/L	n/a	Submerged system + SiO ₂ -modified ceramic membrane	n/a
Run 8	Suncor Energy Pond 7	Inc.	CF with alum 10 mg/L	n/a	Submerged system + TiO ₂ -modified ceramic membrane	n/a

n/a: not available

After comparing Runs 1 – 5 using unmodified ceramic membrane, the optimal condition was selected for the combination with RO to estimate the feasibility of a MF-RO combined treatment (Run 6). Permeate water quality was explored by testing the following: pH, electrical conductivity, turbidity, total suspended solids (TSS), total dissolved solids (TDS), silt density index (SDI₅), total organic carbon (TOC), chemical oxygen demand (COD), a range of anions and cations, the acid extractable fraction (AEF) and naphthenic acids (NAs). The fouling layers on the ceramic membrane surfaces were observed by the scanning electron microscopy (SEM) and energy-dispersive X-ray spectroscopy (EDX) analysis and atomic force microscopy (AFM).

CHAPTER 2: LITERATURE REVIEW

2.1 Oil Sands and OSPW Challenges

Oil sands are a thick, molasses-like, viscous mixture of sand, clay, water and bitumen (Jordaan, 2012). Two technologies are currently available for bitumen extraction from the oil sands: surface mining and *in situ* techniques (Jordaan, 2012). For the deeper depth oil sands deposits, bitumen is extracted through the *in situ* process in which steam is injected to heat and melt bitumen so that it can flow into the lower well and subsequently be pumped to the surface. The shallow oil sand deposits are assessable via the surface mining in which oil sands are removed by the shovel-and-truck operations. Bitumen is separated from the sand and clay by Clarke hot water extraction process that involves oil sands with water, heat and surfactants (Kasperski, 2003). The water after the bitumen extraction and upgrading contains a variety of toxic chemicals, including heavy metal and NAs, which are fatal to aquatic animals, birds and wildlife (Royal Society of Canada, 2010). Therefore, the concern over the environmental impacts associated with OSPW storage is of great importance. In addition, OSPW recycling has become increasingly significant due to a large quantity of water required for the bitumen extraction. Already, about 80% - 85% of the water usage in extraction process relies on recycled OSPW from the tailing ponds (Allen, 2008a).

However, OSPW recycled without any treatments would result in a build-up of dissolved ions and suspended solids that cause a series of operational problems such as low bitumen recovery, scaling and fouling at extraction facilities and boiler (Beier et al., 2009). Studies have shown that divalent cations can cause an increase in the adherence of bitumen to clay and sands, a decline in the adherence of bitumen to air bubbles, surfactants neutralization and clays coagulation by which bitumen recovery is reduced (Kasperski, 2003). Besides, the bitumen recovery can also be interfered by the high concentration of hardness-causing ions and sodium chloride (Allen, 2008a). Extraction infrastructure scaling is usually caused by carbonate, sulphate, and phosphate ions and iron oxides in the water,

while the suspended solids, hardness and high alkalinity are the common components that lead to the facility fouling (Allen, 2008a).

The oil sands companies' goals are to reduce the amount of fresh water withdrawal and to increase the usage of tailings water to the greatest extent (Wang, 2011a). With the OSPW remediation being the first priority, novel technologies associated with the OSPW treatment are being developed.

2.2 Treatment Technologies for OSPW

Currently, the available technologies for the treatment of OSPW include physico-chemical treatment, such as CFS, membrane filtration (MF, UF, NF and RO), adsorption, advanced oxidation, biological treatment, bioremediation and natural wetlands (Gamal El-Din, 2011; Allen, 2008b). The emerging treatment technologies tend to be hybrid treatment systems that are either integrate physical and biological treatments or chemical and biological treatments (Gamal El-Din, 2011). The selection of the treatment techniques is largely dependent on the target components in OSPW, cost, the demands of the oil sands operators for the water and the relevant regulations associated with the OSPW management. As a result, a combination of traditional or/and advanced technologies is more likely to achieve all the challenging goals. Several possible water treatment technologies for OSPW remediation are described in the Sections 2.2.1 to 2.2.6.

2.2.1 Coagulation-flocculation

CF is a low cost and widely used treatment to remove suspended solids and colloidal particulates that are too small to settle out by the gravity within a reasonable time (Santo et al., 2012). It can also reduce the concentration of the high molecular weight organic species in the wastewater. Due to the adverse impacts of the suspended solids and some insoluble hydrocarbons on the treatment processes, such as UV-based advanced oxidation, membrane and

biological treatments, the removal of these pollutants is expected to be dealt firstly in a series of pretreatments (Santo et al., 2012). Fine particles in water can be very stable and are not easily sedimented due to the formation of electrical double layer (EDL) around particles (Crittenden, 2005). Naturally, the positive counter-ions are accumulated and tightly bound to the surface of the negatively charged particles by electrostatic and adsorption forces. The layer of adsorbed cations is known as the fixed charged layer (Crittenden, 2005). To maintain the electric equilibrium with the solution, an excess of cations and anions move around the fixed charged layer, diffusing into the bulk solution. This layer of ions that surrounded fixed charge layer is called diffuse layer. Added together these two layers are the electrical double layer (EDL). The result of the presence of EDL is that particulates in water are unlikely to aggregate or settle down. With the addition of coagulant, the stability among particles in the water is broken and particles become destabilized and easy to gather (Crittenden, 2005). When a charged particle migrate towards the an electrode in the electric field, it will trigger some fraction of water close to the particle's surface to move with it, which forms the shear plane, lying in the diffuse layer. The electrical potential between the shear plane and bulk solution is called zeta potential (Crittenden, 2005).

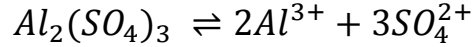
Coagulant can destabilize particles and allow them to aggregate, this involves two mechanisms: charge neutralization and sweep floc (Kim et al., 2007). Charge neutralization mechanism consists of the destabilization of the charged particles and the aggregation of dispersive particles into large particles (flocs) which can be easily removed by the gravity settling. A particular chemical reaction may occur between the negatively charged particles and positively charged coagulants, which disturbs the electric balance among the particles facilitating the agglomeration. In contrast, the sweep floc mechanism requires a formation of precipitates through which particles in water are collided and eventually dragged down. This mechanism postulates that after being dissolved in water, coagulants will rapidly form an amorphous solid-phase (e.g. $\text{Al}(\text{OH})_3$), where the adsorption of solids and some organic matter occurs (Crittenden, 2005).

Inorganic coagulants are the most commonly used coagulants. Typical examples include aluminum sulfate, polyaluminum chloride and ferric chloride, etc. When alum and iron salts are added to water, they dissociated to yield trivalent ions (Al^{3+} or Fe^{3+}), which can be 1000 times more effective in destabilizing particles than monovalent ions (U.S. Army Corps of Engineers, 2001). Table 2-1 shows the advantages and disadvantages of several widely used inorganic coagulants.

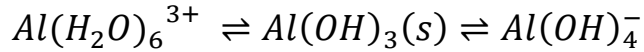
Table 2-1 Advantages and disadvantages of inorganic coagulants (Adapted from U.S. Army Corps of Engineers, 2001).

Coagulants	Advantages	Disadvantages
Alum $\text{Al}_2(\text{SO}_4)_3 \cdot 18\text{H}_2\text{O}$	<ul style="list-style-type: none"> • Most commonly used • Produces less sludge • Most effective between pH 5.8 to 7.7 (Metcalf and Eddy 2003) 	<ul style="list-style-type: none"> • Adds dissolved solids (salts) in water • Effective over a limited pH range
Polyaluminum Chloride (PAC) $\text{Al}_{13}(\text{OH})_{20}(\text{SO}_4)_2\text{Cl}_{15}$	<ul style="list-style-type: none"> • In some applications, floc formed are denser and faster settling than those formed with alum 	<ul style="list-style-type: none"> • Not commonly used • Little full scale data compared to other aluminum derivatives
Ferric Sulfate $\text{Fe}_2(\text{SO}_4)_3$	<ul style="list-style-type: none"> • Effective between pH 5.2 and 8.8 (Metcalf and Eddy 2003) 	<ul style="list-style-type: none"> • Adds dissolve solids (salts) to water • Usually there is a need to increase alkalinity
Ferric Chloride $\text{FeCl}_3 \cdot 6\text{H}_2\text{O}$	<ul style="list-style-type: none"> • Effective between pH 4 and 11 	<ul style="list-style-type: none"> • Adds dissolved solids (salts) to water • Consumes twice as much as alkalinity as alum

The hydrolysis of coagulants can trigger a chain of parallel and sequential reactions and correspondingly produce a series of hydrolysis species. Inorganic metallic coagulant alum, for instance, yields trivalent aluminum ions after dissociation in water, as given below:



The trivalent Al^{3+} then hydrates to form an aquo-metal complex $Al(H_2O)_6^{3+}$. This aquo-metal complex will go through a number of hydrolytic reactions and eventually form hydroxide precipitate as shown below (Metcalf and Eddy, 2003; Crittenden, 2005):



For alum coagulation, the collision of destabilized particles occur first, leading to the formation of small aggregates. This is followed by the collisions of particles to aggregates and eventually aggregates to aggregates. But aggregates are hardly formed in large sizes at lower alum concentration. When alum concentration increases, sweep coagulation is becoming the dominant mechanism and aggregates quickly grow and form hexameric ring structures (Wang et al., 2008; Wu et al., 2009).

Prehydrolyzed metal salts, such as PAC, usually comprise of polynuclear aluminum hydrolysis species (Wu, et al., 2009). The predominant polymeric product is tridecameric polymer with the formula $Al_{13}O_4(OH)_{24}(H_2O)_{12}^{7+}$, often referred as Al_{13} . Al_{13} in PAC improves particles collision and formation of larger aggregates at lower coagulant concentration. When the coagulant concentration increased, the primary aggregates formed by the charge neutralization or adsorption continue to bind with each other to form micro sized flocs. Polycation-patch coagulation and polymer bridging are mainly responsible for the flocs formation at higher doses. PAC coagulated flocs are generally comprised of a Keggin structure, which is a structure that is much more compact and denser than a hexameric ring structure formed by alum (Crittenden, 2005; Wu et al., 2009).

CF is a very effective treatment for petroleum refining produced water on a large-scale application (Santo et al., 2012). The major constituents of the petroleum produced water consist of insoluble hydrocarbons, dissolved and

suspended organic and inorganic matter (Santo et al., 2012). Santo et al. (2012) have studied the CF treatment of petroleum wastewater using PAC, alum and ferric sulfate. The results showed that more than 73% reduction in turbidity was obtained with the addition of coagulants. TOC and COD were decreased by more than 80% for all three coagulants. The highest COD removal was obtained by using a relatively low concentration of PAC (27.2 mg/L), while alum and ferric sulfate achieved a very close COD reduction with the concentrations of 40 and 56 mg/L, respectively.

CF has also been studied for the removal of suspended solids and dissolved organics from OSPW. Wang et al. (2011a) investigated the efficiency of two coagulants, alum and ferric sulphate. The authors reported that 100 mg/L of alum with 10 mg/L cationic polymer CTI TL was the optimal coagulant and flocculent doses, respectively, to achieve 13% TOC and 98% of turbidity removal from OSPW. Ferric sulphate showed a high decrease in the suspended solids; however the residual ferric sulphate caused OSPW discoloration.

Pourrezeai et al. (2011) reported the application of alum and cationic polymer poly DADMAC in CF for the treatment of OSPW. The results revealed that particles destabilization was achieved through the charge neutralization that caused by the adsorption of hydroxide precipitates. CF process substantially removed vanadium and barium by 67-78% and 42-63%, respectively. Moreover, NAs and oxidized NAs concentrations were decreased by 37% and 86%, respectively.

2.2.2 *Membrane Filtration*

Membrane filtration is a physical separation process which relies on the differences in the permeability of water components (Crittenden, 2005). During filtration process, membrane which acts as a selective barrier between the feed stream and permeate stream remains impenetrable to certain species. Some constituents pass through into permeate stream, while others are retained by the

membrane and accumulated on the feed side. Based on the driving force of operation, membrane treatments can be classified into four categories: electrically, thermally, concentration and pressure driven operations (Zeman and Zydney, 1996; Cheryan, 1998). Electrodialysis is an electrically driven process, which utilizes cation and anion exchange membranes under the voltage to remove ionic material from the aqueous solution (Rautenbach and Albrecht, 1989). The main application of electrodialysis is to convert ocean or brackish waters to potable water (Rautenbach and Albrecht, 1989). Membrane processes with thermal driving force are pervaporation and membrane distillation. The typical concentration driven process is dialysis. It has been widely used in the medical field and alcohol-reduced beer production (Rautenbach and Albrecht, 1989). Dialysis is a process that allows small molecules to pass through the membrane and large solute molecules to remain on the retentate side as a response to a difference in trans-membrane concentration of solute (Rautenbach and Albrecht, 1989).

Pressure driven membrane processes can be further divided into two distinguished physicochemical processes: low pressure driven processes and high pressure driven processes (Crittenden, 2005). Low pressure driven process includes MF and UF. These membranes are designed to block solids in the “micro” range and require a relative low pressure during filtration (Cheryan, 1998). The primary removal mechanism of low pressure driven processes is size exclusion (Crittenden, 2005). Therefore MF is widely used as a clarification process, separating suspended particulates from a liquid phase, while UF is used for the purification of macromolecules, as a concentrating and fractionating process in food process and pharmaceutical industries (Cheryan, 1998). NF and RO, on the other hand, are the high pressure driven processes, in which high pressure drives water through a semi-permeable membrane which pore sizes are too small to transfer salts. Diffusive mechanism is usually involved in this process and its separation efficiency depends on the influent concentration and applied pressure (Crittenden, 2005). RO is commonly used for the desalination of seawater or brackish water and removal of low molecular weight dissolved contaminants,

whereas NF is aimed to remove natural organic matter and to decrease the water hardness (Cheryan, 1998). Figure 2-1 shows the properties of the pressure driven membrane processes.

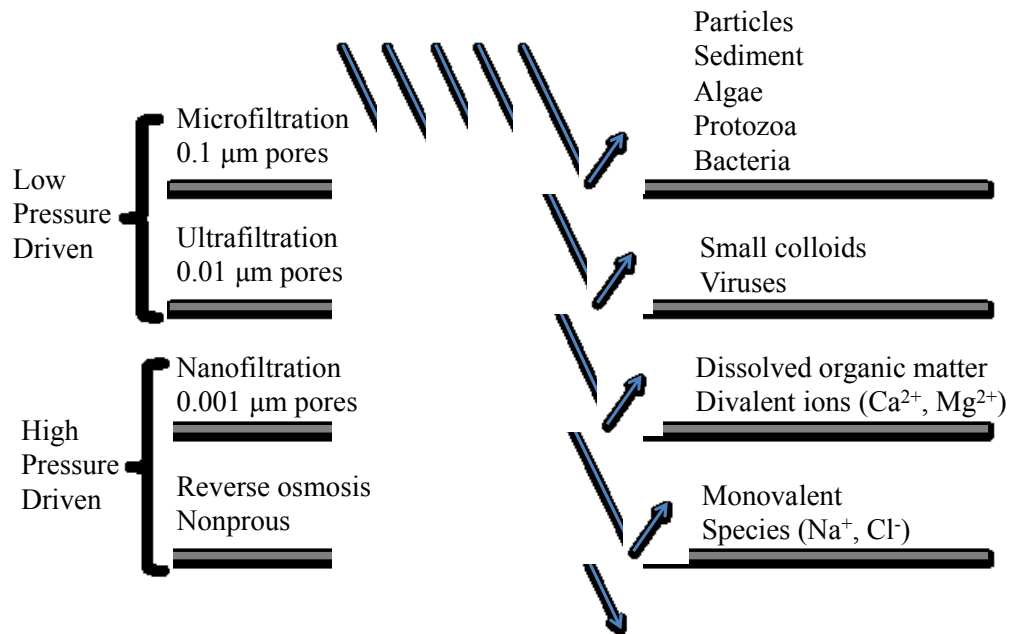


Figure 2-1 Properties of pressure driven membrane processes (adapted from Critenden, 2005).

The most common membranes' geometric forms are hollow fibers, tubular and flat sheets (Cheryan, 1998). Hollow fibers are widespread in water treatment, with an outside diameter ranging from 0.5 to 2 mm. The active layer is often coated inside the fiber (Cheryan, 1998). Tubular membrane is configured as a monolithic structure with a number of channels or tubes throughout the structure. Inorganic materials, such as mineral materials, are the common tubular membrane materials, which have a low surface area to volume ratio but can be performed at a high cross-flow velocity. Thus it is suitable for the high solute concentration wastewater treatment (Cheryan, 1998). The flat sheet membrane has a flat active layer with a high surface area to volume ratio. Spiral wound membrane is frequently stacked in a number of layers and rolled up around a central tube

through which permeate is collected after passing through the spiral flow path (Cheryan, 1998, Crittenden, 2005).

One membrane or several membranes are usually supported in a membrane module in the membrane filtration plant. The specific flow regime throughout the confined space relies on the configuration of a membrane module. Three basic membrane module configurations are currently available: dead end module configuration, cross-flow module configuration and submerged module configuration (Cardew and Le, 1998). Figure 2-2 presents three membrane module configurations. For a dead-end module, the influent perpendicularly moves through the membrane with the particles retained on the membrane surface (Figure 2-2a). In the cross-flow module, the influent flows parallel to the membrane surface and penetrate through membrane (Figure 2-2b). Particles that are separated from the influent and remained on the membrane surface in a cross-flow module can be flushed away by the tangential feed flow, thus preventing the accumulation of solids on the membrane surface. On the contrary, membrane in a dead-end module needs frequent backwashes to detach solids deposition. Typically, the feed water in both dead-end and cross-flow modules is delivered by a feed pump. However in comparison to dead-end, the cross-flow module requires a substantial recirculation flow. As a consequence, it results in a high consumption of pumping energy (Cheryan, 1998; Crittenden, 2005).

In submerged modules, membranes are generally configured in a module that composes of membranes and headers affixed to membranes. The module is immersed in a basin with the wastewater. A mechanical pump creates TMP across the membrane wall and a vacuum suction is applied on the permeate side of the membrane so that permeate can be withdrawn from the feed basin through the membrane and particles are remained on the feed side of the membrane (Crittenden, 2005). Comparing with the cross-flow module, a submerged configuration requires less energy power because the TMP to create vacuum is generally lower than the recirculation pressure (Ueda et al., 1997). However, membrane fouling is a more serious issue in the submerged membrane. Therefore,

in order to minimize membrane fouling, the submerged module is usually equipped with a backwash or aeration system. Air bubbles are usually generated by an air blower on the bottom of membrane modules. The rising bubbles and water scour and agitate the fouling layer to prevent solids from accumulating on the membrane surface (Allen, 2008b).

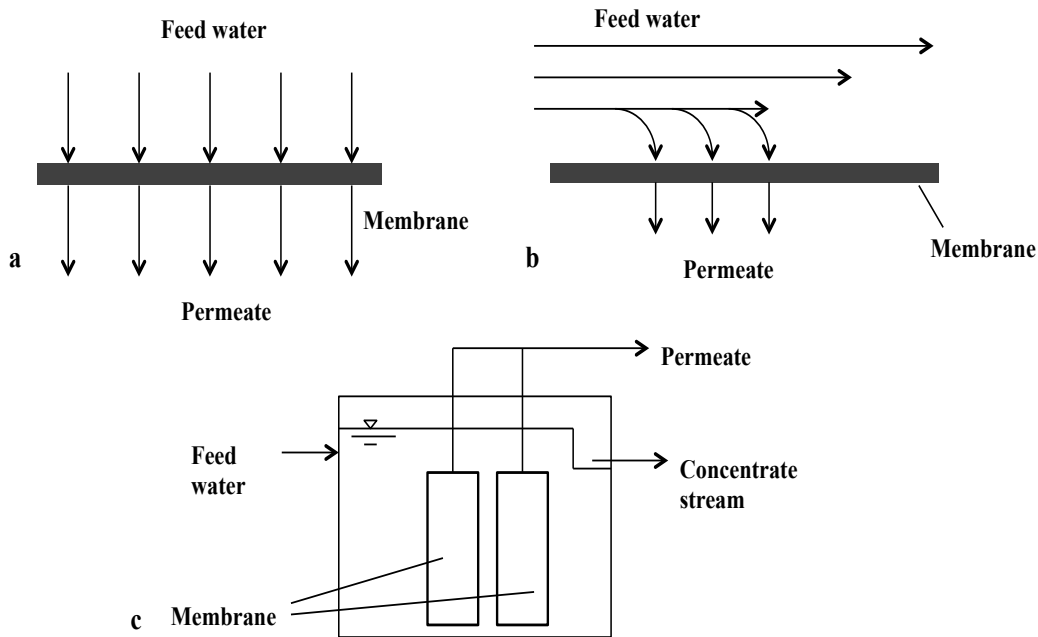


Figure 2-2 Membrane module configurations (a) Dead-end configuration; (b) cross flow configuration; (c) submerged configuration (adapted from Crittenden, 2005).

The applicability of membrane filtration to wastewater treatment has been impeded by the concerns over membrane fouling and durability. Four fouling mechanisms are involved: (a) constriction of internal pore space – permeate restriction by the adsorption of particles smaller than the pore sizes; (b) complete pore sealing – both solvent and solute are stopped by the completely blocked pores; (c) intermediate pore plugging – allows the passage of solvent at a low rate but confines solute to flow through; (d) cake formation – foulants form a separate layer on the membrane surface (Hermia, 1982). These membrane fouling

mechanisms eventually lead to an increasing resistance to the permeate flow and an increasing consumption of energy power. For a submerged membrane system, the essential flow resistance comes from the cake layer (Meng et al., 2007). But in the presence of the aeration stripping, the formation process of a cake layer becomes a dynamic process. This dynamic process is thereby beneficial for the removal of fouling layer (Meng et al., 2007).

Membrane fouling derived from oil, solids and ionic species in oil produced water can cause decreases in rejection and flux rate, and, as a consequence, increase in operating TMP and maintenance costs (Faibish and Cohen, 2001). A variety of approaches that have been studied to address these problems include backwashing, aeration, developing of the novel feed water flow modes, membrane surface modification and pretreatment of the feed water (Allen, 2008b). Pretreatment of the feed water can directly decrease the concentration of potential membrane foulants. For MF and UF, screening, direct coagulation addition and powder activated carbon addition are the most common pretreatments, while for RO and NF; the typical pretreatments are MF or UF (Farahbakhsh et al., 2004).

Many attempts have been made to modify ceramic membranes to alter their surface electrochemical properties (Winkler and Baltus, 2003; Zhang et al., 2009). Surface modification by nanoparticles yields a high degree of control over fouling and an ability to generate desired membrane structure (Kim and Bruggen, 2010). The common nanoparticles coated on ceramic membrane are metal oxides, including titanium dioxide (TiO_2), silica dioxide (SiO_2) and iron oxide (Fe_2O_3) (Kim and Bruggen, 2010). Modified ceramic membrane can achieve a shift isoelectric point towards lower pH. This is because the coated metal oxides (e.g., TiO_2 , SiO_2) surface possesses more strong negative charged sites and the higher ability to bind hydroxide ions than aluminum oxide (Al_2O_3) (Zhang et al., 2009). Figure 2-3 shows the changes in the surface charge of TiO_2 -modified ceramic membrane.

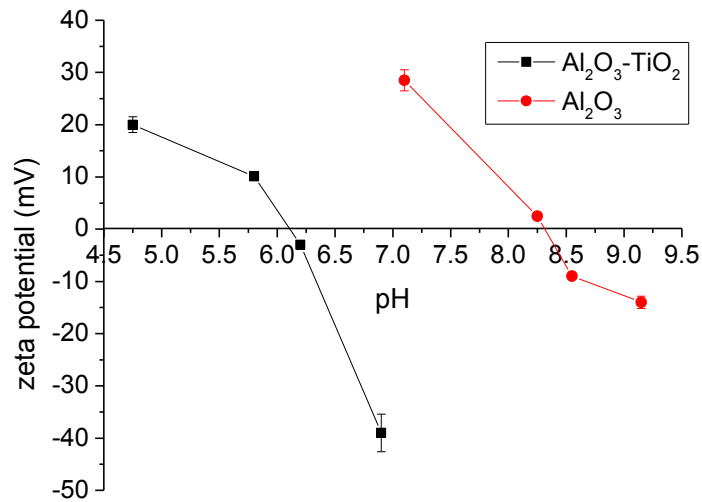


Figure 2-3 pH changes in zeta potential of Al₂O₃ and Al₂O₃ – TiO₂ membranes (adapted from Zhang et al., 2009).

Membrane cleaning is composed of intermittent physical backwashing and periodic chemical cleaning (Cheryan, 1998). Backwashing can restore a portion of membrane permeability caused by the reversible fouling. However, the irreversible fouling can only be removed by the chemical cleaning. The most suitable and usual chemical cleaning agents are alkaline chemicals, acids and chlorine solution (Cheryan, 1998). Although it is expected that chemical cleaning can completely recover TMP, study showed that the efficiency of chemical cleaning was often less than 100% (Ebrahimi et al., 2010). Besides, it was also reported that chemical agents could cause the damage of membrane and impact filtration performance.

The membrane filtration technology has been applied for the remediation of the oil field produced water for a long time (Allen, 2008b). Lin and Lan (1998) investigated a semi-batch UF and RO treating waste drawing oil after pre-filtration by a microfilter. A spiral-wound tube of polymer membrane and a spiral-

wound form polyamide membrane were used in UF and RO units, respectively. UF experimental results indicated that the optimum TMP of 0.24 MPa was able to generate an acceptable combination of permeate flux, permeate volume and total membrane resistance. Also, UF was effective in decreasing concentration of COD and copper as well as reducing turbidity, but results showed no reduction in the permeate's conductivity. Furthermore, with the RO treating UF permeate, the final effluent quality was found to have an over 99% removal of COD, copper, turbidity and conductivity. Polymeric membrane and ceramic membrane have been examined in the oil sands industry focusing on the removal of suspended and dissolved solids, oil, hydrocarbon and salts (Gamal El-Din, 2011). A bench-scale NF membrane system was applied to reduce hardness and NAs concentration in OSPW for potential disposal (Peng et al., 2004). The results showed that a 95% reduction of NAs and an over 90% reduction of divalent ions in OSPW were obtained after NF treatment (Peng et al., 2004).

However, the fouling issue in the membrane treatment of OSPW is particular severe due to the oily and sticky solids and colloids presented in OSPW that may easily block membrane pores and deposit on membrane surface (Gamal El-Din, 2011). Kim et al. (2011) examined pretreatment effects on the OSPW desalination by using commercial NF and RO membranes in the bench-scale experiments. CFS with and without coagulants and coagulant aids were evaluated in this study. Flat sheet membranes were used in NF and RO units. Experimental results exhibited enhanced membrane permeability with the addition of coagulant and coagulant aids. A 30 mg/L alum was found to be the optimum dose for the best performance through both NF and RO filtrations. 98.5% of deionization was obtained for RO after filtration of OSPW pretreated by CFS with alum. It was noted that organic and oily components in OSPW were correlated with the increase in the membrane hydrophobicity and negative surface charge. A 1mM hydrochloric acid in this research was used as chemical cleaning agent, but only 81% of the permeate flux recovery was achieved.

Application of NF membrane was investigated by Peng et al. (2004) to remove the divalent ions and NAs from different OSPWs and surface run off the Aurora mine. The study was conducted using a bench scale flat sheet cross-flow membrane system with 3 different membrane types: Desal 5, NF45 and NF 90. All membrane types yielded an over 90% rejection of divalent cations and NAs from Aurora surface water. But Desal 5 was finally chosen for further OSPW experiments because they achieved stable permeate flux over 16 hours of filtration. The subsequent OSPW experimental results showed that Desal 5 was able to achieve an over 95% rejection of NAs, TOC and divalent ions for all types of OSPW.

Membrane fouling level is dependent on the feed water characteristics such as concentration of suspended and dissolved solids and salts. Dong et al. (2007) studied mechanism of coagulation pretreatments on preventing membrane fouling with respect to the molecular weight of natural organic matter. The authors concluded that the higher molecular weight of hydrophobic compounds was the main reason of the rapid decline in UF membrane flux rate.

Husein et al. (2011) investigated membrane fouling and back contamination of micellar enhanced UF (MEUF) membranes with different molecular weight cut off (MWCO). A cross-flow MEUF module comprised of the tubular TiO₂ ceramic membranes with MWCO of 8, 15 and 50 kDa was employed in the study. Synthetic produced water was mixed with the different types and concentrations of NAs. CPC (cetylpyridinium chloride) surfactant was introduced to the feed water. It was reported that the concentration of CPC in permeate increased with increasing TMP. A linear relation between the permeate flux and TMP was observed for 15 and 50 kDa membranes implying insignificant impact of concentration polarization. A 15 kDa membrane showed a higher removal of contaminants and surfactant in comparison to other membranes with different MWCOs, but a correspondingly higher resistance of the fouling layer was also perceived. Fakhru'l-Razi et al. (2009) conducted a UF treatment of the oil produced water combined with hydrocyclone pretreatment. The experiments were

performed in a cross-flow UF mode. With the hydrocyclone pretreatment, 73% and 54% of solids and oil content, respectively, were successfully removed in permeate.

An appropriate treatment technology selection relies not only on the exceptional treatment performance to achieve a high quality of effluent, but also on the assessment of the economic and environmental sustainability of this technology (Vlasopoulos et al., 2006). Vlasopoulos et al. (2006) performed a life cycle assessment of the environment impacts of 20 different water treatment technologies that are appropriate for treating oil and gas produced wastewater. This assessment was conducted based on the treatment of a volume of 10,000 m³ of produced water (per day) by both individual and combined technologies. In this study, MF was considered as a technology that was capable to clean the produced water to a desired end-use level same as the combined technologies, including dissolved air flotation with absorbents (DAF-ABS) and hydro-cyclone with absorbents (HYDRO-ABS). The authors stated that DAF-ABS and HYDRO-ABS were two treatment combinations that had minimal environmental impacts than other combined technologies including, but not limited to, DAF-activated sludges, DAF- trickling filters. However after the assessment among MF, DAF-ABS and HYDRO-ABS, MF was identified as the most environmentally favorable treatment technology with respect to the impact aspects of abiotic depletion, acidification, eutrophication, global warming and photo-oxidant formation (Figure 2-4). This low environmental impact associated with MF treatment technologies was attributed to its low energy consumption during the equipment operation phase.

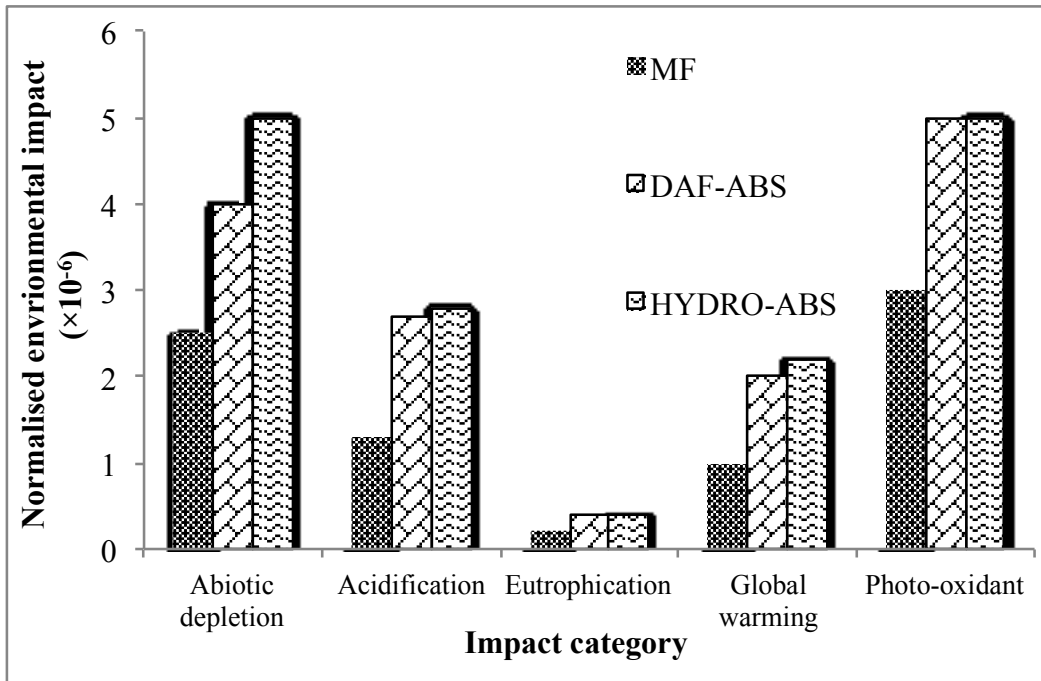


Figure 2-4 Normalized environmental impacts of MF, DAF-ABS and HYDRO-ABS technologies (adopted from Vlasopoulos et al., 2006).

2.2.3 Adsorption

Adsorption is a mass transfer process where ions or molecules in one phase (liquid or air) are attached to the surface of adsorbents (Tchobanoglous et al., 2003). Adsorbents are solids that are able to perform adsorption, while adsorbates refer to the substances capable of being adsorbed. The Van der Waals forces, interacting among ions and compounds, produce the weakly held bonds (electrostatic interactions) that result in the adsorption of components between the two phases (Gregg and Sing, 1982). Adsorption is used to remove organic (natural and synthetic) and inorganic compounds, heavy metal and taste and odour causing compounds from the liquid and gas phases (Jankowska et al., 1991). Carbonaceous materials including activated carbon, zeolites, synthetic polymers and carbon blacks and nanotubes are the most widely used adsorbents in water and wastewater treatments (Parsons and Jefferson, 2006).

Activated carbons are the classical adsorbents used for decolourization, deodorization, dechlorination, detoxication, salt content modification and separation (Bansal et al., 1988). They are originated from a diversity of organic precursors that contain high amount of carbon, such as coal, wood, peat, etc. (Bansal et al., 1988). Given the wide availability of activated carbon, it has sparked an increasing interest in remediation, recycling and contaminant control of industrial wastewaters (Small, 2011). Though researches have demonstrated that the activated carbon was able to remove dissolved organic carbon and NAs from OSPW, it was not effective in removing other target contaminants (e.g., BTEX and oil) (Shawwa et al., 2001).

Petroleum coke (PC) is a byproduct of bitumen upgrading process that is produced through either delayed or fluid coking processes (Furimsky, 1998). Currently, over 6000 tons of PC are generated everyday by Suncor Energy Inc. and Syncrude Canada Ltd, and its total yield is over five million tons per year (Fedorak and Coy, 2006). Due to the high carbon content in PC, it can be activated to better adsorb organic chemicals. The adsorptive capacities of activated PC may be 10 times as higher as that of PC (Shawwa et al., 2001). Therefore, NAs and other organic or inorganic contaminants in OSPW are expected to be more successfully eliminated by PC. Syncrude Canada Ltd. Has started a pilot research on assessing the feasibility of using PC to treat OSPW. The utilization of PC provides a promising OSPW remediation option, not only because it produces a valuable low cost activated carbon, but also addresses the consumption of PC storage on-site (Shawwa et al., 2001).

Zubot et al. (2009) studied the effect of PC adsorption on the removal of dissolved organic components present in the fresh OSPW. Isotherm experiments were performed at a room temperature. OSPW was added to 500mL glass containers to generate solution contained PC of up to 40% by weight. An average 0.26 mg NAs/g PC adsorption capacity was achieved at 60 mg/L of NAs in OSPW. The result showed that pH of OSPW was a key factor to govern the extent of adsorption. When pH of OSPW was reduced to 5.9, the overall NAs removals

were significantly improved. Figure 2-5 displays the NAs concentration remaining in OSPW as a function of the added PC.

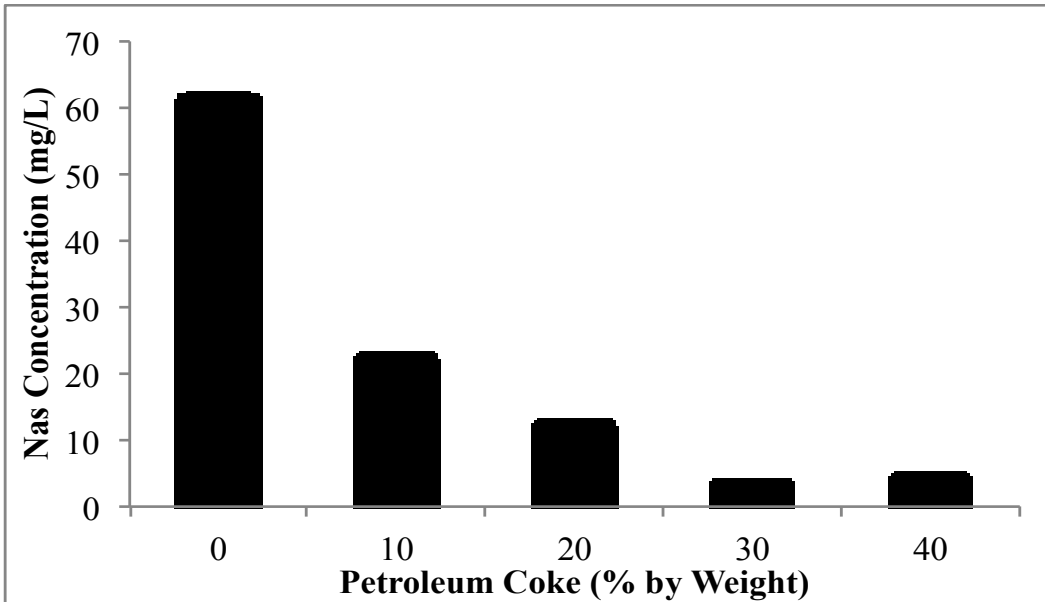


Figure 2-5 NAs concentration at different petroleum coke doses (adapted from Zubot et al., 2010).

The activation of PC for adsorption of NAs was also conducted by Small et al. (2010). Adsorption experiments used Suncor Energy Inc's delayed cokes and Syncrude Canada Ltd's fluid cokes. It was found that the activation under carbon dioxide alone was not efficient to increase the surface area of PC. But with the combination of steam with a rate of 0.5 mL/min at 900 °C, activated delayed coke could eventually attain the greatest surface area after 6 hours of activation. It was also stated that the surface area of petroleum coke affected the adsorption of NAs. AEF reduction test showed that adsorption process removed up to 77% of AEF by 30% wt. of non-activated PC with surface area of 5.7 m²/g, while activated PC (surface area 494 m²/g) achieved 92% AEF reduction with only 5% concentration by weight.

2.2.4 *Advanced Oxidation*

Advanced oxidation processes (AOPs) are chemical oxidation treatment techniques which are enable to oxidize primarily organic and inorganic compounds from contaminated water or air by utilizing highly reactive intermediates, such as hydroxyl radicals (Tarr, 2003). The hydroxyl radical is a very powerful oxidizing agent that is normally generated by the ultraviolet irradiation (UV) or the visible light. It reacts non-selectively with chemical substances because of its strong ability of abstraction of hydrogen atoms from basically all kinds of organic compounds including NAs (Parsons, 2004). The treatment with AOPs not only destructs the target contaminants, but also decreases their toxicity. Generally, the end products of AOP are carbon dioxide and water, with the exception of mineral acids if pollutants contain other elements such as Cl, N, S, etc. AOPs have been proven to be very effective for the treatment of polluted groundwaters and industrial wastewaters (Bolton, 2010). Most of viable AOPs use UV in combination with strong oxidants (e.g., hydrogen peroxide H_2O_2 , ozone O_3) and catalysts. Among all available AOPs, O_3/H_2O_2 , UV/ H_2O_2 , UV/ TiO_2 and neutral pH Fenton are the most commonly used techniques.

AOPs have been considered as a complementary treatment to current biological treatment to expedite the OSPW remediation speed, especially for the degradation of NAs. Ozonation, as a well-known technology, can degrade pollutants directly or via hydroxyl radical reactions. Investigations were conducted to assess the ozonation for removing NAs in OSPW. Experimental results showed a 70% decline in NAs concentration and a non-toxic effluent produced after 50 min of ozonation (Scott et al., 2008). By extending the ozonation time to 130 min, NAs residual concentration decreased to less than 5% of its initial concentration (Scott et al., 2008). Fu et al. (2008) also examined the applicability of ozonation to the treatment of OSPW by conducting a semi-batch experiments. A 64% degradation of the initial AEF of organics was achieved with the ozone concentration of 80 mg/L, while COD slightly deceased from 250 mg/L

to 196 mg/L with the ozone dose of 150 mg/L. Results also showed that the longer OSPW is treated with ozone, the more biodegradable OSPW became. In addition, the numbers of carbon and rings in the NAs structure were found to affect NAs oxidation.

Liang et al. (2011) compared NAs removal efficiency in OSPW by UV/TiO₂, UV/periodate (IO₄⁻), UV/ H₂O₂ and UV/persulfate (S₂O₈²⁻) processes. Half-life estimates for NAs and electrical energy per mass requirement under different AOPs are presented in Table 2-2. After comparison, the authors concluded that the optimum conditions for oxidizing NAs were S₂O₈²⁻ concentration of 20 mM at pH 8 and 10 and H₂O₂ concentration of 50 mM at pH 8.

Table 2-2 Degradation of NAs using AOPs (adapted from Liang et al., 2011).

Treatment	pH	Half-life (min)	(EE/M) _{1/2} (kWh/kg TOC)
UV only	10	>360	-
UV/TiO ₂ (3 g/L)	10	>361	-
UV/IO ₄ (20 mM)	10	>362	-
UV/IO ₄ (4 mM)	10	108	(1.758±0.088) ×10 ⁴
UV/S ₂ O ₈ ²⁻ (20 mM)	8	18.6	(3.67±0.18)×10 ³
UV/S ₂ O ₈ ²⁻ (20 mM)	10	18.3	(3.32±0.17)×10 ³
UV/H ₂ O ₂ (1 mM)	10	>360	-
UV/H ₂ O ₂ (50 mM)	8	17.2	(3.36±0.17)×10 ³
UV/H ₂ O ₂ (50 mM)	10	40	(6.67±0.33)×10 ³

2.2.5 Biological Treatment

Natural biodegradation of organic acids in OSPW is very slow, and the concentration of NAs could hardly be brought down below 19 mg/L (Gamal El-Din, 2011). It is even more difficult to achieve when natural degradation process lasts for more than 10 years because biodegradation process would be significantly deescalated by the deficient in microorganism or specific enzymes (Quagraine et al., 2005a). Exploiting biodegradation through introducing

extraneous microorganisms to remove organic matters from wastewater is defined as biological treatment (Rodgers and Zhan, 2003). This treatment process builds an environment containing organic substances that various microbial cultures can make use of for the subsistence and reproduction (Rodgers and Zhan, 2003). Instead of separating organic substances from wastewater, biological treatment uses the metabolic processes of bacteria to destroy the organic compound structure to decrease the toxicity of wastewater (Quangraine et al., 2005b). Therefore, the factors such as pH, temperature, nutrient sources, dissolved oxygen, etc., that affect microorganism growth and metabolism are critical to the efficiency of biological treatment. Other factors, such as energy consumption, time and cost should also be taken into consideration for the viability of biological treatment (Farhadian et al., 2008).

Biological treatment can be categorized in two distinct types: the suspended growth and the attached growth (Gamal El-Din, 2011). The attached growth biological treatment is known as biofilm reactors treatment and suspended growth treatment involves activated sludge reactors treatment. Study showed that biofilm reactors treatment were superior to active sludge reactors treatment in terms of treatment performance and cost (Rittmann, 2006). Microorganism growing in activated sludge reactors is mobilized and suspended. While in a biofilm reactor, microorganisms are attached to the media (some inert material), such as rocks, sands, ceramic or plastic materials, to form an immobilized biofilm on the surface of the media. This is aimed to optimize the biodegradation level by multi-species microbial communities in the bioreactor and to maintain a relatively clean environment (Langwaldt and Puhakka, 2000). Unlike activated sludge bioreactor, biofilm reactor can function at a high biomass concentration with no necessities of considering biomass retention and recirculation. It also has the advantages of lower energy power, less footprint, lower sensitive to toxic loadings and simple manipulation (Rodgers and Zhan, 2003).

In general, biological treatment of organic substances including NAs is an aerobic process (Herman et al., 1993). It was reported that a rapid aerobic

biodegradation of model and commercial NAs occurred within 10 days of incubation (Whitby, 2010). Clemente et al. (2004) used aerobic cultures to biodegrade the commercial NAs (Kodak NAs and Merichem acids). The NAs concentration dropped to less than 10 mg/L from about 100 mg/L after 10 days of incubation. 60% of carbons in NAs were converted to carbon dioxide. Thus the toxicity of microbial culture supernatant was significantly reduced. However, NAs native to OSPW are more persistent to be aerobically biodegraded than the commercial NAs. The reason is because commercial NAs contain a considerably labile fraction of NAs that is easily biodegradable and a fraction of the greatly branched NAs that is very recalcitrantly biodegradable (Han et al., 2008). OSPW, however, contains only substantially recalcitrant NAs (LO et al., 2006).

Although contaminants in most of the oil sands tailing ponds will eventually become naturally anaerobically degraded, few studies of anaerobic biodegradation of NAs were reported. Holowenko et al. (2001) investigated the anaerobic biodegradation of surrogate NAs. Oil sands mature tailings and sewage sludge were used as an inocula. Results showed that the anaerobic culture partially metabolized cyclohexylpropanoic and cyclohexylpentanoic acids, but did not metabolize cyclohexylbutanoic acid.

2.2.6 Integrated Treatment Process

No individual treatment technology could remove all contaminants from OSPW to achieve a desired water quality output for discharge or reuse. A integrated treatment process which combines multiple treatment processes is a reasonable solution to offer the most effective OSPW remediation. However, few studies have addressed the capacity of integrated OSPW treatment processes (Gamal El-Din, 2011), but the necessary of integrated technologies to treat OSPW has been demonstrated in the literature (Wang, 2011a).

Study by Martin et al. (2010) found that the residual NAs were still remained in OSPW even after the extensive ozone treatment indicating that ozonation

treatment alone cannot completely reduce OSPW toxicity. In order to further remove the remaining NAs fraction, biological treatment was suggested to be the feasible post treatment (Martin et al. 2010). Results showed that the biodegradation rate of the residual NAs was considerably accelerated after ozonation. The authors suggested that the effective biodegradation afterwards was because ozone removed the biologically resistant fraction of NAs (Martin et al. 2010). Wang et al. (2011b) also investigated the OSPW detoxification. The authors showed that after applying 100 mg/L dose of ozone and subsequent biodegradation, OSPW exhibited non-toxic effect on *vibrio fischeri* in Microtox bioassay, implying that combination of two treatments, ozonation and biological degradation, is a promising technology for decreasing OSPW's toxicity.

The economic sustainability of a technology is an important factor in OSPW treatment. Specifically, RO treatment itself can eliminate all types of contaminants in OSPW, producing an extremely high quality effluent, but at an expense of high energy consumption caused by severe membrane fouling (Allen, 2008a; Wang, 2011a). Therefore pretreatment is always needed before the RO process. Kim et al. (2012a) assessed the effects of different CF pretreatment conditions on the RO filtration of OSPW. Compared with the membrane fouling of RO with no pretreatment, CF treatment aimed at maintaining high permeate flux through reducing membrane fouling. With the addition of anionic coagulant aids, CF pretreatment led to the least accumulation of foulants and the most enhanced membrane performance.

2.3 Research Request for OSPW Remediation

Based on the literature review, a wide range of studies has been performed to develop different methods of OSPW decontamination. But these promising treatment processes are lacking the objective assessment of their feasibility for the treatment of OSPW. Most of these studies are mainly focused on decreasing toxicity and salinity in OSPW. Few studies have been conducted on the

investigation of economically and environmentally effective preliminary treatment that would offer high quality of effluent for the subsequent treatment. The pretreatment methods to remove suspended solids and oil content were found in literature, however the application of MF process for the removal of suspended solids and oil content has not been addressed in OSPW research. The research gaps in MF are as follows:

- In present, membrane filtration is widely used as a desalination process (NF and RO), which is usually performed as the end treatment step to reduce OSPW toxicity. Some studies have been employed UF process as a pretreatment step, but they have not tested MF on pretreating OSPW.
- Cross-flow membrane configuration is frequently reported in the literature. However, the feasibility of the submerged membrane configuration requires to be tested for OSPW treatment with regard to TMP changes and permeate quality.
- Membrane fouling associated with MF also needs to be addressed and approaches to minimize MF fouling needs to be developed.

CHAPTER 3: EXPERIMENTAL PROCEDURE AND METHODS

3.1 Experimental Materials and Apparatus

3.1.1 OSPW and Chemicals

Raw OSPW was collected in July 2012 from Pond 7, located at the Suncor Energy Inc. facility in Fort McMurray, Alberta, Canada. The OSPW was preserved in the polyvinyl chloride barrels and stored at 4°C in a temperature controlled room at the University of Alberta. Before experimentation, OSPW was stirred vigorously with a mechanical mixer (Meidensha Corp., Tokyo, Japan) to dissipate suspended solids throughout the water, and warmed to room temperature (22 ± 1 °C). The OSPW characteristics are presented Table 3-1.

Prior to operating CF-MF processes for the treatment of OSPW, different concentrations (0 to 60 mg/L) of alum ($\text{Al}_2(\text{SO}_4)_3 \cdot 18\text{H}_2\text{O}$, Fisher Scientific, Fair Lawn, NJ, USA) and (0 to 60 mg/L) of PAC ($\text{Al}_2(\text{OH})_n\text{Cl}_{6-n}$, Fisher Scientific, Fair Lawn, NJ, USA) were examined to determine the optimum dose of alum and PAC for the efficient membrane filtration. Chemicals used in all experiments were analytical grade and were used without further purification. Fresh stock solutions of coagulants (25.0 g/L as alum or PAC) were prepared for all experiments and were diluted before application. Milli-Q water (Millipore Corp., Bedford, MA, USA) with a resistivity of 18.2 M Ω -cm and conductivity less than 1 $\mu\text{S cm}^{-1}$ was used for dilution and other use.

Table 3-1 Characterization of the Suncor Energy Inc. Pond 7's OSPW.

Parameters	Average
pH	7.20
Conductivity, $\mu\text{S}/\text{cm}$	3671.5
Turbidity, NTU	25.9
Total organic carbon (TOC), mg/L	41.2
Chemical oxygen demand (COD), mg/L	134.6
Total suspended solids (TSS), mg/L	21.2
Total dissolved solids (TDS), mg/L	1906.2
Acid extractable fraction (AEF) mg/L	31.9
Silt density index (SDI ₅)	6.25
Average particle size, nm	696.8
Magnesium, mg/L	30.62
Calcium, mg/L	25.90
Iron, mg/L	0.24
Manganese, mg/L	0.08
Silicon, mg/L	5.66
Fluoride, mg/L	1.90
Chloride, mg/L	1291.3
Bromide, mg/L	n/d
Phosphate, mg/L	n/d
Sulfate, mg/L	60.6
Nitrate, mg/L	0.92
Sodium, mg/L	705.1
Potassium, mg/L	13.1
NAs, mg/L	7.2

n/d: not detected

3.1.2 Microfiltration and Reverse Osmosis Membranes

Four membranes were used in the present study: three types of flat-sheet ceramic membranes: unmodified, SiO₂-and TiO₂-modified ceramic membranes (Meidensha Corp., Tokyo, Japan) were applied for MF treatment and one commercial flat-sheet polymeric membrane (GE Osmonics, Fairfield, CT, USA) was used for RO treatment. The MF membranes are designed to remove particulates, and the RO membrane is purported to desalinate OSPW. The ceramic MF membrane units consisted of two layers: a ceramic membrane active layer and a base layer. The surface charges of modified and unmodified membranes were measured by Zetasizer Nano ZS (Malvern Instruments Co, Malvern, UK). For the alumina-based ceramic membrane, the iso-electric point determined from measuring the zeta potential is usually within the range of 8-9.4 (Kosmulski, 2009; Mullet et al., 1997). Figure 3-1 present a cross-sectional image of the tested ceramic MF membrane unit structure.

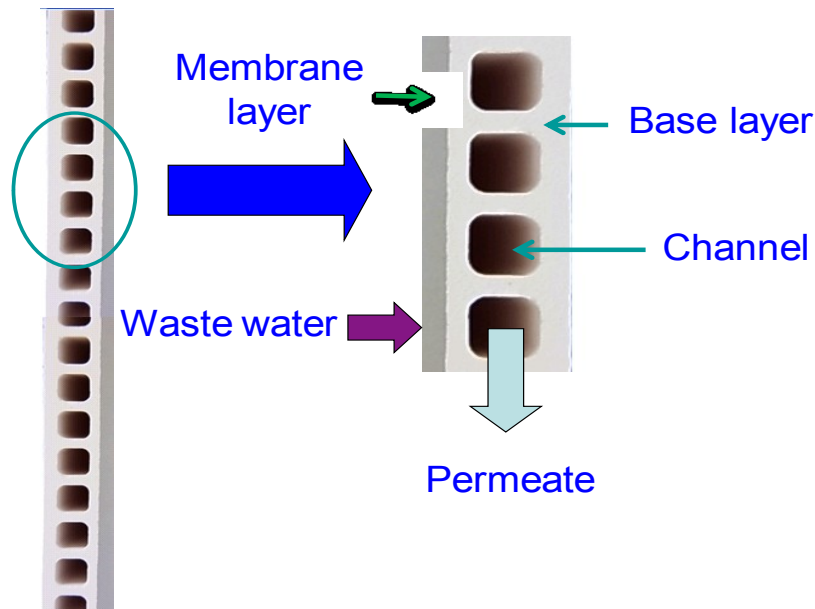


Figure 3-1 Cross-section of ceramic membrane (Meidensha Corp., Tokyo, Japan).

The polymeric RO thin-film composite (TFC) membranes were purchased from the GE Osmonics (Fairfield, CT, USA). Before experimentation, the RO membrane was soaked into Milli-Q water for at least 24 hours and then compressed to achieve stable permeate flux. The properties of the ceramic MF membranes and the polymeric RO membrane are listed in Table 3-2.

Table 3-2 Physico-chemical properties of membranes.

Membrane type	Material	Rejection (%)	pH range	Porosity (%)	Thickness of membrane active layer
MF Flat-sheet	Unmodified ceramic (Al ₂ O ₃)	95.1 of 0.1µm particles (latex)*	2-12	44.4	49
MF Flat-sheet	SiO ₂ -modified ceramic	97.1 of 0.1µm particles (latex)*	2-12	44.7	53
MF Flat-sheet	TiO ₂ -modified ceramic	97.0 of 0.1µm particles (latex)*	2-12	45	52
RO Flat-sheet	Polyamide TFC	99.5 of NaCl	4-11	-	-

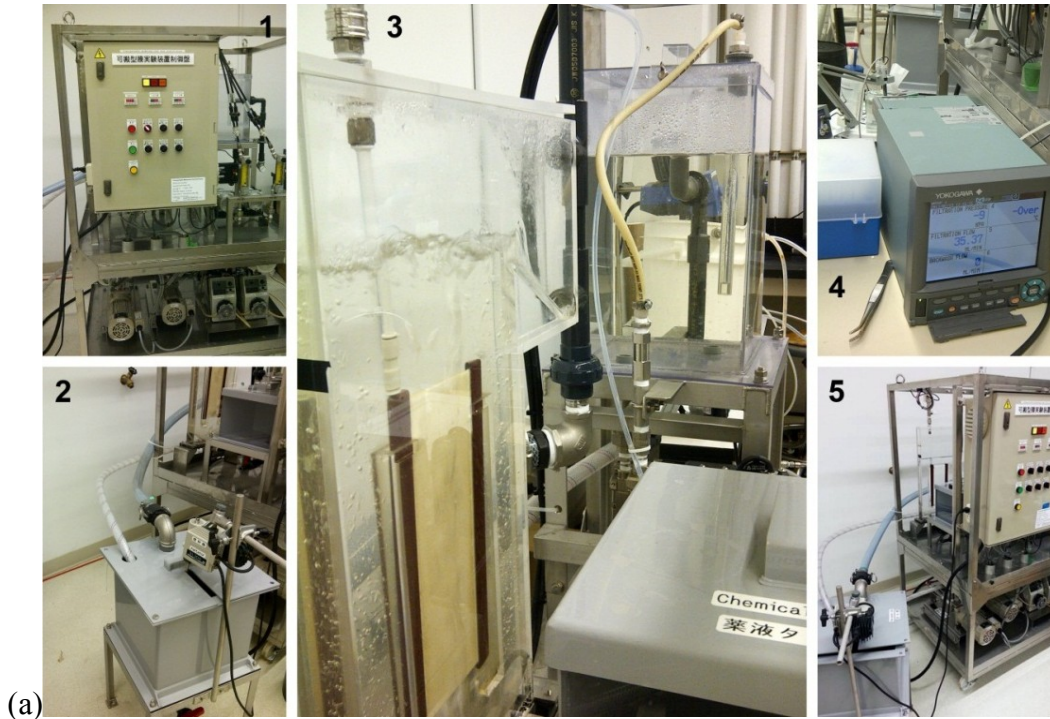
*Supplied by JSR. Dynospheres™

3.1.3 Microfiltration and Reverse Osmosis Membrane Treatment System

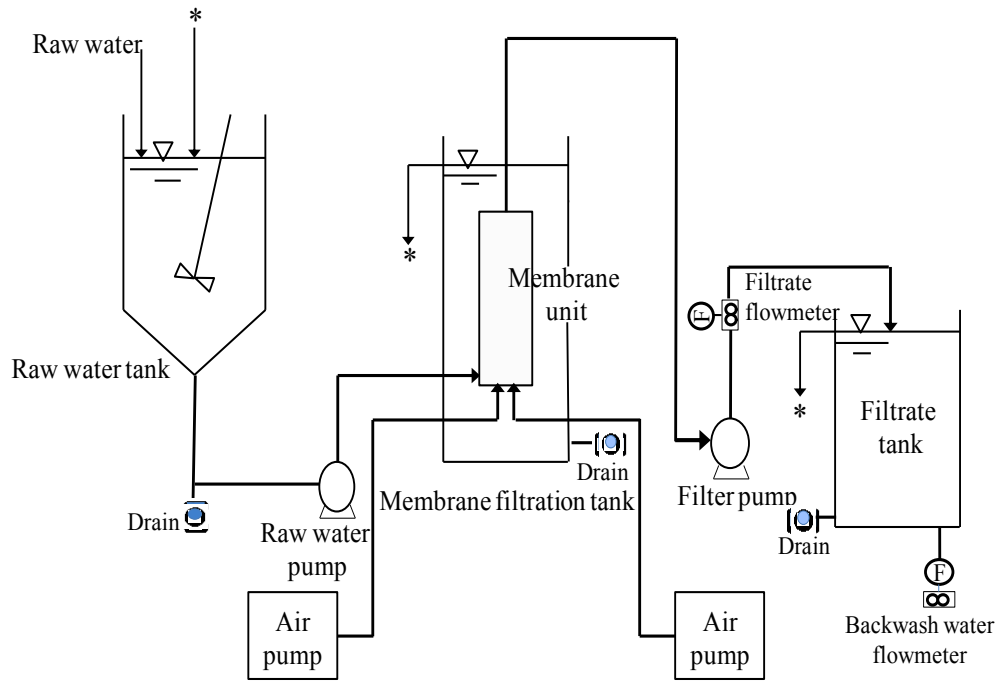
Raw OSPW and CF-pretreated OSPW were filtered through a low-pressure submerged MF membrane system that consisted of the flat-sheet ceramic MF membrane, a 30-L feed tank with a stainless steel mechanical stirrer, four mechanical pumps (i.e., a feed water pump, two air pumps and a filter pump), a membrane tank and a permeate tank. A data recorder was connected to the system and automatically recorded the variations in TMP and filtration flow rate every 10 s. The MF system was automatically backwashed every 10 min for 30 sec. The MF ceramic membrane filtration setup is shown in Figure 3-2.

The RO filtration was conducted through a lab-scale cross-flow filtration module (SEPATM CF II plate and frame cell, GE Osmonics, Fairfield, CT, USA),

which had 140 cm² of effective membrane area. Water was fed from a feed tank (20 L) by a mechanical pump and transported by flexible stainless-steel tubes to inlet ports of the module. TMP and feed flow rate were controlled by a pressure gauge, back-pressure regulators, and bypass valves. Membrane coupons were cleaned and soaked in Milli-Q water and precompactd under 1378 kPa for 24 to 48 hours until a steady-state flux was obtained. Photographs and a schematic diagram of the RO membrane setup are shown in Figure 3-3.

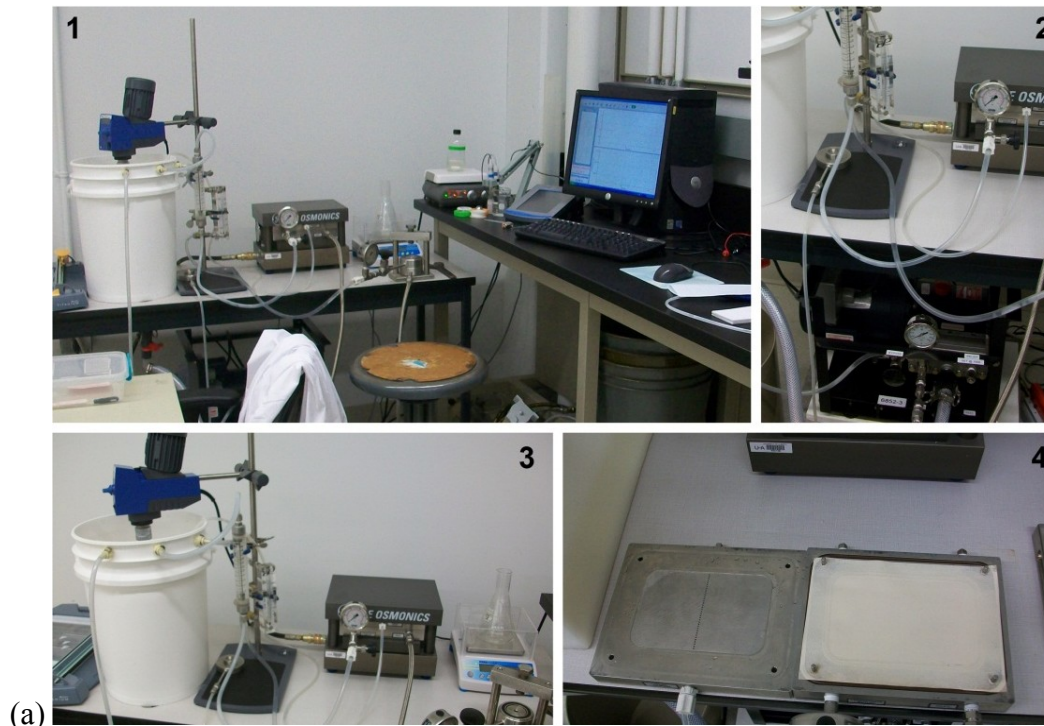


(a)

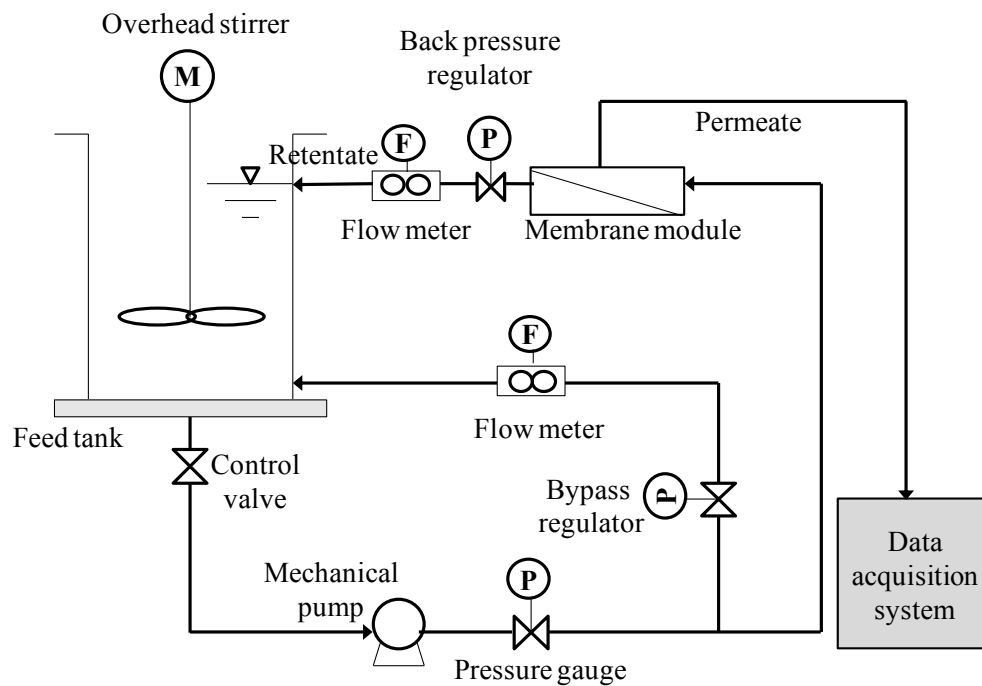


(b)

Figure 3-2 (a) Images of MF ceramic membrane treatment system (1) transportable membrane test unit panel, water pumps, air pumps and flow meters; (2) feed tank and a mechanical stirrer; (3) membrane and permeate tanks; (4) data recorder; (5) membrane test unit and feed tank. (b) Schematic diagram of MF filtration process.



(a)



(b)

Figure 3-3 (a) Images of RO polymeric membrane treatment system: (1) RO filtration system; (2) RO membrane module and mechanical pump; (3) feed tank, overhead stirrer and electrical scale; and (4) RO membrane and membrane module. (b) Schematic of RO filtration system.

3.2 Experimental Procedure

3.2.1 Coagulation-Flocculation Experiment

The optimal concentrations of coagulants in CFS and CF were determined prior to MF runs. The reason that CF process was selected for the chemical modification of feed water was to mitigate the formation of fouling in the MF process that was largely caused by solid materials, such as sand, silt and clay. Coagulation tests were conducted with aluminum-based coagulants. PAC and alum were added in different doses (0.5 mg/L, 1 mg/L, 2 mg/L, 5 mg/L, 10 mg/L, 20 mg/L, 40 mg/L, and 60 mg/L). The optimization of coagulant concentrations in CF process was based on changes in zeta potential and average particle size. CF was also conducted at pH 10 (see section 4.2.1 for explanation), 1 M sodium hydroxide (NaOH) was used to adjusted pH. The optimization of coagulants concentrations in CFS was based on turbidity changes before and after CF. A jar tester unit consisting of six 2-L square jars and mechanical paddles (PB-700™ Standard JarTester, Phipps & Bird Inc., Richmond, VA, USA) was used for the CF process. The mixing intensity and times were as follows: rapid mixing for 30 seconds at 120 rpm and slow mixing for 10 minutes at 30 rpm (Pourrezaei et al., 2011). CF experiments were conducted at room temperature (22 ± 1 °C). Samples were collected through the sampling ports on each jar directly after the CF process for measurements of zeta potential and average particle size. Zeta potential and average particle size were measured by Zetasizer Nano (Malvern Instruments Co, Malvern, UK). Turbidity was measured before and after sedimentation. An image of the coagulation test set-up is shown in Figure 3-4.



Figure 3-4 Jar test unit with coagulated OSPW.

3.2.2 *Microfiltration Experiment*

The ceramic MF membrane was immersed in a membrane tank filled with the feed water. Under pressurized suction, permeate moved across the membrane surface into the channel and then permeate flowed into the permeate tank. Each membrane filtration run in this study comprised of two stages. The purpose of the first stage was to concentrate impermeable constituents in the feed water. In the first stage, 25 L of OSPW were continuously filtered by the membrane for 11 hours to generate 20 L of permeate: 10 L were stored in a permeate tank in the membrane system and the other 10 L were kept in a separate container without recycling to the membrane system. Retentate generated in the membrane tank was recycled to the feed tank. In total, 15 L of OSPW remained in membrane system after the first stage. The second stage commenced after the first stage, operating the remaining OSPW in the system for additional 7 days or more. In this stage,

permeate continually flow back to feed water tank as well as the retentate. The purpose of this stage was to test membrane stability under highly concentrated feed water conditions. The MF treatment was generally operated until TMP decreased to -35kPa, after which chemical cleaning with 0.1% (v/v) sodium hypochlorite (NaOCl) was conducted. NaOCl is a caustic and oxidizing chemical agent that can effectively dissolve organic and inorganic foulants (Zondervan and Roffel, 2007). Its high instant cleaning rate and overall membrane cleaning effectiveness have been reported (Zondervan and Roffel, 2007). During chemical cleaning, membrane was soaked in NaOCl solution for 1 hour. Milli-Q water was used to wash the remaining NaOCl solution off the membrane before membrane was placed back to membrane tank. For Runs 5 and 6, feed water pH was adjusted to 10 by adding 1 M NaOH after CF process. MF filtration process is presented as the flow chart below (Figure 3-5). Detailed descriptions of 8 runs are listed in Table 3-3.

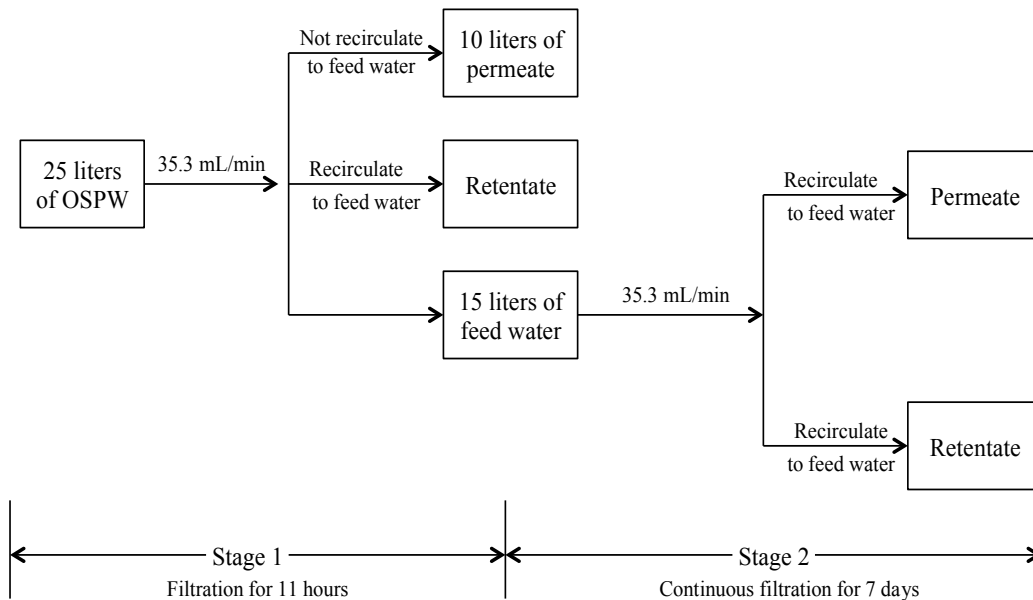


Figure 3-5 Membrane filtration processes.

Table 3-3 Detailed descriptions of OSPW filtration runs.

Run #	Description of Run	Conditions
Run 1	MF (unmodified ceramic membrane) with raw OSPW	<ul style="list-style-type: none"> • Net flux = 45 L/m²h (suction pump set at 35.3 mL/min) • Flow rate of membrane aeration = 1.13 mL/min • Backwash cycle = 10 min, backwash duration = 0.5 min
Run 2	Direct CF (20 mg/L PAC) followed by MF (unmodified ceramic membrane)	<ul style="list-style-type: none"> • Net flux = 45 L/m²h (suction pump set at 35.3 mL/min) • Flow rate of membrane aeration = 1.13 mL/min • Backwash cycle = 10 min, backwash duration = 0.5 min
Run 3	Direct CF (10 mg/L alum) followed by MF (unmodified ceramic membrane)	<ul style="list-style-type: none"> • Net flux = 45 L/m²h (suction pump set at 35.3 mL/min) • Flow rate of membrane aeration = 1.13 mL/min • Backwash cycle = 10 min, backwash duration = 0.5 min
Run 4	Direct CF (30 mg/L alum) followed by MF (unmodified ceramic membrane)	<ul style="list-style-type: none"> • Net flux = 45 L/m²h (suction pump set at 35.3 mL/min) • Flow rate of membrane aeration = 1.13 mL/min • Backwash cycle = 10 min, backwash duration = 0.5 min
Run 5	Direct CF (10 mg/L alum with OSPW pH adjusted to 10) followed by MF (unmodified ceramic membrane)	<ul style="list-style-type: none"> • Net flux = 45 L/m²h (suction pump set at 35.3 mL/min) • Flow rate of membrane aeration = 1.13 mL/min • Backwash cycle = 10 min, backwash duration = 0.5 min
Run 6	Direct CF (10 mg/L alum with OSPW pH adjusted to 10) followed by MF (unmodified ceramic membrane) and RO	<ul style="list-style-type: none"> • Net flux = 45 L/m²h (suction pump set at 35.3 mL/min) • Flow rate of membrane aeration = 1.13 mL/min • Backwash cycle = 10 min, backwash duration = 0.5 min

Run 7	Direct CF (10 mg/L alum) followed by MF (SiO ₂ -modified ceramic membrane)	<ul style="list-style-type: none"> • Net flux = 45 L/m²h (suction pump set at 35.3 mL/min) • Flow rate of membrane aeration = 1.13 mL/min • Backwash cycle = 10 min, backwash duration = 0.5 min
Run 8	Direct CF (10 mg/L alum) followed by MF (SiO ₂ -modified ceramic membrane)	<ul style="list-style-type: none"> • Net flux = 45 L/m²h (suction pump set at 35.3 mL/min) • Flow rate of membrane aeration = 1.13 mL/min • Backwash cycle = 10 min, backwash duration = 0.5 min

3.3 Sample Analysis Techniques

Raw OSPW, permeates after the first and the second stage were characterized in terms of pH, conductivity, turbidity, AEF, TOC, SDI₅, COD, TSS, TDS, average particle size, metals (sodium, potassium, magnesium, calcium, iron, manganese and silicon) anions (chloride, bromide, phosphate, sulfate and nitrate) and NAs. The pH, conductivity, turbidity and TOC were monitored every day during the second stage. Feed water after second stage was also characterized for pH, conductivity, turbidity and TOC.

3.3.1 *pH*

pH is a measure of acidity or basicity of aqueous or other liquid solutions (Wang, 2011a). pH can significantly affect water and wastewater treatment with respect to efficiency and effluent quality. An Accumet XL60 pH/conductivity meter (Fisher Scientific, Fair Lawn, NJ, USA) was used to measure the pH of OSPW. Three buffers with pH of 4, 7 and 10 were used to calibrate the pH meter. pH analysis was conducted according to Standard Method 4500-H (American Public Health Association, 2005).

3.3.2 *Conductivity*

Conductivity is a measure of an aqueous solution's ability to conduct an electric current (Wang, 2011a). An Accumet XL60 pH/conductivity meter (Fisher Scientific Inc., Fair Lawn, NJ, USA) was used to determine the conductivity of OSPW at a room temperature (22 ± 1 °C). Conductivity was analyzed based on EPA Method 9050 A (EPA, 1996).

3.3.3 *Turbidity*

Turbidity is the haziness of a liquid caused by silt, sands bacteria chemical precipitates, etc. that are not visible to naked eyes (Wang, 2011a). In the experiments, turbidity was measured in nephelometric turbidity units (NTU) by using a digital nephelometric turbidimeter (Orbeco-Hellige Inc., Sarasota, FL, USA). Procedures were based on Standard Method 2130 (American Public Health Association, 2005).

3.3.4 *Total Organic Carbon*

TOC is the total amount of carbon bounds in organic compounds (Wang, 2011a). In this study, TOC in the sample was measured by an Apollo 9000 TOC combustion analyzer (FOLIO Instrument Inc., Kitchener, ON, Canada). The TOC analyzer used the high-temperature combustion method, where organic carbons were oxidized to carbon dioxide by combustion at 680 °C and continually flushed pure oxygen. All samples were analyzed in relation to a blank (Milli-Q water). Blank and potassium hydrogen phthalate standards were used to calibrate the instrument. The standard curve was calculated using Apollo software TOC Talk (Teledyne Tekmar, Mason, IA, USA). All calibrations and sample operation procedures were based on the Apollo 9000 TOC system Manual (American Public Health Association, 2005).

3.3.5 *Chemical Oxygen Demand*

COD is an indirect method to determine the concentration of organic compounds in water (Wang, 2011a). In this project, a COD digestion reactor (Bioscience Inc., Allentown, CO, USA) and a DR 3900 Benchtop Spectrophotometer (HACH company, Loveland, CO, USA) were used for COD determination. HACH COD digestion reagent vials that contained digestion reagent ranging from 3 to 150 mg/L were used for COD measurements. A 2 mL

of sample was added into reagent vials for digestion. In the experiments, sample vials were inserted in COD digestion reactor and heated at 150 °C for 2 hours and cooled down to the room temperature (22 ± 1 °C) before colorimetric determination. The spectrophotometer was utilized to measure the absorbance at 420 nm. The reference solution was a digested blank with 2 mL of Milli-Q water. Pre-programmed COD calibration method within the spectrophotometer was applied to directly yield the COD concentrations.

3.3.6 *Total Suspended Solids*

TSS was determined by gravimetric analysis referred to Standard Methods 2540 D (American Public Health Association, 2005). The well-mixed sample was filtered through a weighted standard fiberglass filter with 1 μm pore size and 24 mm diameter. The residual retained on the filter was dried to a constant weight at 103 ~ 105 °C. This weight is defined as TSS. The concentration of solids is expressed as the ratio of mass per volume (mg/L). 200 mL of sample was used for determination of TSS, as the TSS in OSPW after membrane filtration was expected to be low.

All Gooch crucibles were dried with filters in them at 105 ± 2 °C overnight and placed in desiccators to cold them down to room temperature before using.

3.3.7 *Total Dissolved Solids*

TDS is a measure of the portion of total solids in a solution that passes through the filter. More specifically, a well-mixed sample was filtered through a standard glass fiber filter. The filtrate was evaporated and dried to a constant weight in a weighted evaporating dish. The increase in the dish weight was defined as TDS. Before measurement, evaporating dishes were rinsed and heated in an oven at 105 ± 2 °C overnight. The dishes were placed in desiccators and

dried to ambient temperature before using. TDS measurement was referred to Standard Method 2540 C (American Public Health Association, 2005).

3.3.8 *Ion Chromatography*

Ion chromatography (IC) is a measure of the anions such as: chloride, bromide, phosphate, sulfate, nitrate, nitrite, etc., and cations such as: sodium, calcium, potassium, magnesium, etc. in mg/L quantities. The measurement is based on the different levels of affinity between the ionic species and basic anion exchanger (American Public Health Association, 2005). Ion chromatograph (DX-600, Dionex, Sunnyvale, CA, USA) with an autosampler (Dionex, Sunnyvale, CA, USA) was employed to analyze chloride, bromide, phosphate, sulfate and nitrate ions in samples.

3.3.9 *Inductively Coupled Plasma-Mass Spectrometry*

Inductively coupled plasma-mass spectrometry (ICP-MS) is designed to determine the trace metals such as: sodium, calcium potassium, magnesium, etc. in water (Wang, 2011a). This measurement is achieved by sample atomization and ionization after passing by an inductively heated plasma torch at high temperature. Ions identification is conducted according to their mass to charge ratios. A multi-collector Nu PlasmaTm inductively coupled plasma mass spectroscope (Nu Instruments Ltd., Wrexham, UK) was used in the experiments.

3.3.10 *Naphthenic Acids*

NAs represent a complex mixture of carboxylic acids including linear and/or saturated ring structures (Allen, 2008a). The classical formula of NAs is $C_nH_{2n+z}O_2$. In this study, the chromatographic separation of NAs was performed by an ACQUITY UPLC System (Waters Corp., Milford, MA, USA). Samples

were filtered through the 0.45 filter, and filtrates were used for the analysis (Alpatova et al., 2013).

3.3.11 Acid Extractable Fraction

AEF is referred to NAs, oxidized NAs and other acid-extractable organic fraction in OSPW whose concentrations can be determined together by using Fourier Transform Infra Red (FT-IR) spectroscopy (Pourrezaei et al., 2013). To determine the concentration of AEF in OSPW, samples were acidified first and targeted organics were extracted from the aqueous phase in OSPW with the methylene chloride (Fisher Scientific, Fair Lawn, NJ, USA). Then Fourier Transform Infra Red (FT-IR) spectroscopy (100 FT-IR Spectrometer, PerkinElmer, Waltham, MA, USA) was used to measure the concentration of AEF by recording the two peak heights of the spectrum at 1743 and 1706 cm^{-1} . The combined peak heights were then compared to the standard calibration curve that was obtained with a Fluka NAs to calculate the AEF concentration of an unknown sample. The extraction and FT-IR analysis procedures were performed according to Jivraj et al. (1996).

3.3.12 Silt Density Index

SDI is a measure of fouling potential of water in RO. SDI measure referred to the Standard Test Method for Silt Density Index (SDI) of Water (American Society for Testing Materials, 1995). A SDI-PU kit (Applied Membranes Inc., Vista, CA, USA) was employed in the experiments. In this study, OSPW was run through a 0.45 micron filter at the constant pressure of 206.7kPa throughout the test. The SDI 5 minutes was performed with 500 ml sample size test.

Formula for calculating the SDI is as follows:

$$\text{SDI} = (1 - T_{\text{initial}}/T_{\text{final}}) * 100/t$$

T_{initial} : the time to filter initial 500 mL of water

T_{final} : the time to filter final 500 mL of water

t: in this project t is 5 min

3.3.13 *Scanning Electron Microscopy and Energy-dispersive X-ray Spectroscopy*

SEM is a microscopic method that produces a focused beam of high-energy electrons to generate various signals at a solid sample surface (Welton, 2003). It reveals information about the external morphology and composition of a sample. EDX is an analytical technique for identifying the elemental composition or chemical characteristics of material (Welton, 2003). It depends on the observation of an interaction of the excitation of X-ray spectrum in a sample. In this study, membrane surfaces before and after OSPW treatment were analyzed by SEM (Vega3, Tescan Inc., Cranberry, PA, USA) and EDX (Oxford Instruments, Abingdon, UK). Prior to SEM-EDX imaging, membrane specimens were sputter coated with an approximately 10 nm layer of gold to make them electrically conductive.

3.3.14 *Atomic Force Microscopy*

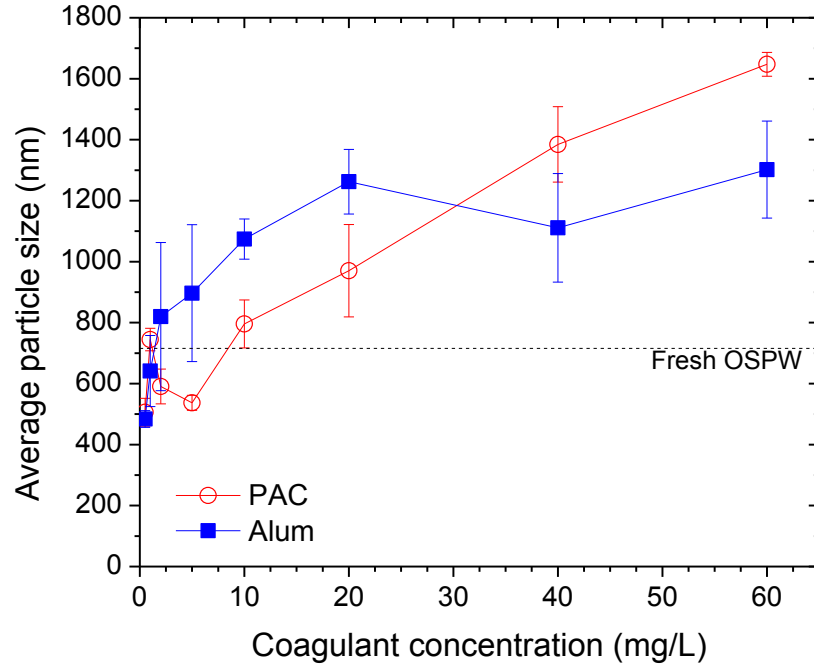
AFM images were obtained using a MFP-3D microscope (Asylum Research, Santa Barbara, CA, USA) in air at a room temperature (22 ± 1 °C) in the tapping mode. A rectangular silicon probe (aluminium reflex coated) with a cantilever spring constant of 42 N/m and a frequency of 300 kHz was used. A nominal tip height was 11 μm with an apex radius of 9 nm and a side angle of 35°. Samples were scanned at a rate of 1.0 Hz at 500 nm depth, with a scan size 20 μm by 20 μm .

CHAPTER 4: RESULTS AND DISCUSSION

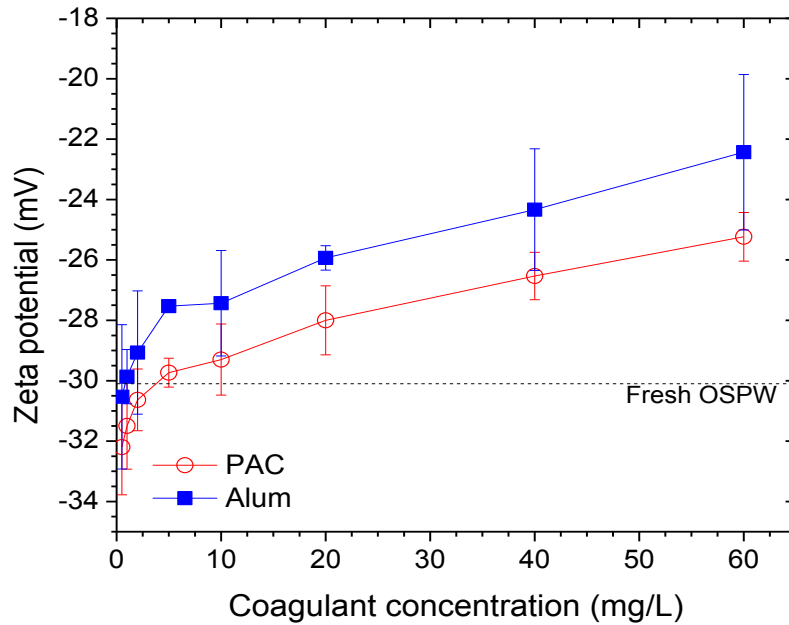
4.1 Optimization of alum and PAC Dose for MF Process

4.1.1 CF Test for Selecting Optimal Doses Of alum and PAC

Fine particulates in OSPW can flocculate and settle naturally, but in a very slow manner due to the high zeta potential of particles, which causes strong interparticles' repulsion forces (Wang, 2011a). Coagulation destabilizes the stable suspensions of particles by reducing zeta potential (Metcalf and Eddy, 2003). Destabilized fine particulates coalesce or adsorb to aluminum hydroxide (Al(OH)_3) precipitates, forming larger flocs which can be easily gravity settled or membrane filtered (Crittenden, 2006; Tansel et al., 1995). In addition, zeta potential of the flocs also affects the attraction forces between the membrane and flocs, which can lead to the build-up of fouling on membrane surfaces (Kim et al., 2007). The effect of PAC and alum concentrations on OSPW average particle size and zeta potential at neutral pH are shown in Figure 4-1.



(a)



(b)

Figure 4-1 (a) Average particle size and (b) zeta potential after coagulation with different doses of PAC and alum at neutral pH.

The average particle size in the raw OSPW is approximately 700 nm. As PAC and alum concentrations increase, average particle size in OSPW increases due to the formation of insoluble metal hydroxides after addition of aluminum-based coagulants (Kim et al., 2011). The ceramic membrane used in this study could reject all particulates over the sizes of 100 nm; therefore alum and PAC concentrations around 10 and 20 mg/L, respectively, could allow the removal of particulates by the ceramic membrane (Figure 4-1a). The charge neutralization of PAC and alum is different; it relies on the ion's valence, hydrolysis products, and coagulant dosages (Aktas, 2013). As alum and PAC concentrations increase, particulate's zeta potentials in OSPW rise from -31 to -22 mV and from -32 to -26 mV for alum and PAC coagulated particles, respectively. Figure 4-2 shows the correlation between the zeta potential of unmodified ceramic membrane and solution's pH. The outcome of membrane fouling depends on the balance between electrostatic interaction and hydrophobic/hydrophilic interaction between membrane and fouling materials (Liu et al., 2001). Electrostatic interaction results from the surface charges of membrane and fouling, and hydrophobic interaction originates from the Van der Waals attractive force between two moleculars when they approach each other. Therefore, electrostatic repulsive force is a principal mechanism to keep membrane and foulants apart (Liu et al., 2001). The unmodified ceramic membrane is positively charged at neutral pH, while the zeta potential of the OSPW solid matters is negative at the same pH (i.e., -30.1mV in neutral pH). This can lead to a strong electrostatic attraction between the membrane surface and particles. Although increasing the dosage of coagulants can largely lessen these attractive interactions, a high dose of coagulants, on the other hand, can increase operational costs and raise the concern about the environmental impact due to the residual coagulants in OSPW. Thus, using a relatively lower dose of chemical coagulant is beneficial from both environmental and economical points of view. A 10 mg/L of alum and 20 mg/L of PAC appear to be the minimum concentrations enabling optimization of average particle size and zeta potential of coagulated OSPW. Therefore, those concentrations were selected for the conditions of Runs 2 and 3 in membrane filtrations.

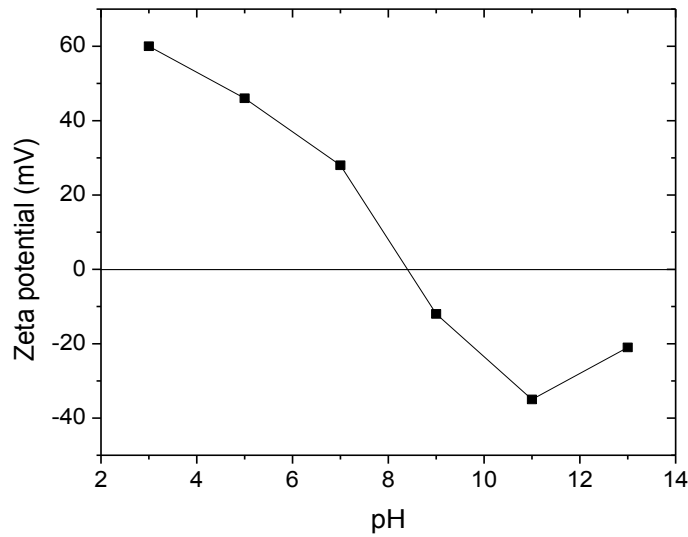
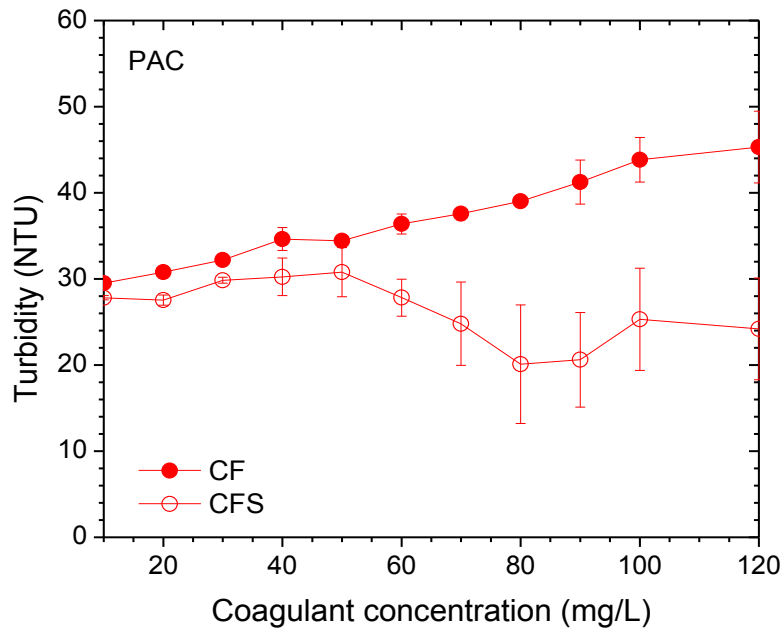


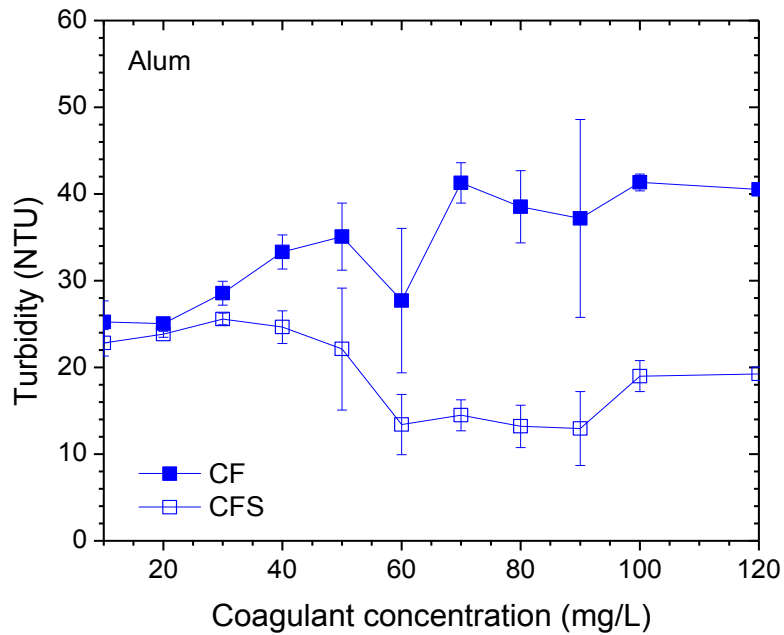
Figure 4-2 Zeta potential of unmodified ceramic membrane at different pHs.

4.1.2 CFS Test for Selecting Optimal Doses of alum and PAC

Figure 4-3 shows the effect of alum and PAC concentrations on OSPW turbidity in the CFS treatment. The optimum concentration of alum and PAC in CFS process is generally determined based on the lowest turbidity of the supernatant after sedimentation (Kim et al., 2011; Pourrezaei et al., 2011). The results show that more than 50% of OSPW turbidity is removed when alum and PAC were applied in the ranges of 60 to 90 mg/L and 80 to 90 mg/L, respectively; beyond these ranges an increase in turbidity occurred. This phenomenon may be resulted from a restabilization of the suspended solids after increasing the concentration of positively charged hydrolysis products (Pourrezaei et al., 2011). Thus, 60 mg/L alum and 80 mg/L PAC are the minimum doses of coagulants which allow for the removal of maximum amount of solids. Comparing coagulant concentrations used in CFS process to the concentration of alum and PAC used in CF-MF process, it is obvious that not only did CF-MF substantially lower the concentration of alum demanded (which is beneficial for both operational cost and environmental impact), but also produced an extremely low turbidity of the effluent (0.8 NTU) (Table 4-2).



(a)



(b)

Figure 4-3 (a) Turbidity versus PAC concentrations after CF and CFS pretreatments; and (b) turbidity versus alum concentrations after CF and CFS pretreatments.

4.2 Unmodified Ceramic Membrane Filtration Performance

4.2.1 Unmodified Membrane Filtration Performance

The membrane filtrations of raw and coagulated OSPWs were evaluated by the changes in TMP over the operation time. The detailed experimental plan is shown in Table 3-3. The TMP in the second stage in Runs 1 to 4 started decreasing at approximately -9 kPa because it had already slightly declined by 2 kPa from -7 kPa during the 11 hours in the first stage as shown in Figures 4-4a, 4-5a, 4-6a, while TMP in Runs 5 and 6 did not change during the first stage (Figures 4-7a and 4-8a). The average turbidity of OSPW at the beginning of all runs was 25.9 NTU (Table 3-1). After the first stage, the feed OSPW was concentrated with the membrane rejects, showing a turbidity two-to-three times higher than the initial OSPW (as shown in the Table of each run in Appendix B). This indicates that the TSS was highly concentrated after the first stage. For all runs, the membrane surface was clean and fouling layer was not visually apparent in the first stage, in the second stage TMP decreased as more particles accumulated on the membrane.

Run 1. MF membrane treatment with raw OSPW. In the Run 1 (Figure 4-4b), two chemical cleanings were performed after 27 and 94 hours of operation. A steep decline in TMP within first 24 hours was observed due to the higher level of deposition of solids on the membrane surface. After first chemical cleaning, 96% of TMP was recovered, and after second chemical cleaning, 90% of the TMP was recovered, suggesting that NaOCl was able to removal almost of irreversible foulants on the membrane surface. But as the time of chemical cleaning increases, the efficiency of chemical cleaning for raw OSPW fouled membrane seemed to be diminished.

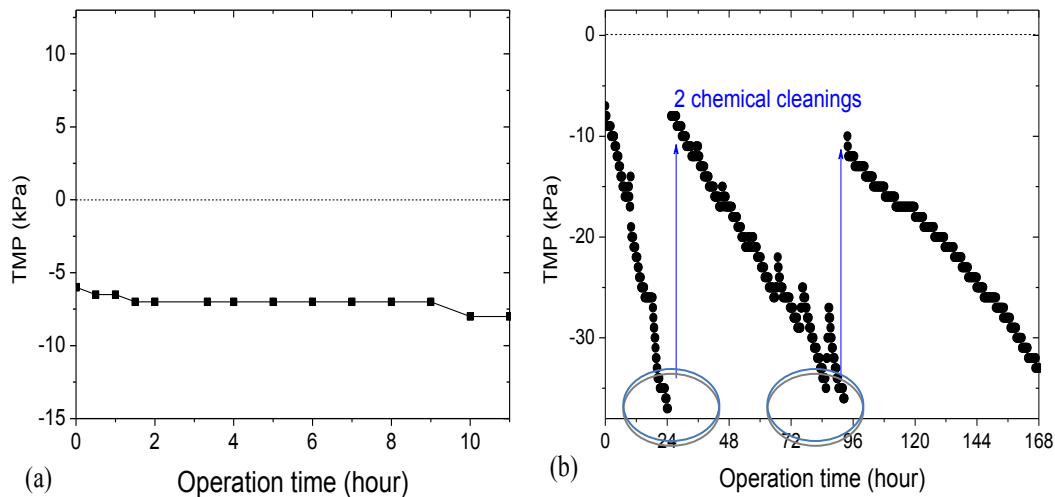


Figure 4-4 Simplified TMP data at (a) first stage and (b) second stage of Run 1. The original TMP data are shown in Figure A1 in Appendix A.

Run 2. CF-MF membrane treatment with 20 mg/L PAC-coagulated OSPW.

Figure 4-5b shows TMP changes during the second stage of Run 2. In the second stage, only one chemical cleaning was performed after 49 hours, and TMP reached -35 kPa at the end of filtration. A 93% recovery of TMP in Run 2 showed that chemical cleaning was capable of restoring the TMP of fouled membrane with PAC-coagulated OSPW. Comparing to Run 1, CF pretreatment in Run 2 contributed to a slow accumulation of membrane fouling and, as a consequence, less frequent demand of chemical cleaning. With the addition of PAC, the rate of TMP decrease slowly declined, which may be attributed to the enlarged size of particles. The use of PAC decreased the adsorption of small particles in the membrane pores and promoted a build-up of a more permeable cake layer than the cake layer formed by the raw OSPW particles (Guigui et al., 2002). The large and porous particles deposited on the membrane surface can also be easily scrubbed away by the automatically generated air bubbles, thus protecting the membrane from foulants (Howe and Clark, 2006). Another possible reason of the membrane fouling reduction is that the zeta potential of OSPW increased with PAC addition, as shown in Figure 4-1b. This resulted in a reduction in attractive forces between the particles and the membrane surface (Crittenden, 2005). The above mentioned

mechanisms led to a decrease in flow resistance, and correspondingly a lower pressure was required for water molecules transport as compared with the higher pressure needed in Run 1.

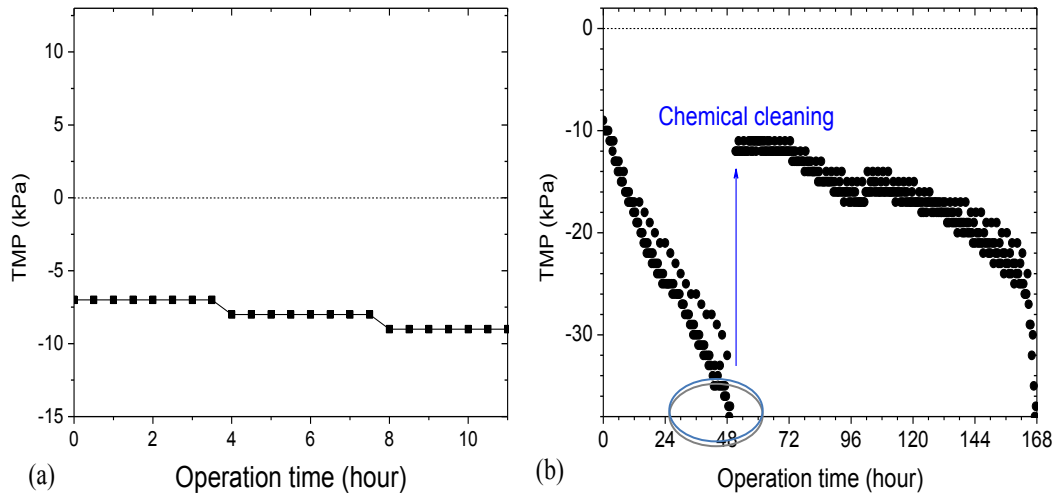


Figure 4-5 Simplified TMP data at (a) first stage and (b) second stage of Run 2. The original TMP data are shown in Figure A2 in Appendix A.

Run 3. CF-MF membrane treatment with 10 mg/L alum-coagulated OSPW.

Run 3 was performed with 10 mg/L alum-coagulated OSPW. Two chemical cleanings were performed after 74 and 144 hours and both chemical cleanings recovered 100% of TMP. After the first chemical cleaning, the TMP gradually dropped to -20 kPa, but it steeply decreased from -20 kPa to -35 kPa in the second stage. This sudden drop in TMP was likely a result of a shift in the position of the air bubbles during membrane filtration. As such, the air bubbles were not able to displace fouling, resulting in a quick accumulation of foulants on the membrane surface. As shown in Figure 4-6b, the rate of TMP decrease in second stage of Run 3 was much slower than in Run 2. Our results demonstrated that 10 mg/L alum-coagulated OSPW particles (Run 3) exhibited similar zeta potentials and average particle size values as 20 mg/L PAC-coagulated OSPW particles (Run 2, shown in Figure 4-1), indicating the observed slow decrease of TMP in Run 3 was

not resulted from the coagulated particle surface charge or average particle size, It is hypothesized that TMP decreasing rate was affected by the membrane's permeability that was directly determined by the coagulated particles' structure (strength and shape). Floc characterization study has shown that alum and PAC form very distinctive solid phases (Wang et al., 2008). PAC-coagulated flocs normally appear as clusters of small spheres or chain-like structures (kegging structure) that are denser than alum precipitates, which are composed of the fluffy and porous structures (hexametric ring structure) of alum hydrolyzed species (Shen, 1992; Bertsch, 1987). From the reported membrane fouling studies, PAC forms a tighter cake layer compared to alum's loose cake layer (Exall, 2011; Harif et al., 2012). With respect to these findings, the difference in the rate of TMP decrease between Runs 2 and 3 may be attributed to the effect of the lower cake formation potential of alum as compared to PAC. Therefore, alum can generate better membrane performance than PAC in terms of TMP decreasing rate. Future characterization of the surface morphology and particular chemical properties of OSPW-fouled membranes by different coagulants should be conducted to clearly understand the mechanism of coagulated OSPW fouling.

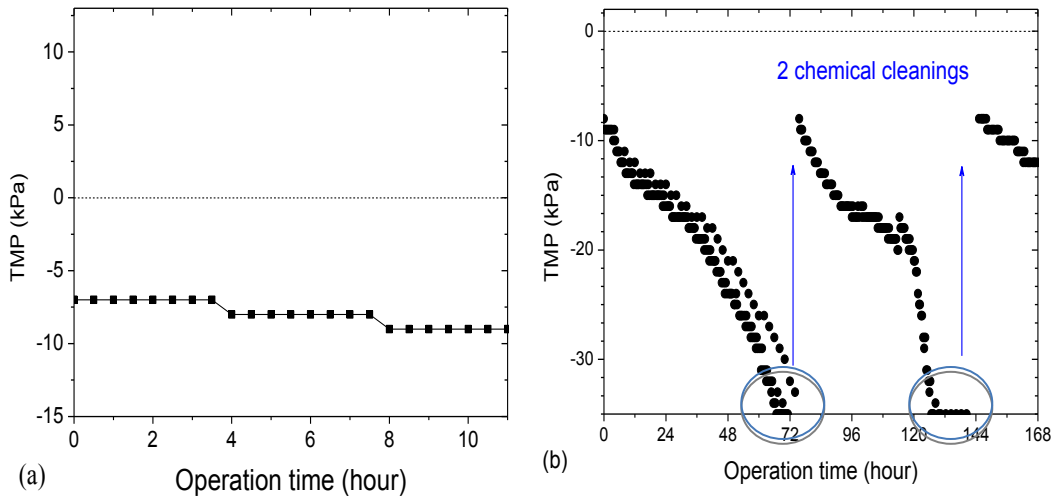


Figure 4-6 Simplified TMP data at (a) first stage and (b) second stage of Run 3. The original TMP data are shown in Figure A3 in Appendix A.

Run 4. CF-MF membrane treatment with 30 mg/L alum-coagulated OSPW.

In order to investigate the effect of higher alum concentration on membrane fouling behavior, the concentration of alum was increased to 30 mg/L. Chemical cleaning was conducted after 102 hours and 96% of TMP was recovered. The TMP changes as a function of operation time are shown in Figure 4-7. A relatively slow decrease in TMP was achieved in Run 4 after increasing the concentration of coagulant. This improvement in membrane performance was mainly arising from the increase in zeta potential of OSPW particles (Figure 4-1b) instead of average particle sizes, as the average particle sizes at both alum concentrations (10 and 30 mg/L) were similar (Figure 4-1a). The zeta potential of alum-coagulated OSPW particles was slightly increased by 12.2%, from -28.5 mV at 10 mg/L alum to -25 mV at 30 mg/L alum (Figure 4-1b). The higher zeta potential of OSPW resulted in a reduction in the attraction of particles to the membrane surface which was positively charged at pH 7-8 (Figure 4-2). But the increase in alum concentration from 10 mg/L to 30 mg/L did not significantly reduce the rate of TMP decrease. Correspondingly, the membrane fouling was less significantly influenced by the alum concentrations.

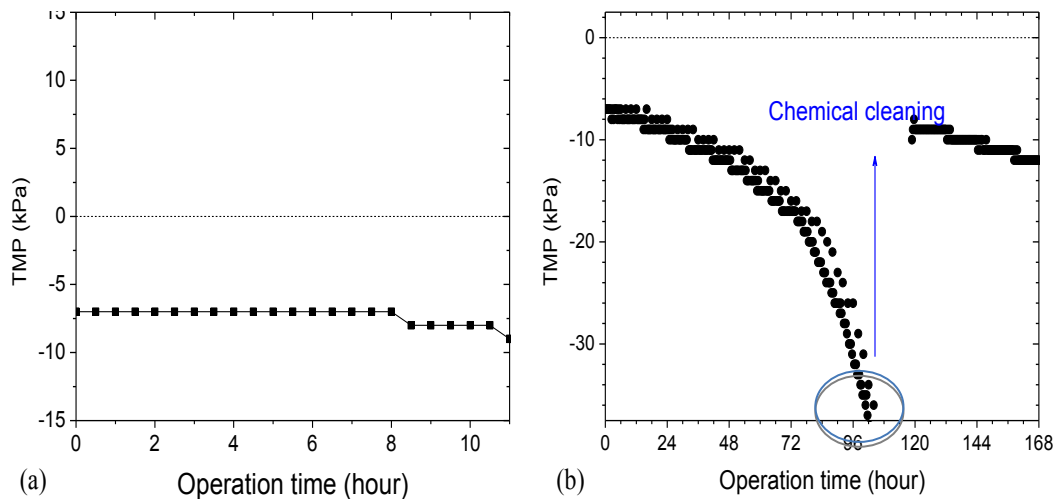


Figure 4-7 Simplified TMP data at (a) first stage and (b) second stage of Run 4. The original TMP data are shown in Figure A4 in Appendix A.

Run 5. CF-MF membrane treatment with 10 mg/L alum-coagulated OSPW at pH 10. It is generally accepted that membrane surface charge can exert a pronounced influence on the membrane fouling and filtration performance (Clark, 1991). To further investigate the relationship between membrane surface charge and membrane fouling, membrane filtration was performed with increasing pH of 10 mg/L alum-coagulated OSPW to 10. The isoelectric point (IEP) of the unmodified ceramic membranes used in this study was found to be between pH 8 to 9. Membrane surface is positively charged at pH below IEP and negatively charged at pH above IEP (as shown in Figure 4-2). The pH of OSPW used in this study is in the range 7 - 8 (Table 3-1). Therefore, the unmodified ceramic membrane would exhibit a positively charged surface in the presence of OSPW and this positively charge resulted in the attractive forces between the negatively charged particles in OSPW and the membrane's surface (Kim et al., 2011). When the pH of feed water was increased to 10, the surface charge of unmodified ceramic membrane was negative. As such, the repulsive forces between the particles and the membrane may lead to a significant decrease in the membrane's fouling.

However, pH changes may influence the value of zeta potential and average particle size of coagulated OSPW, making the optimal coagulant condition no longer suitable for MF at a higher pH (Kim et al., 2006; Slavik et al., 2012; Zhao et al., 2011). Therefore, before conducting Run 5 we examined the zeta potential and average particle size of coagulated OSPW with 10 and 20 mg/L of alum and with 10 and 20 mg/L of PAC at pH 10. These results were compared with the corresponding ones measured at neutral pH before (in Section 4.1.1). Figure 4-8 shows the zeta potential and average particle size of alum- and PAC- coagulated OSPW at pH 7 and 10. Overall, pH showed strong influence on the zeta potential and average particle size of PAC-coagulated OSPW, but had little impact on the zeta potential and average particle sizes of alum-coagulated OSPW. As it can be seen, for 10 mg/L and 20 mg/L of alum, the zeta potentials of OSPW at pH 7 were very similar to the zeta potentials of OSPW at pH 10 (Figure 4-8a), while the average particle sizes of 10 mg/L alum-coagulated OSPW at pH 7 and 20 mg/L alum-coagulated OSPW at pH 7 were relatively decreased after pH increased to 10 (Figure 4-8b). In contrast, higher pH caused a fairly large increase in both zeta potential and average particle size for PAC-coagulated OSPW. Thus, it can be concluded that pH adjustment did not significantly affect the CF with alum.

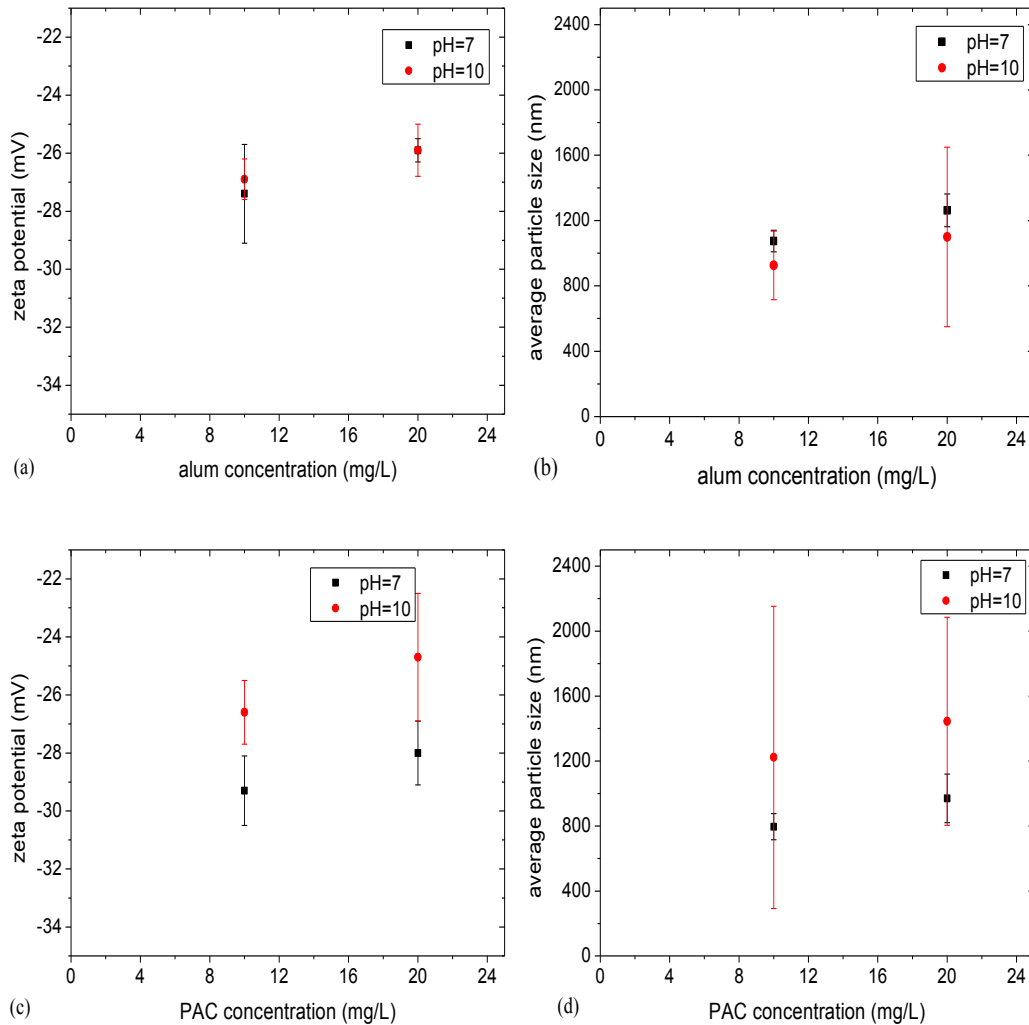


Figure 4-8 Effect of pH on (a) the zeta potential of alum-coagulated OSPW; (b) the average particle size of alum-coagulated OSPW; (c) zeta potential of PAC-coagulated OSPW; (d) average particle size of PAC-coagulated OSPW.

For Run 5, 10 mg/L of alum was applied for CF pretreatment of OSPW and the feed water pH was adjusted to 10. As it can be seen in Figure 4-9a, TMP did not decline during the first stage. Figure 4-9b shows that no chemical cleaning was required during 7 days of the second stage operation. In order to further evaluate the membrane's sustainability with the conditions of Run 5 (i.e., 10 mg/L alum with feed water pH adjusted to 10), the second stage's operation was extended to 11 days (as indicated by the red dashed line in Figure 4-9b). As

expected, the TMP was maintained for considerably longer time in Run 5 than in Run 3 due to the significantly slower fouling accumulation. The TMP dropped to -35 kPa at 228 hours and a 93% recovery of TMP after chemical cleaning indicated that NaOCl was still effective in detaching the fouling layer after longer operation times. It is noted that the high pH and/or long operation time may impact the effectiveness of TMP recovery because a relatively fast decrease in TMP after the chemical cleaning was only observed in Run 5.

Since the zeta potential and average particle size of OSPW particles were not significantly affected by the increasing pH, the reduced affinity between the particles and the membrane surface was a result of decreasing zeta potential of the unmodified ceramic membrane. As shown in Figure 4-2, zeta potential of the membrane surface decreased from 10 mV at the natural OSPW pH to -25 mV at pH 10. It is likely that an electrostatic repulsion was generated between the particles and the membrane surface, which eventually mitigated membrane fouling (Zhang et al., 2009). Correspondingly, membrane fouling was significantly influenced by the unmodified ceramic membrane surface charge.

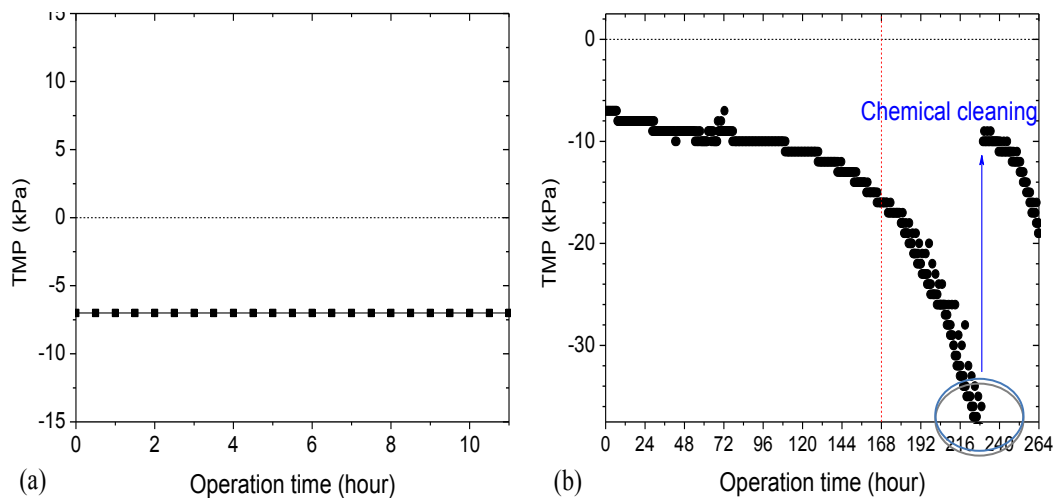


Figure 4-9 Simplified TMP data (a) first stage and (b) second stage of Run 5.

The original TMP data are shown in Figure A5 in Appendix A.

Run 6. CF-MF membrane treatment with 10 mg/L alum-coagulated OSPW at pH 10. Run 6 was conducted under the same operating conditions as Run 5 in order to perform a RO treatment after the MF treatment. In Run 6, the operation was performed for 7 days, and the permeate was used as the feed water for the following RO filtration. As can be seen in Figure 4-10, the TMP decreasing rate within 7 days in Run 6 was in the accordance with the Run 5.

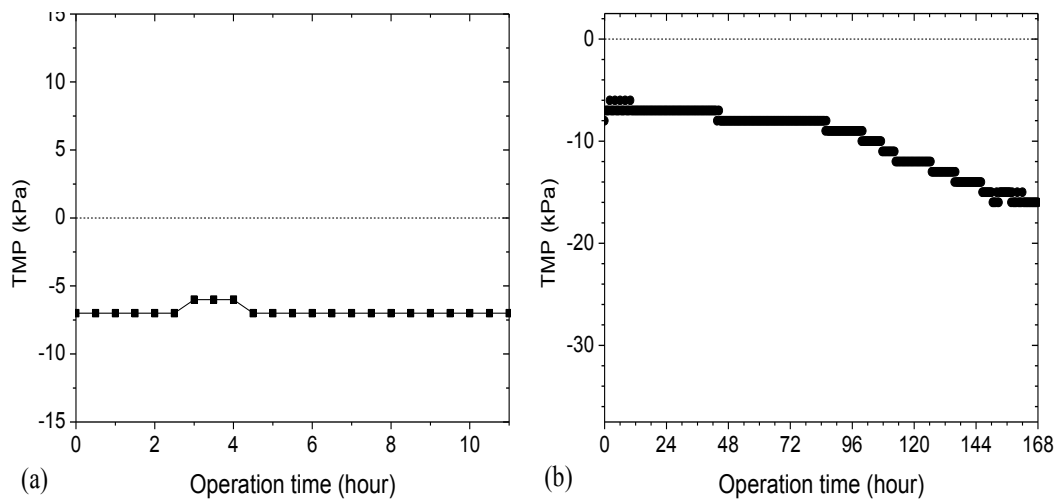


Figure 4-10 Simplified TMP data (a) first stage and (b) second stage of Run 6. The original TMP data are shown in Figure A6 in Appendix A.

4.2.2 Permeate Quality after Unmodified ceramic MF Treatment

Tables 4-1 and 4-2 present MF permeates quality and selected components' removal after first and second stages, respectively. The results show that membrane filtration with unmodified ceramic membrane can achieve satisfactory permeate quality even under high concentration of rejects and high pressure in the second stage. After MF or CF-MF processes, the turbidity, TOC, COD, TSS and SDI₅ of permeates in each run decreased, while other parameters, such as pH, conductivity, TDS, AEF and NAs were maintained at their initial values. No further reduction in each parameter after MF process with CF was observed as

compared to those after the MF process without CF, implying that the influence of CF pretreatment on permeate quality was less significant regardless of coagulants' types or concentrations (Pate, et al., 1994). The removals of TSS and turbidity were more than 93% in each run, indicating that ceramic MF treatment was able to remove a large portion of suspended solids. However, in most cases, MF and CF-MF treatments did not effectively remove the organic species measured as COD or TOC (Tables 4-1 and 4-2). This suggests that the large majority of organic matter was either dissolved in OSPW, thereby was not trapped by coagulant flocs during CF process, or was of a molecular weight too low to be rejected by the membrane pores (Mah and Kotecha, 2011). pH also did not influence the removal of organic and inorganic species because no enhancement in permeate quality was observed in Runs 5 and 6 as compared to other runs. The less removal of organic species in all runs may be due to the insufficient coagulant dose to initiate the sweep flocculation.

The SDI₅ removal was more than 69 % regardless of the CF pretreatment conditions. Raw OSPW has a SDI₅ of 6.25 and therefore it could not be directly applied as a feed to the RO system. With the CF-MF pretreatment, SDI₅ of MF effluent was decreased to lower than 2, which is applicable to the direct RO treatment (SDI₅ < 3) (ASTM, 2007). Moreover, in all 6 runs, the SDI₅ and turbidity of permeate after second stage showed lower values than the corresponding SDI₅ and turbidity of permeate after (Tables 4-1 and 4-2). It is likely because solids that were smaller than the membrane pore sizes were removed by a cake of larger particles that was formed on the membrane surface in second stage (Crittenden, 2005; Gao et al., 2011). As mentioned in Section 4.2.1, membrane's fouling after first stage was not visually apparent, and the slight decrease in TMP during 11 hours of operation may imply that the cake layer was not formed in first stage, which led to the slightly higher turbidity and SDI₅ values (Gao et al., 2011). However, Run 6 showed unexpected higher values of SDI₅ and turbidity after second stage than after first stage. This may be caused by the experimental error during the measurement of SDI₅ and turbidity.

Table 4-1 MF permeate quality and removal of selected components after first stage of 6 runs (all water quality parameters tested for raw OSPW, permeate after first, second and during second stage in 6 membrane filtration runs are shown in Appendix B).

		Turbidity, NTU	TOC, mg/L	COD, mg/L	TSS, mg/L	SDI ₅
Run 1	Feed, mg/L	25.33	41.40	124.00	22.17	6.22
	Permeate, mg/L	0.96	36.23	112.33	1.00	1.89
	Removal, %	96.20	12.49	9.41	95.49	69.61
Run 2	Feed, mg/L	24.05	40.00	144.60	16.06	6.73
	Permeate, mg/L	1.06	34.40	131.33	0.00	2.01
	Removal, %	95.60	14.00	9.18	100.00	70.13
Run 3	Feed, mg/L	29.50	42.20	145.30	19.20	6.36
	Permeate, mg/L	0.75	39.2	134.7	0.00	1.85
	Removal, %	96.80	7.11	7.30	100.00	69.30
Run 4	Feed, mg/L	24.63	41.71	138.67	21.17	6.15
	Permeate, mg/L	0.79	35.18	125.33	1.00	1.89
	Removal, %	96.78	15.65	9.62	100.00	69.27
Run 5	Feed, mg/L	26.23	41.40	128.33	22.00	5.92
	Permeate, mg/L	0.92	38.45	122.00	1.33	1.98
	Removal, %	96.49	7.13	4.93	93.95	66.55
Run 6	Feed, mg/L	23.73	40.57	126.67	26.67	6.10
	Permeate, mg/L	0.62	36.05	117.00	1.75	1.64
	Removal, %	97.39	11.14	7.63	93.44	73.11

Table 4-2 MF permeate quality and removal of selected components after second stage of 6 runs (all water quality parameters tested for raw OSPW, permeate after first, second and during second stage in 6 membrane filtration runs are shown in Appendix B).

		Turbidity, NTU	TOC, mg/L	COD, mg/L	TSS, mg/L	SDI ₅
Run 1	Feed, mg/L	25.33	41.40	124.00	22.17	6.22
	Permeate, mg/L	0.68	36.11	114.33	1.50	1.52
	Removal, %	97.30	12.78	7.80	93.23	75.56
Run 2	Feed, mg/L	24.05	40.00	144.60	16.06	6.73
	Permeate, mg/L	0.90	35.77	133.50	0.00	1.44
	Removal, %	96.26	10.58	7.68	100.00	78.60
Run 3	Feed, mg/L	29.50	42.20	145.30	19.20	6.36
	Permeate, mg/L	0.92	39.2	139	0.00	1.35
	Removal, %	96.88	7.11	4.30	100.00	78.90
Run 4	Feed, mg/L	24.63	41.71	138.67	21.17	6.15
	Permeate, mg/L	0.63	34.90	126.67	0.00	1.30
	Removal, %	97.44	16.33	8.65	100.00	78.86
Run 5	Feed, mg/L	26.23	41.40	128.33	22.00	5.92
	Permeate, mg/L	0.61	36.93	121.50	0.67	1.29
	Removal, %	97.67	10.80	5.32	96.95	78.21
Run 6	Feed, mg/L	23.73	40.57	126.67	26.67	6.10
	Permeate, mg/L	0.77	36.05	117.00	1.75	n/a
	Removal, %	96.76	9.19	5.27	95.31	n/a

n/a: not available

4.2.3 *Permeate Quality Analysis after RO Treatment*

As shown in Table 4-3, RO treatment achieved high removal of organic species in the OSPW as measured by TOC, COD, AEF, and NAs; the reductions in TOC and COD were 98.0% and 100.0%, respectively. The most toxic components in OSPW, NAs, were removed by 99.3% which coincides with the 100% removal of AEF. Meanwhile, inorganic components (i.e., conductivity and TDS) were removed from the raw OSPW by more than 98.0%. The residual ions in RO permeate primarily consisted of chloride and sodium, having concentrations of 40.1 mg/L and 20.9 mg/L respectively. The removals of chloride and sodium were 96% and 97%, respectively; this follows the typical removals of monovalent ions during the RO membrane treatment (> 95.0) (Kim et al., 2012b). The results of RO filtration demonstrated that the combined treatment of RO and MF generated a highly qualified permeate with respect to the overall removal of organic and inorganic compounds. Thus, the optimized CF-MF process can be applied as an effective OSPW pretreatment to reduce suspended solids and SDI₅ contents prior to RO treatment.

Table 4-3 The removal of organic and inorganic compounds after RO treatment.

Parameter	Removal, %
Conductivity, $\mu\text{S}/\text{cm}$	98.2
Turbidity, NTU	98.6
TOC, mg/L	98.0
COD, mg/L	100.0
TDS, mg/L	98.1
AEF, mg/L	100.0
NAs, mg/L	99.3
Magnesium, mg/L	96.6
Calcium, mg/L	99.0
Iron, mg/L	100.0
Manganese, mg/L	100.0
Silicaon, mg/L	98.0
Fluoride, mg/L	94.6
Chloride, mg/L	96.0
Sulfate, mg/L	98.6
Nitrate, mg/L	100.0
Sodium, mg/L	97.0
Potassium, mg/L	95.2

4.2.4 *Unmodified Ceramic Membrane Surface Characterization*

Bare membrane and fouled membranes after Runs 3, 4 and 6 were analyzed by the SEM-EDX. The TMPs at the end of Runs 3, 4 and 5 were -12, -12 and -16 kPa, respectively. Figure 4-11 presents SEM images of the tested membranes. As it can be seen in Figure 4-11a, coarse grains of Al_2O_3 were well distributed on bare ceramic membrane surface. Fouled membranes treated with coagulated OSPW had an obvious formation of a fouling layer and an aggregation of particles on the membrane surface (Figures 4-11b, 4-11c and 4-11d).

Compared to the bare membrane, all OSPW-fouled membranes were completely covered with foulants. Deposition of large aggregates was observed on the surfaces of fouled membranes from Runs 3 and 4 (Figures 4-11b and 4-11c). This was probably due to the strong attraction of positively charged membrane surface to foulants. On the other hand, fouled membrane from Run 6 (Figure 4-11d) had a flatter and smoother surface than the other two membranes. Though relatively higher TMP (-16 kPa) at end of Run 6 than that of Runs 3 and 4 (both -12 kPa) implied that more fouling was accumulated on the membrane surface after Run 6, no visible large aggregates were adhered to this membrane. This may be due to the lower attraction of membrane surface to foulants at higher pH feed water. The higher final TMP in Run 6 was likely due to a consecutive 7 days of membrane filtration with no chemical cleaning (Figure 4-10). In contrast, membranes from Runs 3 and 4 both experienced chemical cleanings after TMP reached -35 kPa (Figures 4-6 and 4-7). The differences in membrane fouling morphology between Run 6 and Runs 3 and 4 may demonstrate that the less accumulation of particle aggregates led to a slow TMP decrease during membrane filtration which eventually extended the membrane performance and reduced frequency of chemical cleanings.

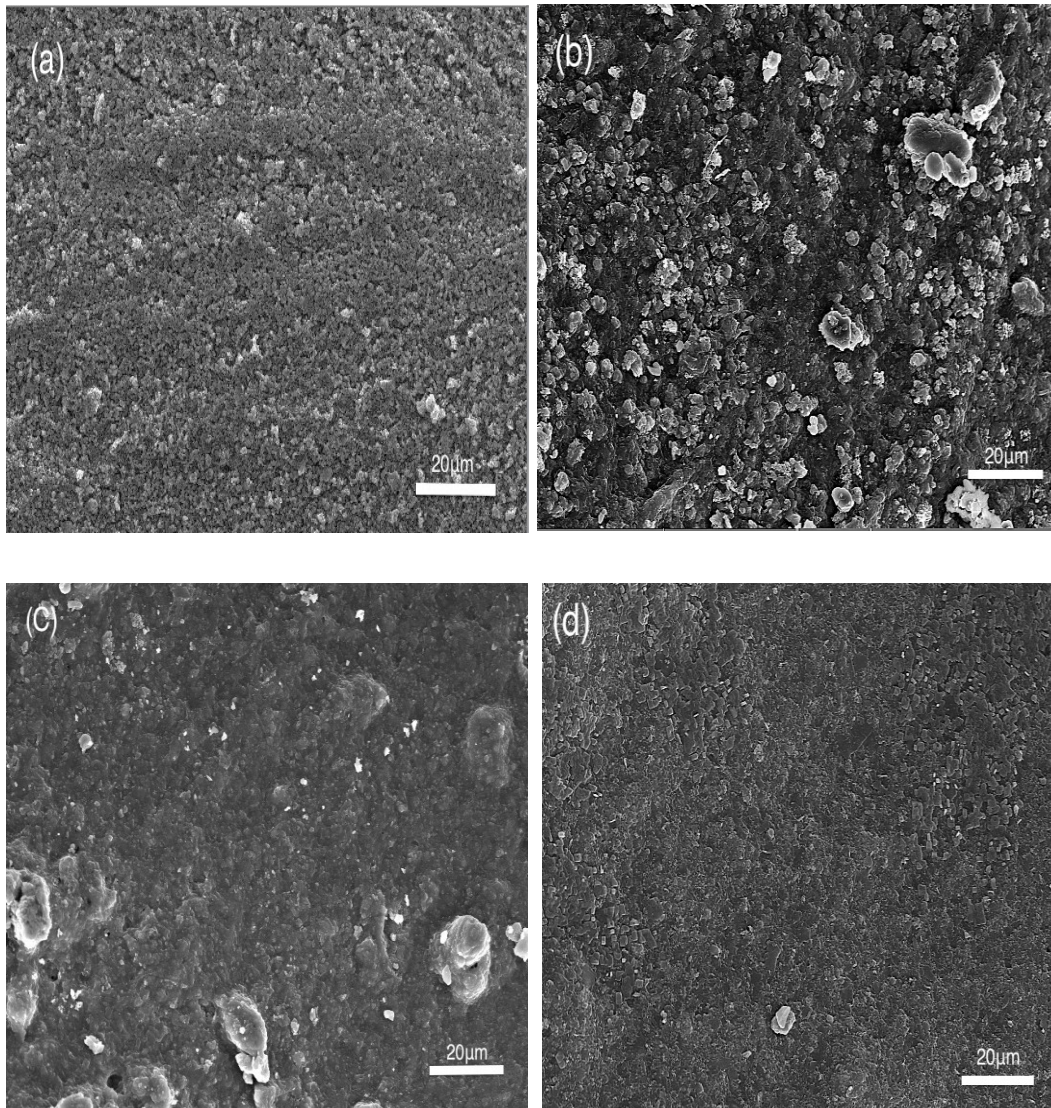
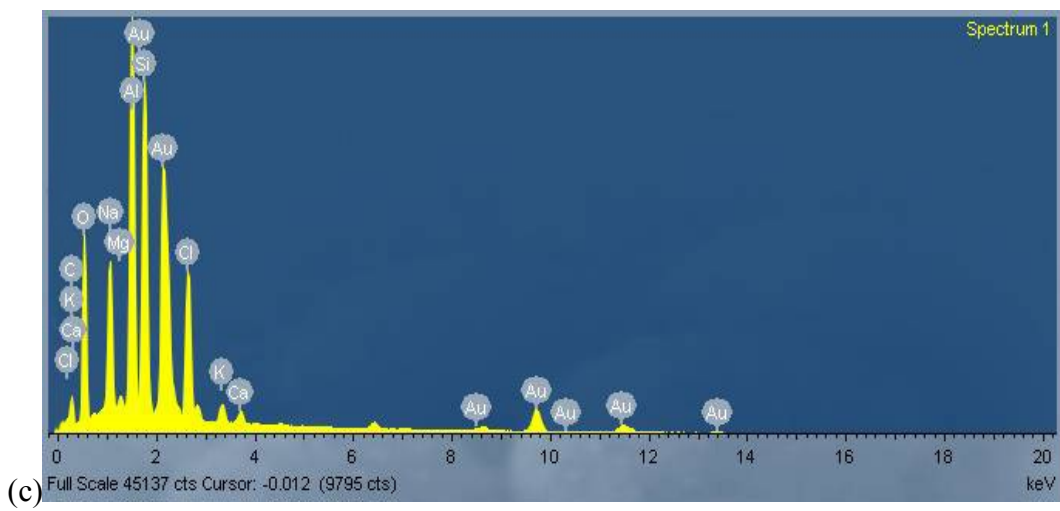
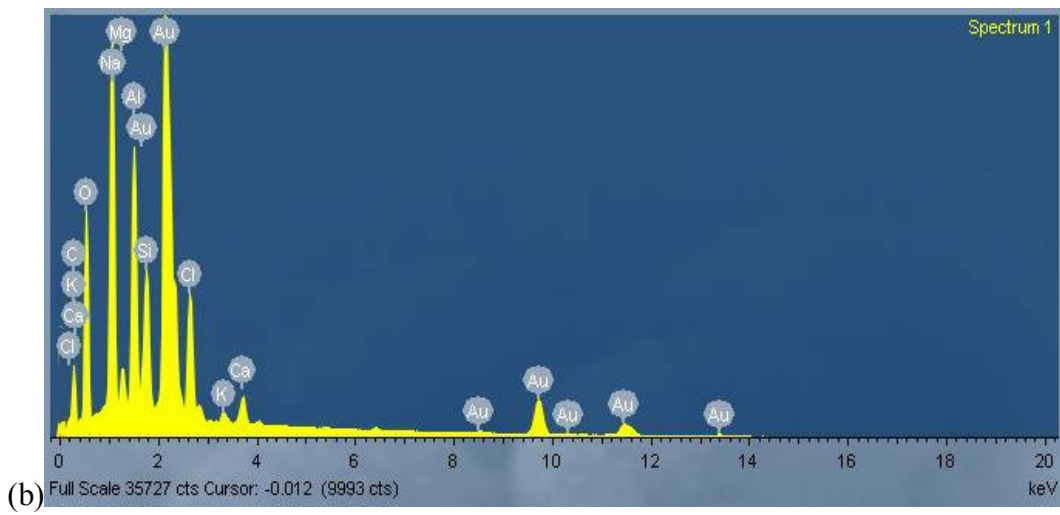
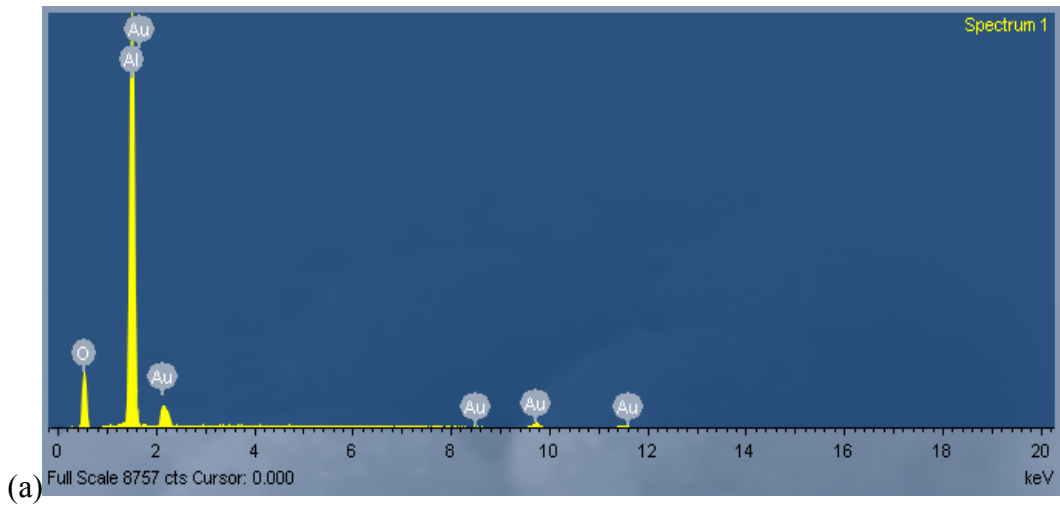


Figure 4-11 SEM images of (a) bare membrane; (b) membrane treated with 10 mg/L alum-coagulated OSPW; TMP at end of filtration was -12 kPa (Run 3); (c) membrane treated with 30 mg/L alum-coagulated OSPW; TMP at end of filtration was -12 kPa (Run 4); and (d) membrane treated with 10 mg/L alum-coagulated OSPW at pH 10; TMP at end of filtration was -16 kPa (Run 6).

Figure 4-12 shows the EDX spectrums of bare and fouled membranes from Runs 3, 4 and 6. The atoms showed in the EDX spectrum represent the composition of ceramic membrane and the membrane foulants. Aluminum and gold (Au) were the most abundant components, due to the composition of the ceramic membrane (i.e., Al_2O_3), coagulants (i.e., $\text{Al}_2(\text{SO}_4)_3 \cdot 18\text{H}_2\text{O}$ and $\text{Al}_2(\text{OH})_n\text{Cl}_{6-n}$) and surface coating (Au). Figure 4-12a shows the bare membrane surface's composition. Bare ceramic membrane was only comprised of aluminum and oxygen. Due to membrane fouling, all three fouled membranes showed various atoms on the surface, including silica, sodium, calcium, potassium, magnesium and carbon. These atoms were originated from the composition of the solid species within the OSPW, such as kaolinite ($\text{Al}_2\text{Si}_2\text{O}_5(\text{OH})_4$), illite ($((\text{K},\text{H}_3\text{O})(\text{Al},\text{Mg},\text{Fe})_2(\text{Si},\text{Al})_4\text{O}_{10}[(\text{OH})_2,(\text{H}_2\text{O})])$) and montmorillonite ($((\text{Na},\text{Ca})_{0.33}(\text{Al},\text{Mg})_2(\text{Si}_4\text{O}_{10})(\text{OH})_2 \cdot n\text{H}_2\text{O})$) which have shown to be the primary constituents of clay in oil sands (Chalaturnyk et al., 2002; FTFC, 1995) (Figures 4-12b, 4-12c and 4-12d). These atoms presented at high intensity in EDX spectrum of fouled membranes from Runs 3 and 4 (Figures 4-12b and 4-12c). Therefore, the identified membrane foulants mainly consisted of the solid particles in OSPW. As mentioned above in Section 4.2.2, membrane filtrations achieved significantly lower TOC and COD removals (Table 4-2), indicating that organic substances dissolved in OSPW could rarely be retained by membrane. Therefore carbon (C) atoms that were detected at relatively lower intensity by EDX might stem from carbonate ions or/and organics that adhered to the particles rather than from the dissolved organic substances.

Fouled membrane from Run 6 presented the most “clean” membranes surface. In comparison to the fouled membranes from Runs 3 and 4 (which exhibited very similar composition of atoms), the intensity of calcium, sodium and potassium atoms on fouled membrane from Run 6 was lower and no potassium atoms was detected. Based on the comparisons of SEM images of Runs 3, 4 and 6, it is speculated that the significantly lower intensity of atoms may be ascribed to the less accumulation of particle aggregates. Therefore, membrane surface charge could significantly impact membrane fouling behavior.



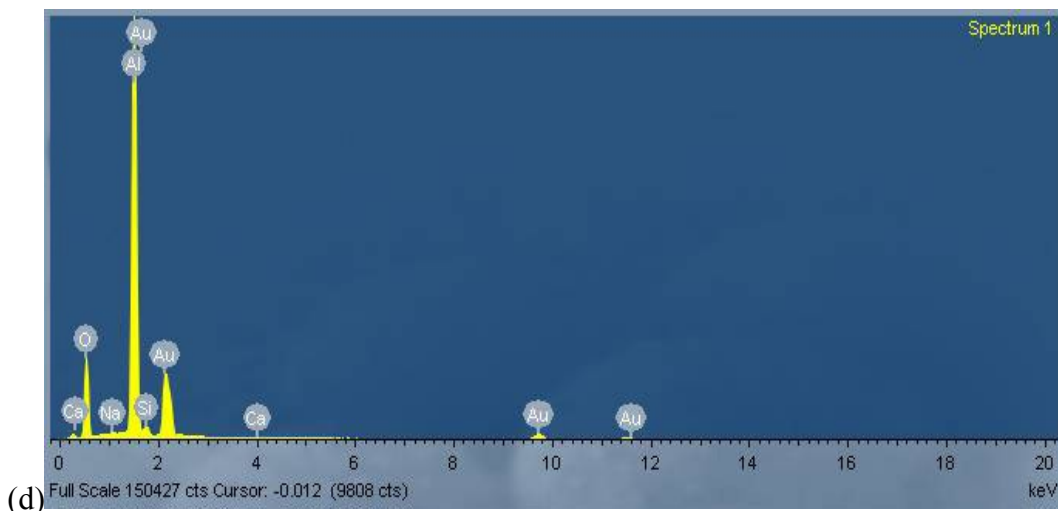


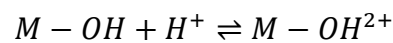
Figure 4-12 EDX spectrums of (a) bare membrane; (b) membrane treated with 10 mg/L alum-coagulated OSPW; TMP at end of filtration was -12 kPa (Run 3); (c) membrane treated with 30 mg/L alum-coagulated OSPW; TMP at end of filtration was -12 kPa (Run 4); and (d) membrane treated with 10 mg/L alum-coagulated OSPW at pH 10; TMP at end of filtration was -16 kPa (Run 6).

4.3 Surface Modified Ceramic Membrane Filtration Performance

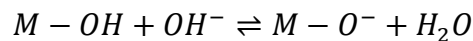
4.3.1 Modified Membrane Filtration Performance

To investigate the effect of the membrane surface charge on the membrane fouling behavior, SiO₂- and TiO₂-modified ceramic membranes were selected for further experiments. Membrane filtrations through two modified membranes treated with 10 mg/L of alum-coagulated OSPW (in the same condition as Run 3) were conducted in Runs 7 and 8. The pH dependence of the zeta potential of two new modified membranes is shown in Figure 4-13. The results show that surface zeta potential values of two modified membranes were significantly decreased as compared to the unmodified ceramic membrane. The IEPs for unmodified membrane and TiO₂-modified membrane were around 8.2 and 4.0, respectively; while the IEP of SiO₂-modified membrane was outside the tested pH range. This finding is consistent with other studies that showed that the IEP of Al₂O₃ particles

range within 6.9-10.5, whereas IEP of SiO₂ and TiO₂ particles range within 1.9 - 4.5 and 3.8 to 7.2, respectively (Yoko et al., 1988; Zhong and Clark, 1993). Surface charge of metal oxide (e.g. silica and titania) is pH dependent (McCafferty and Wightman, 1997; Tamura et al., 1999). Their surface charge relies on the reactivity of surface functional group (hydroxyl groups) with potential-determining ions in the solution (Cornell and Schwertmann, 2003). Hydroxyl groups can become hydrated or hydroxylated in the solution through acquiring hydrogen ions and hydroxide ions from aqueous solutions, respectively. If solution's pH is lower than the IEP, hydrogen ions will be the potential-determining ions on the membrane surface, resulting in a positive surface charge;



If the pH is higher than the IEP, hydroxide ions will be the potential-determining ions on the membrane surface, resulting in a negative charge.



The hydroxylation ability of hydroxyl groups on SiO₂ and TiO₂ surfaces is higher than the ability of hydroxyl groups on Al₂O₃ surfaces (McCafferty and Wightman, 1997; Tamura et al., 1999; Zhang et al., 2009). Thus SiO₂ and TiO₂ surfaces tend to be negatively charged in relatively low pH solutions (Zhang et al., 2009). Therefore, when Al₂O₃-based ceramic membranes were coated with SiO₂ or TiO₂, the IEP of membrane surface would shift towards lower pHs. Aside from zeta potential changes after surface coating, the modified and unmodified ceramic membranes had similar particles retention, porosity and the thickness of membrane active layer as listed in Table 3-2.

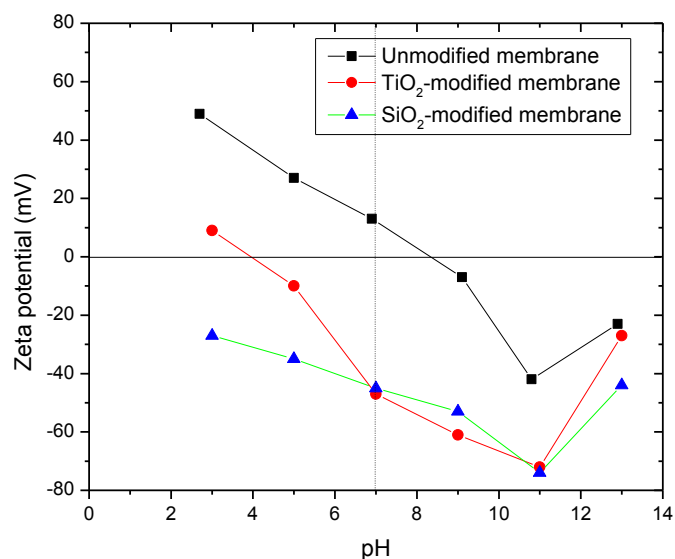
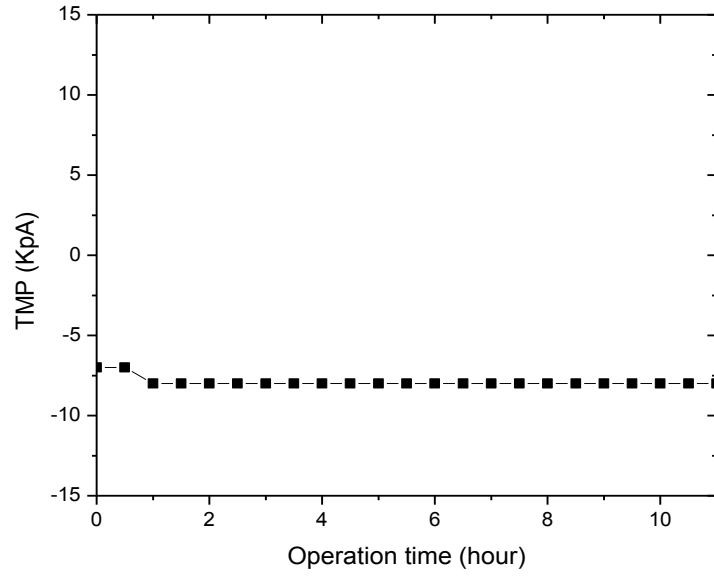
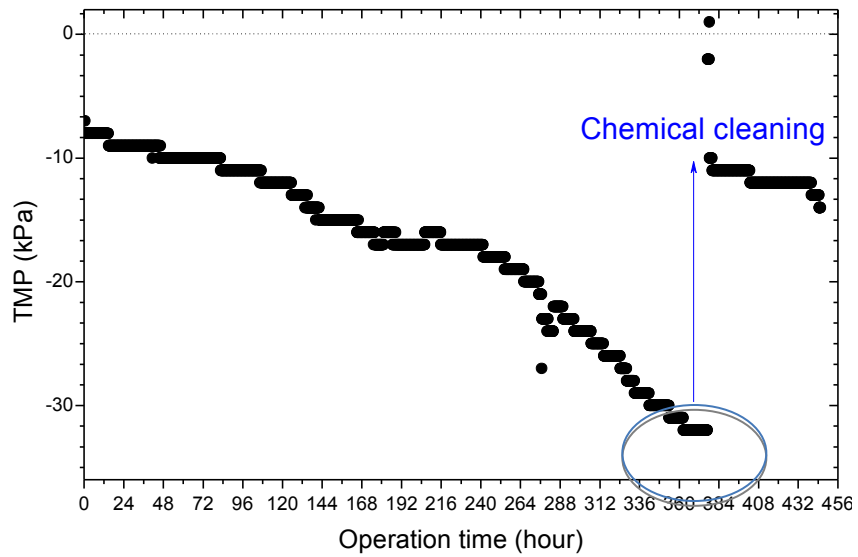


Figure 4-13 Membrane zeta potential as a function of solution pH for tested ceramic membranes.

Run 7. SiO₂-modified membrane treated with 10 mg/L alum-coagulated OSPW. For SiO₂-modified membrane, TMP was retained at -8 kPa during the first stage, with a slightly higher value of TMP (-7 kPa) observed at the beginning of the first stage due to the system's instability (Figure 4-14a). In the second stage, TMP decreasing rate was significantly reduced in contrast to that of unmodified membrane at the same filtration condition (Figure 4-6). This phenomenon was expected because SiO₂-modified membrane and particles in OSPW at pH 7-8 are both negatively charged. The negative charge of modified membrane promoted the repulsive interactions between the particles and membrane thus inhibiting the deposition of particles on the membrane surfaces. Therefore, a stable TMP through the filtration process was achieved. Chemical cleaning was performed for SiO₂-modified membrane after 384 hours (16 days) of membrane filtration. A 92.3% of TMP of SiO₂- modified membrane was restored after chemical cleaning. This result showed that NaClO was still effective in removing irreversible fouling from surface- modified ceramic membrane.



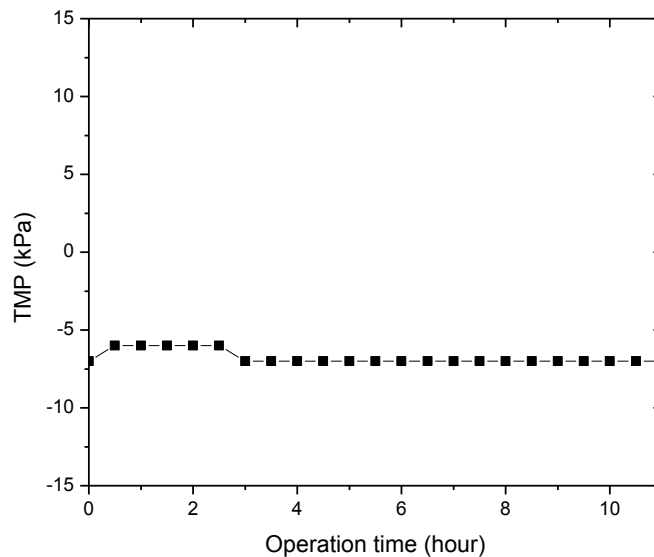
(a)



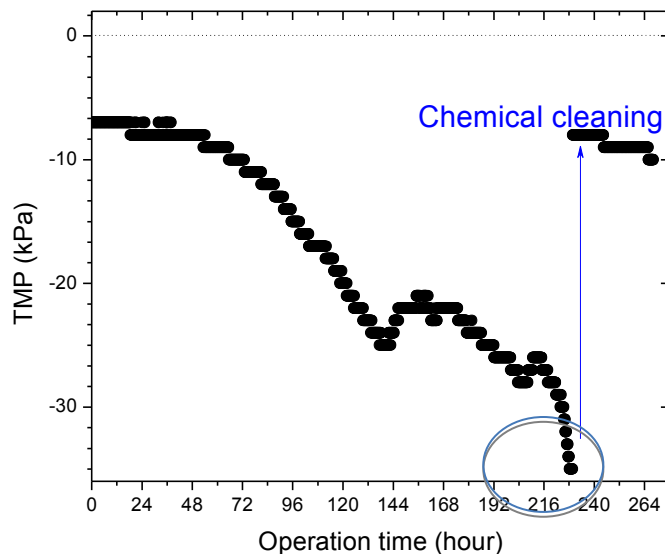
(b)

Figure 4-14 Simplified TMP data at (a) first stage and (b) second stage of Run 7 (SiO_2 -modified ceramic membrane). The original TMP data are shown in Figure A7 in Appendix A.

Run 8. TiO_2 -modified membrane treated with 10 mg/L alum-coagulated OSPW. Figure 4-15 shows TMP changes as a function of operation time for TiO_2 -modified membrane. Same as Run 7, TMP in Run 8 fluctuated initially but eventually stabilized at -7 kPa during the first stage. In the second stage, chemical cleaning was performed after 228 hours (9.5 days) of membrane filtration. Membrane achieved 96.5% of TMP recovery. It is noticed that an unexpected steep decline occurred at the end of this run. This may be due to the shift of the air scrubbing which resulted in a fast fouling accumulation. The improvement of TiO_2 -modified membrane performance was also because of the decrease in the membrane's surface charge. However, although two modified membranes exhibited similar negative zeta potential values within pH range of 7-8 (Figure 4-13), the rates of TMP decrease in two filtration runs were substantially different. It indicates that for OSPW filtration through surface-modified membranes, membrane surface charge may not be the primary factor that was accounted for the membrane fouling behavior.



(a)



(b)

Figure 4-15 Simplified TMP data at (a) first and (b) second stage of Run 8 (TiO₂-modified ceramic membrane). The original TMP data are shown in Figure A8 in Appendix A.

4.3.2 Surface Roughness of Unmodified and Modified Membranes

In order to elucidate the effect of membrane roughness on membrane fouling behavior, membrane surface roughness measurements were conducted. AFM images of bare unmodified and two modified ceramic membranes are shown in Figure 4-16 and revealed the different extents of the surface roughness. Physical parameters, including root mean square (RMS), roughness average deviation (R_a) and maximum peak-to-valley obtained from AFM analysis are presented in Table 4-4.

Unmodified membrane shows a rough surface (Figure 4-16a), with RMS, R_a and maximum peak-to-valley distance of 203.906 nm, 162.56 nm and 1174.19 nm, respectively, whereas SiO₂-modified ceramic membrane surface differed distinctively from the unmodified ceramic membrane. It is recognized that surface modification influences the roughness of ceramic membranes (Kim and Bruggen,

2010). Corneal et al. (2010) reported that the maximum peak-to-valley height of a surface modified ceramic membrane was reduced as a result of the coating materials filling the valleys between two peaks. As it can be seen in Figure 4-16b, SiO₂-modified membrane shows a smoother surface than unmodified membrane. The maximum peak-to-valley slightly decreased from 1174.192 to 1164.54 nm and RMS decreased from 203.906 to 155.704 nm. TiO₂-modified ceramic membrane, on the other hand, exhibits a similar morphological structure to the unmodified ceramic membrane (Figure 4-16c), but with significantly different roughness values. TiO₂ coating resulted in an increase in RMS from 203.906 to 232.951 nm. R_a and maximum peak-to-valley value of TiO₂-modified ceramic membrane also presented the highest values among all three membranes. The higher surface roughness of TiO₂-modified ceramic membrane was apparently responsible for the more rapid TMP decrease when comparing with the TMP decreasing rate of SiO₂-modified ceramic membrane (Figures 4-14 and 4-15).

Vrijenhoek et al. (2001) investigated the correlation of membrane surface characteristics with the initial rate of colloidal silica fouling and reported the mechanistic reason of the impact of surface roughness on fouling behavior. According to authors, water and particles are prone to convect towards the thinnest section on the active layer, the bottom of valley, because this position offers the lowest resistance to penetration. Therefore, particles are easily accumulated in the valley, as they move towards the center of a valley under the permeation drag forces. Although the bottom of valley will not be completely plugged, it could still substantially constrict the water flow through the membrane, leading to a rapid fouling deposition and TMP decrease during the initial stage of filtration. In direct contrast, a smoother surface has an evenly spaced fouling deposition rather than clogged valleys. As a result, the initial fouling rate will be slower. Therefore, TMP declined slowly during the filtration through SiO₂-modified membrane due to the lower membrane surface roughness than TiO₂-modified membrane.

It is noteworthy to mention that though TiO_2 -modified membrane showed higher roughness than the unmodified membrane, TiO_2 -modified membrane did not lead to a faster rate of TMP decrease (Figure 4-15) as a response to easy accumulation of foulants than unmodified membrane (Figure 4-6). It is possible that membrane fouling was more significantly affected by positive membrane surface charge (unmodified membrane) rather than by surface roughness. Therefore, the negatively charged TiO_2 -modified membrane maintained a stable TMP for 228 hours before TMP dropped to -35 kPa, in contrast to the 72 hours for unmodified membrane.

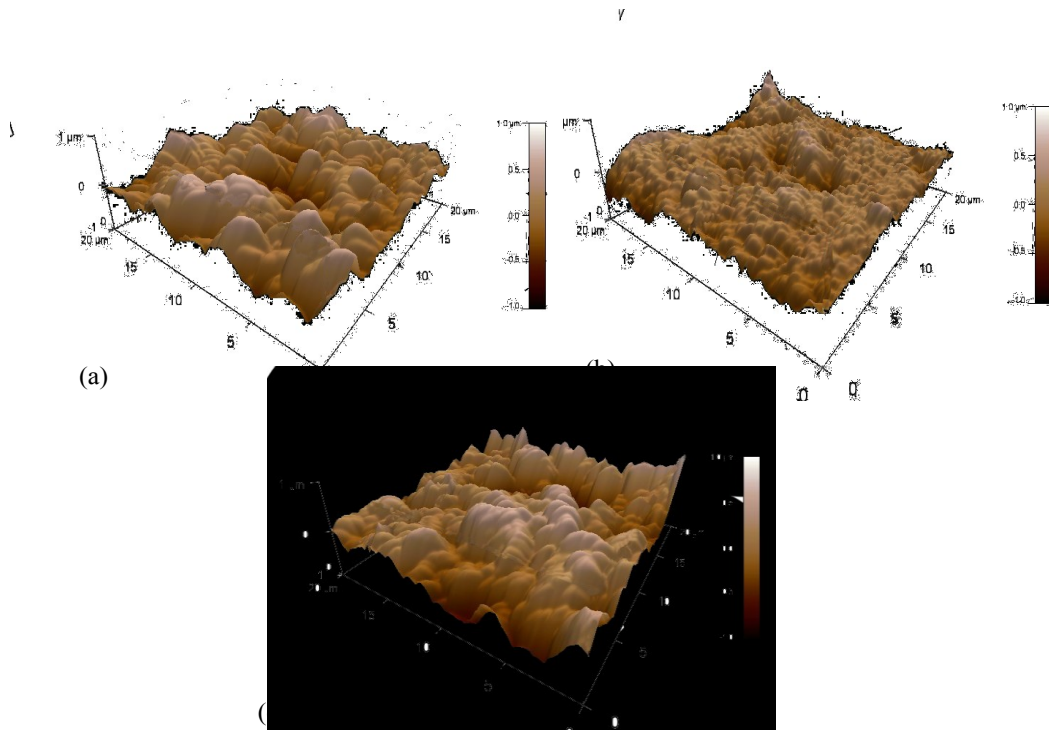


Figure 4-16 AFM images of (a) unmodified ceramic membrane; (b) SiO_2 -modified ceramic membrane; (c) TiO_2 -modified ceramic membrane

Table 4-4 Roughness of unmodified and modified ceramic membranes.

Membrane types	RMS, nm	R _a , nm	Maximum peak-to-valley distance, nm
Unmodified ceramic membrane	203.91	162.56	1174.19
SiO ₂ -modified ceramic membrane	155.70	122.12	1164.55
TiO ₂ -modified ceramic membrane	232.95	188.45	1527.51

4.3.3 Permeate Quality after Modified Membrane Filtration

Tables 4-5 and 4-6 present the MF permeate quality and removal of selected components after first and second stages of filtration through two modified membranes. As shown in Tables 4-5 and 4-6, permeate quality was not improved after filtration through the two modified ceramic membranes as compared to the permeate quality of unmodified ceramic membrane (Tables 4-2 and 4-3). Surface modified membranes also exhibited a high inorganic matter removal and low organic matter removal. For the two modified membranes, turbidity and TSS removals after second stage of membrane filtrations were more than 97%, while the TOC and COD removals were less than 10 %. SDI₅ values in both filtrations were decreased to less than 2 after MF treatment, demonstrating that membrane filtrations through the modified ceramic membranes can still provide an effluent that was applicable to serve as the influent for RO treatment (SDI₅ < 3) (ASTM, 2007).

It is noted that for both modified ceramic membranes, the permeate quality after second stage remained at the same level as the permeate quality after the first stage, despite the substantially longer operation time. The additional solids removal by cake layer formed during the second stage was also observed, as the turbidity and SDI₅ show a consistent decrease after the second stage in both filtrations through the modified membranes.

Table 4-5 MF permeate quality and removal of selected components after first stage of filtrations through two modified membranes (all water quality parameters tested for raw OSPW, permeate after first, second and during second stage in all membrane filtration runs are shown in Appendix B).

	SiO ₂ -modified membrane			TiO ₂ -modified membrane		
	Feed, mg/L	Permeate, mg/L	Removal, %	Feed, mg/L	Permeate, mg/L	Removal, %
Turbidity, NTU	28.50	0.90	96.84	32.50	0.90	97.23
TOC, mg/L	38.20	36.31	4.95	40.90	36.06	11.83
COD, mg/L	124.00	118.00	4.84	127.00	112.67	11.28
TSS, mg/L	22.67	0.00	100.00	21.78	0.00	100.00
SDI ₅	6.20	1.96	68.39	6.08	1.98	67.43

Table 4-6 MF permeate quality and removal of selected components after second stage of filtrations through two modified membranes (all water quality parameters tested for raw OSPW, permeate after first, second and during second stage in all membrane filtration runs are shown in Appendix B).

	SiO ₂ -modified membrane			TiO ₂ -modified membrane		
	Feed, mg/L	Permeate, mg/L	Removal, %	Feed, mg/L	Permeate, mg/L	Removal, %
Turbidity, NTU	28.50	0.76	97.33	32.50	0.72	97.78
TOC, mg/L	38.20	35.43	7.25	40.90	36.82	9.98
COD, mg/L	124.00	117.00	5.65	127.00	116.67	8.13
TSS, mg/L	22.67	0.00	100.00	21.78	0.00	100.00
SDI ₅	6.20	1.41	77.26	6.08	1.90	68.75

4.3.4 *Modified Membrane Surface Characterizations*

Fouling layers on modified membrane surfaces were directly observed by SEM. Figure 4-17 shows the surfaces of bare unmodified membrane, fouled unmodified membrane, bare SiO₂-modified membrane, fouled SiO₂-modified membrane, bare TiO₂-modified membrane and fouled TiO₂-modified membrane. Surface coating did not change the thickness of membrane active layer, porosity and rejection characteristics (Table 3-2), but it is very clearly that for bare membrane, the coating of SiO₂ altered ceramic membrane surface morphology (Figure 4-17c). The SiO₂-modified membrane was fully covered the by small grains of SiO₂ and showed much smoother surface than the unmodified and TiO₂-modified membranes, while TiO₂-modified membrane showed a similar coarsening of the grains to unmodified membrane (Figure 4-17e). The SEM images of three bare membranes were very consistent with the AFM images that showed distinct surface morphology between unmodified and SiO₂-modified membranes and similar morphology between unmodified and TiO₂-modified membranes

For the fouled membranes, very different fouling surfaces were observed. Unmodified membrane showed a very rough surface with the deposition of large particle aggregates (Figure 4-17b). The fouling layers on the surfaces of SiO₂- and TiO₂-modified membranes, however, were much flatter (Figures 4-17d and 4-17f), which may be a result of the reduced membrane attraction to particle aggregates. It is hypothesized that the less accumulation of large particle aggregates promoted stable TMPs during filtrations through the two modified membranes (Figures 4-14b and 4-15b) compared to the TMP during filtration through the unmodified membrane (Figure 4-6b). However, to prove this hypothesis, cross-sectional SEM images of fouling membranes should be conducted to determine the thickness of the fouling layers.

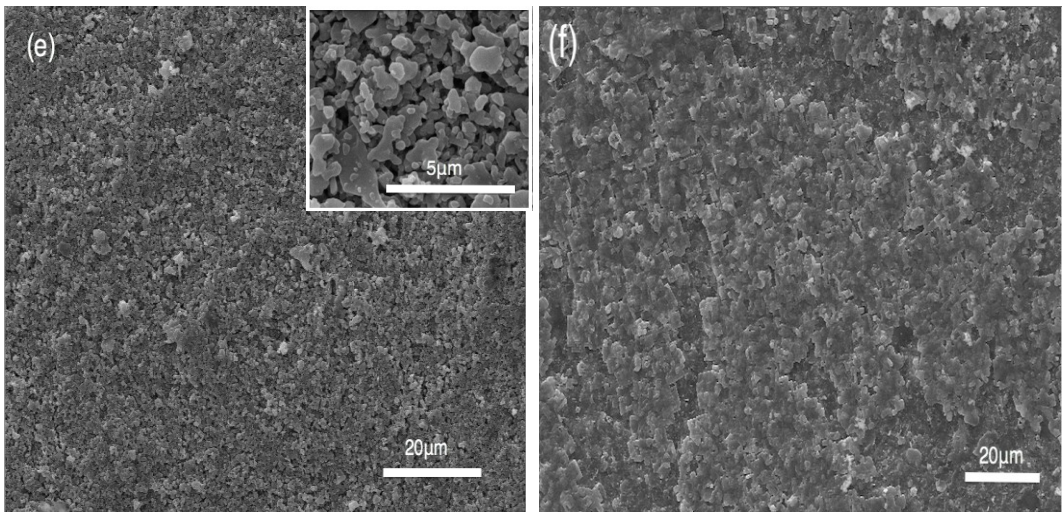
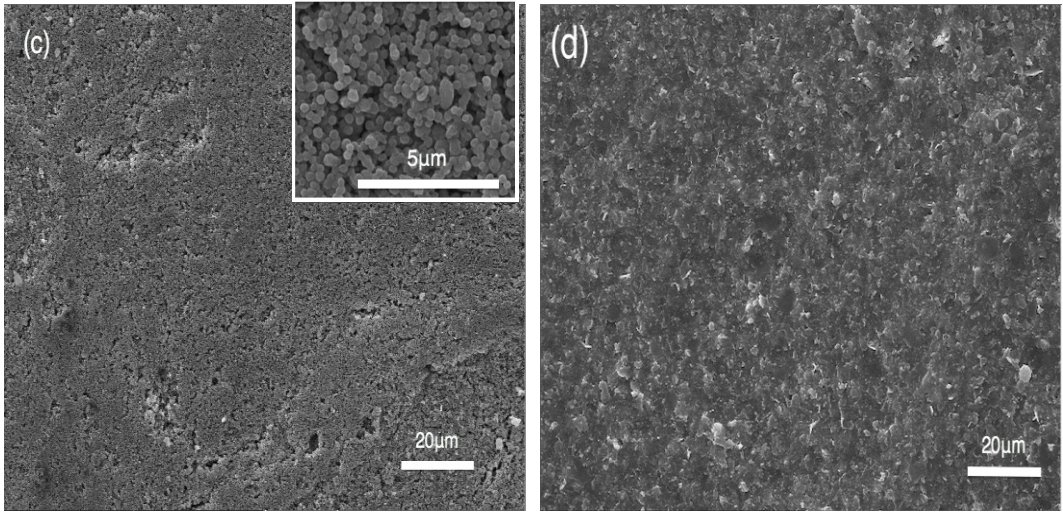
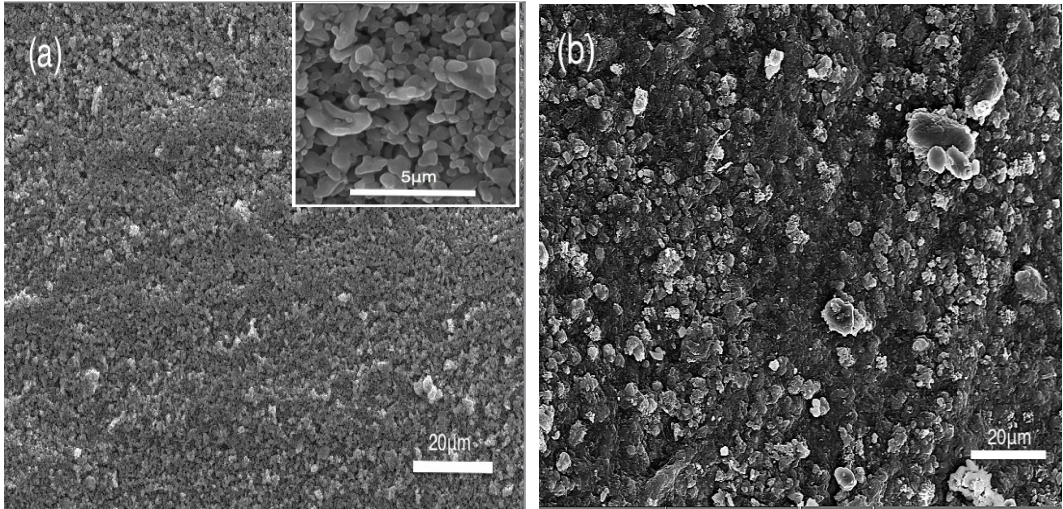
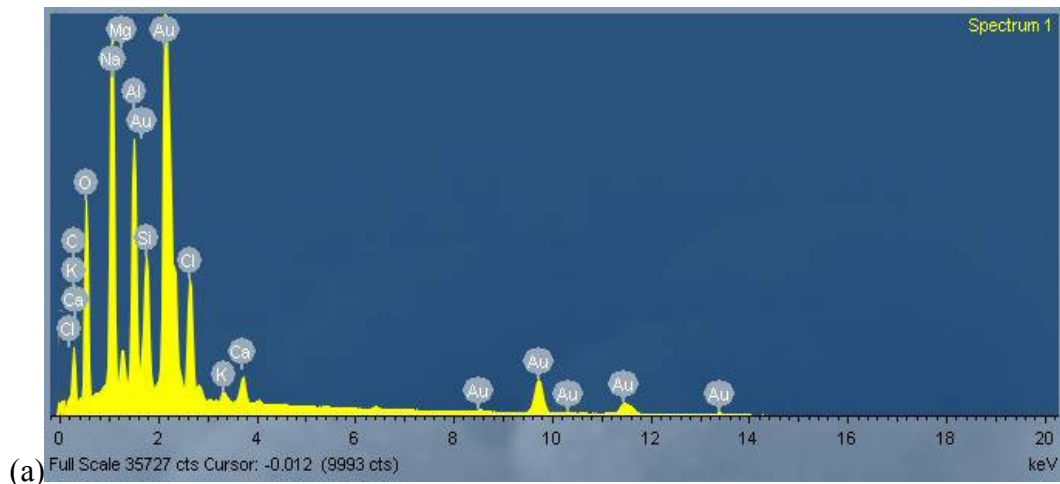


Figure 4-17 SEM images of (a) bare unmodified membrane; (b) fouled unmodified membrane, TMP at the end of filtration was -12 kPa; (c) bare SiO₂-modified membrane; (d) fouled SiO₂-modified membrane, TMP at the end of filtration was -16 kPa; (e) bare TiO₂-modified membrane; (f) fouled TiO₂-modified membrane, TMP at the end of filtration was -11kPa; All three membranes were treated with 10 mg/L alum-coagulated OSPW.

The EDX spectra of fouled modified and unmodified ceramic membranes are presented in Figure 4-18. Al and Au atoms were detected at the highest intensity because Al and Au stemmed from ceramic membrane materials and the surface coating material for SEM specimens, respectively. Though modified membranes seemed to be more severely fouled as TMPs at the end of filtration were relatively high, EDX spectra of modified membranes, however, did not show significantly higher intensity of atoms (Figures 4-18b and 4-18c) as compared to the unmodified membrane (Figure 4-18a). Same as the explanation above in Section 4.2.4, this may be mainly caused by the less deposition of large particle aggregates (as shown in Figure 4-17), which is a consequence of lower attraction of membrane surface to foulants.



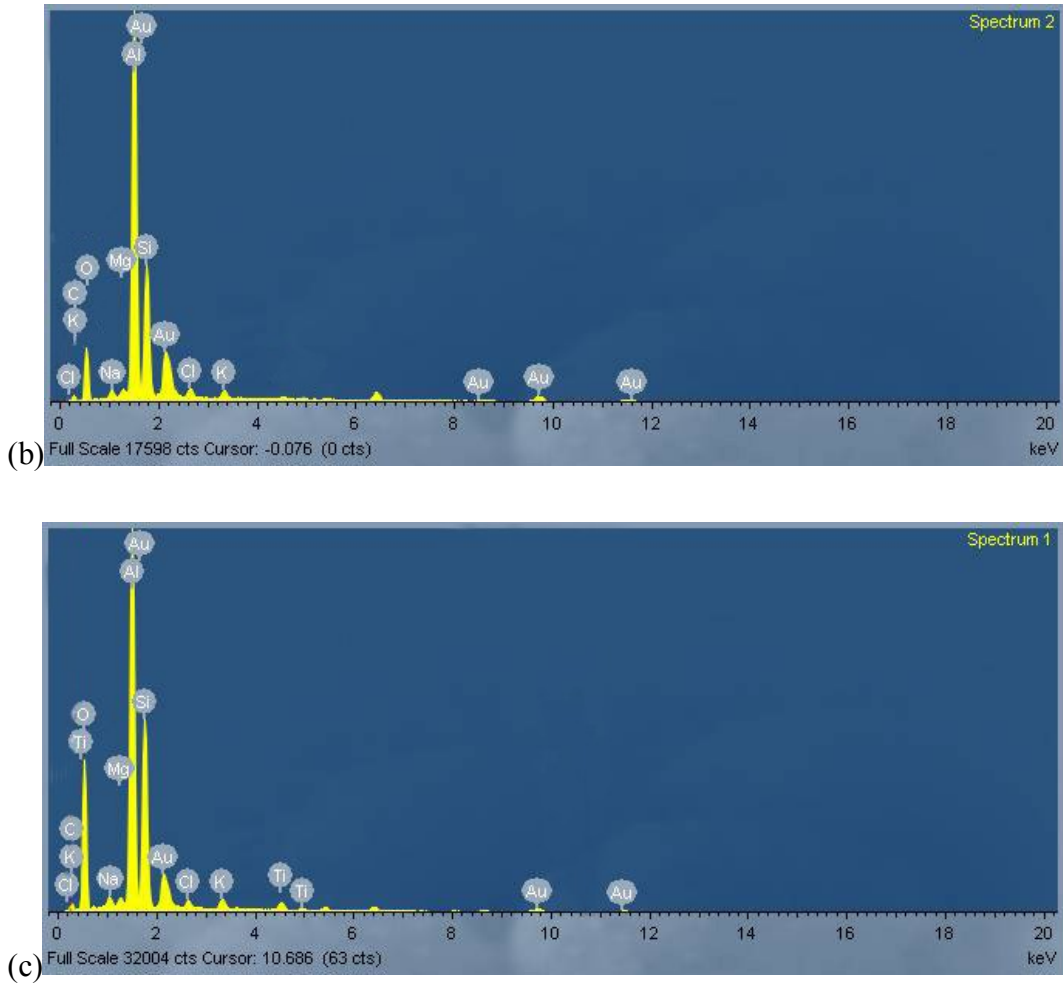


Figure 4-18 EDX spectrums of (a) fouled unmodified membrane; TMP at end of filtration was -12 kPa; (b) fouled SiO₂-modified membrane; TMP at the end of filtration was -16 kPa; (c) fouled TiO₂-modified membrane; TMP at the end of filtration was -23kPa. All three membranes were treated with 10 mg/L alum-coagulated OSPW.

CHAPTER 5: CONCLUSIONS AND RECOMMENDATIONS

In this study, a submerged ceramic membrane MF treatment was investigated for the treatment of OSPW from Suncor Energy Inc. Pond 7. Eight membrane filtration runs were conducted to examine the effect of CF and membrane materials on membranes' performance. Each run was operated for at least seven days. The following conclusions are drawn from this study:

- Our experimental results showed that the direct CF process substantially decreased TMP decreasing rate by reducing fouling of unmodified membrane. Alum coagulant showed a better ability to improve membrane performance in terms of TMP than PAC coagulant.
- Higher alum concentration did not effectively reduce the rate of TMP decrease.
- Filtration of OSPW with pH adjustment can significantly decrease the rate of TMP decrease due to the reduction of fouling through indirectly altering membrane surface charge from positive to negative.
- The importance of the effect of membrane surface charge on fouling control was directly proved by investigations of SiO₂- and TiO₂-modified ceramic membrane filtrations, where the negatively charged membranes generated a substantially low rate of TMP decrease.
- The electrostatic interactions between particles and membrane surface also influenced fouled membrane surface morphology and fouling compositions which were concluded based on the observations of SEM and EDX results.
- TMP, AFM and SEM analyses of two surface modified membranes demonstrated the effect of membrane surface roughness on fouling accumulation. Low roughness of SiO₂-modified membrane captured less fouling than high roughness of TiO₂-modified membrane.
- In all filtration runs, chemical cleaning with NaOCl was found to be very effective to remove irreversible fouling to restore more than 90% TMP to its original values regardless of different filtration conditions or membrane material.

- Permeate water quality measurements showed that membrane filtration conditions and membrane materials did not impact the removal of OSPW's components. Membrane filtration can recover more than 93% TSS, but can hardly remove more than 10% of organic matter (expressed as COD, TOC, AEF and NAs) from OSPW.
- For all filtration runs, MF can decrease SDI₅ index to a level acceptable to allow the treated OSPW to serve as RO feed. Treatment combining RO with MF generated a highly qualified permeate with respect to the overall removal of organic and inorganic compounds, indicating the applicability of MF-RO for the treatment of OSPW.
- CF-MF was compared with the CFS process. The results showed that CF-MF not only reduced the coagulant's concentration in economical and environmental point of views, but also generated a high quality effluent in terms of turbidity as compared to CFS process.

The following recommendations are suggested for the future investigations:

In present study, membrane surface charge and roughness tests have only been performed on bare unmodified and modified ceramic membranes. Further studies on the assessment of the zeta potential and surface roughness of fouled membranes should be conducted to fully understand OSPW fouling mechanisms. Besides, surface characterizations (SEM and EDX) should be performed either on membranes with the similar fouling degrees (or TMP values) or after the same operation time in order to clarify the effect of CF or membrane materials on the membrane morphology.

Future study should include evaluation of ceramic membrane hydrophobicity in order to further evaluate the interaction between ceramic membrane and OSPW fouling. It is also important to include the study of OSPW fouling mechanisms (i.e., cake layer formation, complete pore sealing, standard pore sealing and intermediate pore sealing) modeling to elucidate the internal and external membrane fouling and to determine the predominant fouling mechanism.

One limitation of this study is that the experiments were performed in the recirculation mode instead of the continuous OSPW flow mode. The experiments with the recirculating feed water could provide more accurate results in the case of short filtration time than in the case of long filtration time. Because OSPW was recirculated, the composition of OSPW was changing as filtration progressed, and concentration of solid materials decreased due to their deposition on membrane surface. To exclude this effect, pilot scale study with continuous OSPW filtration is required.

REFERENCES

- Ahn, K. H., and Song, K. G. 2000. Application of microfiltration with a novel fouling control method for reuse of wastewater from a large-scale resort complex. *Desalination*, 129(3), 207-216.
- Aktas, T.S., Takeda, F., Maruo, C., Fujibayashi, M., and Nishimura, O. 2013. Comparison of four kinds of coagulants for the removal of picophytoplankton. *Desalination and Water Treatment*, 51(16-18): 3547-3557.
- Alberta Department of Energy, 2010. Facts and statistics. Available: <http://www.energy.gov.ab.ca/OilSands/791.asp>
- Alberta Energy. 2012. Progress report: responsible actions: a plan for Alberta's oil sands. Edmonton.
- Alfredo, K.A. 2012. Drinking water treatment by alum coagulation: competition among fluoride, natural organic matter, and aluminum [electronic resource]. Austin, Texas; University of Texas at Austin.
- Allen, E. 2008a. Process water treatment in Canada's oil sands industry: I. Target pollutants and treatment objectives. *Journal of Environmental Engineering and Science*; 7: 123-138.
- Allen, E. 2008b. Process water treatment in Canada's oil sands industry: II. A review of emerging technologies. *Journal of Environmental Engineering and Science*; 7: 499-524.
- Alpatova, A., Kim, E-S., Dong, S., Sun, N., Chelme-Ayala, P., and Gamal El-Din, M., 2014. Treatment of oil sands process-affected water with ceramic ultrafiltration membrane: Effects of operating conditions on membrane performance. *Separation and Purification Technology*, 122: 170-182.

- America Public Health Association. 2005. Standard methods for the examination of water and wastewater, Washington, DC.
- American Society for Testing and Materials (ASTM), 1995. Standard Test Method for Silt Density Index (SDI) of Water, D4189–4195.
- American Society for Testing and Materials (ASTM). 2007. Standard Test Method for Silt Density Index (SDI) of water; ASTM D4189-07; American Society for Testing and Materials: Philadelphia, PA.
- Bansal, R.C., Donnet, J., and Stoeckli, F. 1988. Active carbon. Marcel Dekker, Inc., New York. 482 pp.
- Basile, A., Nunes, S. 2011. Advanced Membrane Science and Technology for Sustainable Energy and Environmental Applications. Woodhead Publishing Limited, Sawston, Cambridge, UK.
- Benko, K.L. 2009. Ceramic Membranes for Produced Water Treatment. World Oil, 230(4; 200920): 103-105.
- Beier, N., Alostaz, M., and Segó, D. 2009. Natural dewatering strategies for oil sands fine tailings. IN: Tailings and Mine Waste '09, Banff, Alberta. University of Alberta, Department of Civil & Environmental Engineering, Edmonton, Alberta
- Bertsch, P. M. 1987. Conditions for Al_13 polymer formation in partially neutralized aluminum solutions, Soil Science Society American Journal, 51: 825-828.
- Bolton, J. R. 2010. Ultraviolet applications handbook, 3rd Ed., Bolton Photosciences Inc., Edmonton, AB, Canada for an extensive discussion of advanced oxidation technologies.
- Cardew, P. T. and Le, M. S. 1998. Membrane processes: a technology guide. Royal society of chemistry, Cambridge.

- Chalaturnyk, R.J., Scott, D., Ozum, B. 2002. Management of oil sands tailings. *Petroleum Science and Technology*, 20(9&10): 1025-1046.
- Cheryan, M. 1998. *Ultrafiltration and micro filtration handbook*. Technomic Publishing Co. Lancaster, Pennsylvania.
- Clark, W, M, Bansal. A, Sontakke. M, Ma.Y. H. 1991. Protein adsorption and fouling in ceramic ultrafiltration membranes, *J. Membr. Sci.* 55 (1991) 21.
- Clemente, J.S., MacKinnon, M.D., Fedorak, P.M. 2004. Aerobic biodegradation of two commercial naphthenic acids preparations. *Environmental Science & Technology*, 38, 1009–1016.
- Cornell, R. M., and Schwertmann, U. 2003. *The iron oxides : structure, properties, reactions, occurrences, and uses*. Wiley-VCH, Weinheim.
- Corneal, L.M., Masten, S.J., Simon H.R. Davies, Tarabara, V.V., Byun, S., and Baumann, M.J. 2010. AFM, SEM and EDS characterization of manganese oxide coated ceramic water filtration membranes. *Journal of Membrane Science*, 360: 292-302.
- Crittenden, John C. 2005. *Water treatment principles and design*. Hoboken, N.J.: J. Wiley.
- Dokholyan, V.K., Magomedov, A.K. 1983. Effects of sodium naphthenate on survival and some physiological-biochemical parameters of some fishes. *Journal of Ichthyology*, 23, 125– 132.
- Dong, B.Z., Chen, Y., Gao, N.Y., Fan, J.C. 2007. Effect of coagulation pretreatment on the fouling of ultrafiltration membrane. *Journal of Environmental Sciences*, 19(3), 278–283.
- Ebrahimi, M., Willershausen, D., Ashaghi, K.S., Engel, L., Placido, L., Mund, P., Bolduan, P., and Czermak, P. 2010. Investigations on the use of different

- ceramic membranes for efficient oil-field produced water treatment. *Desalination*, 250(3): 991-996.
- EPA. 1996. Method 9050A: Specific conductance.
- Exall. K. N. 2001. Examination of the behaviour of aluminium-based coagulants during organic matter removal in drinking water treatment, Thesis, Queen's University, Kingston, Ontario, Canada.
- Faibish, R.S., Cohen, Y. 2001. Fouling-resistant ceramic-supported polymer membranes for ultrafiltration of oil-in-water microemulsions. *Journal of Membrane Science*, 185(2), 129–143.
- Fakhru'l-Razi, A., Pendashteh, A., Abdullah, L.C., Biak, D.R.A., Madaeni, S.S., Abidin, Z.Z. 2009. Review of technologies for oil and gas produced water treatment. *Journal of Hazardous Materials*, 170(2–3), 530–551.
- Farahbakhsh, K., Svrcek, C., Guest, R.K., and Smith, D.W. 2004. A review of the impact of chemical pretreatment on low-pressure water treatment membranes. *Journal of Environmental Engineering & Science*, 3(4): 237-253.
- Farhadian, M., Duchez, D., Vachelard, C., Larroche, C. 2008. Monoaromatics removal from polluted water through bioreactors – A review. *Water Research*, 42(6–7), 1325–1341.
- Fedorak, P.M., and Coy, D.L. 2006. Oil sands cokes affect microbial activities. *Fuel*; 85: 1642-1651.
- Fine Tailings Fundamentals Consortium (FTFC). 1995. Advances in oil sands tailings research, Alberta Department of Energy, Oil Sands and Research Division, Edmonton, Alberta, Canada
- Fu, J., Gamal El-Din, M., Smith, D.W., MacKinnon, M.D., Zubot, W. 2008. Ozone treatment of naphthenic acids in Athabasca oil sands process-affected

- water. In: First International Oil Sands Tailing Conference, December 7-10, 2008, Edmonton, Alberta, pp. 228–231.
- Furimsky, E. 1998. Gasification of oil sands coke: review. *Fuel Processing Technology*; 56: 263-290.
- Gamal El-Din, M. 2011. Review of remediation technologies for oil sands process-affected waters. Environmental engineering technical report 11-01, University of Alberta, Edmonton, A.B.
- Gamal El-Din, M. 2012. Treatment and management of oil sands tailings water for detoxification and decontamination [online]. Available from http://www.aiees.ca/media/8699/2012-waterresources-gamal_el_din_treatment_of_oil_sands_water-public_version.pdf
- Gao, W.J., Lin, H.J., Leung, K.T., Schraft, H., and Liao, B.Q. 2011. Structure of cake layer in a submerged anaerobic membrane bioreactor. *Journal of Membrane Science*, 374(1–2): 110-120.
- Gregg, S.J., and Sing, K.S.W. 1982. Adsorption, surface area and porosity. Academic Press Incorporated, London; pp. 1-39.
- Guigui, C., Rouch, J.C., Durand-Bourlier, L., Bonnelye, V., and Aptel, P. 2002. Impact of coagulation conditions on the in-line coagulation/UF process for drinking water production. *Desalination*, 147(1-3): 95-100.
- Han, X. M.; MacKinnon, M. D.; Martin, J. W. 2009. Estimating the in situ biodegradation of naphthenic acids in oil sands process waters by HPLC/HRMS. *Chemosphere*, 76 (1), 63–70.
- Han, X., Scott, A.C., Fedorak, P.M., Bataineh, M., Martin, J.W. 2008. Influence of molecular structure on biodegradability of naphthenic acids. *Environmental Science & Technology*, 42, 1290–1295.

- Harif, T., Khai, M., and Adin, A. 2012. Electrocoagulation versus chemical coagulation: Coagulation/flocculation mechanisms and resulting floc characteristics. *Water Research*, 46(10): 3177-3188.
- Herman, D.C., Fedorak, P.M., Costerton, J.W. 1993. Biodegradation of cycloalkane carboxylic acids in oil sands tailings. *Canadian Journal of Microbiology*, 39, 576–580.
- Hermia, J. 1982. Constant pressure blocking filtration laws-application to power-law non-Newtonian fluids. *Trans. Inst. Chem. Eng.* 60 (3), 183e187.
- Holowenko, F.M., MacKinnon, M.D., Fedorak, P.M. 2001. Naphthenic acids and surrogate naphthenic acids in methanogenic microcosms. *Water Research*, 35, 2595–2606.
- Howe, K. J., and Clark, M. M. 2006. Effect of coagulation pretreatment on membrane filtration performance. *J. Am. Water Works Assoc.*, 984, 133–146.
- Husein, M. M., A. Deriszadeh, and T.G. 2011. Experimental and modeling study of MEUF removal of naphthenic acids, *Desalination*, 273(2-3), 352–358.
- Jankowska, H., Swiatkowski, A., Choma, J. 1991. *Active carbon*. Ellis Harwood, New York, NY, USA.
- Jiang, J.T. 2010. Ozonation of oil sands process-affected water accelerates microbial bioremediation. *Environmental Science & Technology*, 44(21), 8350–8356.
- Jivraj, M. N., MacKinnon, M., Fung, B. 1996. Naphthenic acid extraction and quantitative analysis with FT-IR spectroscopy; Syncrude Canada Ltd. Internal Report: Edmonton: Syncrude Canada Ltd.
- Jordaan, S.M. 2012. Land and water impacts of oil sands production in alberta. *Environmental Science & Technology*, 46(7): 3611-3617.

- Kasperski, K.L. 2003. Review of research on aqueous extraction of bitumen from mined oil sands. Unpublished report. CANMET Energy Technology Centre, Natural Resources Canada, Devon, Alta.
- Kim, E.-S., Liu, Y., and Gamal El-Din, M., 2012a. Evaluation of membrane fouling for in-line filtration of oil sands process-affected water: The Effects of Pretreatment Conditions. *Environmental Science & Technology*, 46(5): 2877-2884.
- Kim, E.-S., Mohamed Gamal El-Din, Yang Liu. 2012b. Comparison of deionization technologies for the treatment of basal depressurization water and oil sands process-affected water. Final report, Department of Civil and Environmental Engineering University of Alberta, Edmonton, A.B.
- Kim, E.-S., Liu, Y., Gamal El-Din, M. 2011. The effects of pretreatment on nanofiltration and reverse osmosis membrane filtration for desalination of oil sands process-affected water. *Separation and Purification Technology*, 81(3): 418–428.
- Kim, J., and Van der Bruggen, B. 2010. The use of nanoparticles in polymeric and ceramic membrane structures: Review of manufacturing procedures and performance improvement for water treatment. *Environmental Pollution*, 158(7): 2335-2349.
- Kim, J., Nason, J.A., and Lawler, D.F. 2006. Zeta potential distributions in particle treatment processes. *Journal of Water Supply: Research & Technology-AQUA*, 55(7): 461-470.
- Kim, S., Park, N., Kim, T., Park, H. 2007. Reaggregation of flocs in coagulation-cross-flow microfiltration. *Journal of Environmental Engineering*, 133(5): 507-514.

- Kosmulski, M. 2009. Compilation of PZC and IEP of sparingly soluble metal oxides and hydroxides from literature. *Advances in Colloid and Interface Science*, 152, pp. 14–25
- Langwaldt, J.H., Puhakka, J.A. 2000. On-site biological remediation of contaminated groundwater: a review. *Environmental Pollution*, 107(2), 187–197.
- Lee, D., Liao, G., Chang, Y., and Chang, J. 2012. Coagulation-membrane filtration of *Chlorella vulgaris*. *Bioresource Technology*, 108(0): 184-189. doi: <http://dx.doi.org/10.1016/j.biortech.2011.12.098>.
- Legrini, O., Oliveros, E and Braun, A.M. 1993. Photochemical processes for water treatment, *Chem, Rev.*, 93,671-698
- Liang, X., Zhu, X., Butler, E.C. 2011. Comparison of four advanced oxidation processes for the removal of naphthenic acids from model oil sands process water. *Journal of Hazardous Materials*, in press.
- Liu, Charles, et al. 2001. Membrane chemical cleaning: from art to science. Pall Corporation, Port Washington, NY 11050.
- Lo, C.C., Brownlee, B.G., Bunce, N.J. 2006. Mass spectrometric and toxicological assays of Athabasca oil sands naphthenic acids. *Water Research*, 40(4) 655–664.
- Mah, R., Guest, R., and Kotecha, P. 2011. Piloting conventional and emerging industrial wastewater treatment technologies for the treatment of oil sands process-affected water. *Proceedings of the International Water Conference*, IWC 11-21.
- Martin, J.W., Barri, T., Han, X.M., Fedorak, P.M., Gamal El-Din, M., Perez, L., Scott, A.C., Jiang, J.T. 2010. Ozonation of oil sands process-affected water accelerates microbial bioremediation. *Environmental Science & Technology*, 44(21), 8350–8356.

- McCafferty, E., and Wightman, J.P. 1997. Determination of the surface isoelectric point of oxide films on metals by contact angle titration. *Journal of Colloid and Interface Science*, 194(2): 344-355.
- Meng, F., Zhang, H., Yang, F., and Liu, L. 2007. Characterization of cake layer in submerged membrane bioreactor. *Environmental Science & Technology*, 41(11): 4065-4070.
- Metcalf, and Eddy. 2003. *Wastewater engineering treatment and reuse*, McGraw-Hill Higher Education.
- Meiser E. 2001. Field evaluation of ceramic microfiltration membranes in drinking water treatment, Montana University System Water Center
- Mueller, J., Cen, Y., Davis, R.H. 1997. Crossflow microfiltration of oily water. *Journal of Membrane Science* 129:221-235.
- Mullet. M, Fievet. P, Reggiani. J.C, Pagetti. J. 1997. Surface electrochemical properties of mixed oxide ceramic membranes: zeta-potential and surface charge density. *Journal of Membrane Science*, 123, pp. 255–265
- Oluwaseun, O., Burnett, D., Hann, R., and Haut, R. 2008. Application of membrane filtration technologies to drilling wastes. Society of petroleum engineering annual technical conference and exhibition, Denver, Colorado. 21-24 Spetember 2008. Society of Petroleum Engineers.
- Parsons, S. 2004. *Advanced oxidation process for water treatment*. IWA Publishing, London, U.K.
- Parsons, S.A., Jefferson, B. 2006. *Introduction to potable water treatment Processes*. Blackwell Publishing Ltd., Oxford, UK.
- Patel, R., Penisson, A.C., Hill, R.D., Wiesner, M.R. 1994, Membrane microfiltration of secondary wastewater effluent, in: *Chemical Water and*

- Wastewater Treatment III, R. Klute and H.H.Hahn, eds., SpringerVerlag, Berlin, pp.29-36.
- Peng, H., Volchek, K., MacKinnon, M., Wong, W.P., Brown, C.E. 2004. Application of nanofiltration to water management options for oil sands operations. *Desalination*, 170(2), 137–150.
- Pourrezaei, P. 2013. Physico-chemical processes for oil sands process-affected water treatment. Doctor of Philosophy Dissertation submitted to the Faculty of Graduated Studeies and Research, Department of Civil and Environmental Engineering, University of Alberta, Edmonton, Canada.
- Pourrezaei, P.; Drzewicz, P.; Wang, Y.; Gamal El-Din, M.; Perez- Estrada, L. A.; Martin, J. W.; Anderson, J.; Wiseman, S.; Liber, K.; Giesy, J. P. 2011. The impact of metallic coagulants on the removal of organic compounds from oil sands process-affected water. *Environmental Science and Technology*, 45(19): 8452–8459.
- Quagraine, E. K., Headley, J. V., and Peterson, H. G. 2005a. Is biodegradation of bitumen a source of recalcitrant naphthenic acid mixtures in oil sands tailing pond waters? *J Environ Sci Health A Tox Hazard Subst Environ Eng*, 40(3), 671-84.
- Quagraine, E. K., Peterson, H. G., and Headley, J. V. 2005b. In situ bioremediation of naphthenic acids contaminated tailing pond waters in the Athabasca oil sands region--demonstrated field studies and plausible options: a review. *J Environ Sci Health A Tox Hazard Subst Environ Eng*, 40(3), 685-722.
- Rautenbach, R. and Albrecht, R. 1989. Membrane processes. John Wiley & Sons Ltd. New York.
- Rittmann, B.E. 2006. Microbial ecology to manage processes in environmental biotechnology. *Trends in Biotechnology*, 24(6), 261–266.

- Rodgers, M., Zhan, X.M. 2003. Moving medium biofilm reactors. *Reviews in Environmental Science and Bio/Technology*, 2(2–4), 213–224.
- Royal Society of Canada. 2010. Environmental and health impacts of Canada's oil sands industry; Report of the Royal Society of Canada expert panel: Ottawa, Ontario, 2010.
- Sanders, R.S., Ferre, A.L., Maciejewski, W.B., Gillies, R.G., and Shook, C.A. 2000. Bitumen effects on pipeline hydraulics during oil sand hydrotransport. *Canadian Journal of Chemical Engineering*, 78(4): 731-742.
- Santo, C. E.; Vilar, V. J. P.; Botelho, C. M. S.; Bhatnagar, A.; Kumar, E.; Boaventura, R. A. R. 2012. Optimization of coagulation-flocculation and flotation parameters for the treatment of a petroleum refinery effluent from a Portuguese plant. *Chemical Engineering Journal* 2012, 183, 117-123.
- Scott, A.C., Zubot, W., MacKinnon, M.D., Smith, D.W., Fedorak, P.M. 2008. Ozonation of oil sands process water removes naphthenic acids and toxicity. *Chemosphere*, 71(1), 156–160.
- Shawwa, A.R., and Smith D.W., and Segó, D.C. 2001. Color and chlorinated organics removal from pulp mills wastewater using activated petroleum coke. *Water Resources*; 35: 745-749.
- Shen. Y. H. 1992. Synthesis and characterization of polyaluminum coagulants for water treatment, Thesis, University Park, PA, Pennsylvania State University.
- Simon, A., Price, W.E., and Nghiem, L.D. 2013. Changes in surface properties and separation efficiency of a nanofiltration membrane after repeated fouling and chemical cleaning cycles. *Separation and Purification Technology*,: 42.
- Singh, V., Purkait, M.K., and Das, C. 2011. Cross-flow microfiltration of industrial oily wastewater: experimental and theoretical consideration. *Separation Science & Technology*, 46(8): 1213-1223.

- Slavik, I., Muller, S., Mocosch, R., Azongbilla, J.A., and Uhl, W. 2012. Impact of shear stress and pH changes on floc size and removal of dissolved organic matter (DOM). *Water Research*, 46(19): 6543-6553.
- Small, C.C. 2011. Activation of delayed and fluid petroleum coke for the adsorption and removal of naphthenic acids from oil sands tailings pond water. M.Sc. thesis, Department of Civil and Environmental Engineering, University of Alberta, Edmonton, A.B.
- Tamura, H., Tanaka, A., Mita, K., and Furuichi, R. 1999. Surface hydroxyl site densities on metal oxides as a measure for the ion-exchange capacity. *Journal of Colloid and Interface Science*, 209(1): 225-231.
- Tansel, B., Regula, J., and Shalewitz, R. 1995. Treatment of fuel oil and crude oil contaminated waters by ultrafiltration membranes. *Desalination*, 102: 301-311.
- Tarr, M.A. 2003. *Chemical degradation methods for wastes and pollutants*. Marcel Dekker, New York, N.Y., USA.
- Tchobanoglous, G., Burton, F.L., Stensel, H.D. 2003. *Wastewater engineering. treatment, disposal, and reuse*. 4th edition. McGraw-Hill Inc., New York, N.Y., USA.
- Tingley, D. 1992. *Alberta environmental protection & enhancement act*. Edmonton, Alta. : Legal Education Society of Alberta.
- U.S. Army Corps of Engineers. 2001. Manual No. 1110-1-4012 engineering and design: Precipitation/coagulation/flocculation. Department of the Army, ed., Washington, DC20314-1000.
- Ueda, T., Hata, K., Kikuoka, Y., and Seino, O. 1997. Effects of aeration on suction pressure in a submerged membrane bioreactor. *Water Research*, 31(3): 489-494.

- Vlasopoulous, N., Memon, F.A., Butler, D., and Murphy, R. 2006. Life cycle assessment of wastewater treatment technologies treating petroleum process waters. *Science of the Total Environment*; 367: 58-70.
- Vrijenhoek, E.M., Hong, S., and Elimelech, M. 2001. Influence of membrane surface properties on initial rate of colloidal fouling of reverse osmosis and nanofiltration membranes. *Journal of Membrane Science*, 188(1): 115-128.
- Wang, J., Guan, J., S.R. Santiwong, and David Waite, T. 2008. Characterization of floc size and structure under different monomer and polymer coagulants on microfiltration membrane fouling. *Journal of Membrane Science*, 321: 132-138.
- Wang, Y. 2011a. Advanced physic-chemical treatment of oil sands process-affected waters. Master of Sciences Thesis submitted to the Faculty of Graduate Studies and Research, Department of Civil and Environmental Engineering, University of Alberta, Edmonton, Canada.
- Wang, N. 2011b. Ozonation and biodegradation of oil sands process water. Master of Sciences Thesis submitted to the Faculty of Graduate Studies and Research, Department of Civil and Environmental Engineering, University of Alberta, Edmonton, Canada.
- Welton, J. E. 1984. SEM petrology atlas. Available [online]: <http://www.doganaydal.com/nesneler/kutuphanekitaplar/SEM-ATLAS.PDF>. Accessed November 15, 2013.
- Winkler, B.H., and Baltus, R.E. 2003. Modification of the surface characteristics of anodic alumina membranes using sol-gel precursor chemistry. *Journal of Membrane Science*, 226(1-2): 75-84.
- Wu, X., Ge, X., Wang, D., and Tang, H. 2008. Distinct mechanisms of particle aggregation induced by alum and PACl: Floc structure and DLVO

- evaluation. *Colloids and Surfaces A: Physicochemical and Engineering Aspects*, 347: 56-63.
- Yan, M., Wang, D., Yu, J., Ni, J., Edwards, M., and Qu, J. 2008. Enhanced coagulation with polyaluminum chlorides: Role of pH/Alkalinity and speciation. *Chemosphere*, 71(9): 1665-1673.
- Yoko, T., Kamiya, K., Yuasa, A., Tanaka, K., and Sakka, S. 1988. Applications: Monoliths, fibers, coating films, etc.: Surface modification of a TiO₂ film electrode prepared by the sol-gel method and its effect on photoelectrochemical behavior. *Journal of Non-Crystalline Solids*, 100: 483-489.
- Zaidi, A., Simms, K., and Kok, S. 1992. The use of micro/ultrafiltration for the removal of oil and suspended solids from oilfield brines. *Water Science & Technology*, 25(10): 163.
- Zeman, L.J. and Zydney, A.L. 1996. *Microfiltration and ultrafiltration : principles and applications / Leos J. Zeman, Andrew L. Zydney*. New York : M. Dekker, c1996.
- Zhang, Q., Fan, Y.Q., and Xu, N.P. 2009. Effect of the surface properties on filtration performance of Al₂O₃-TiO₂ composite membrane. *Separation and Purification Technology*, 66(2): 306-312.
- Zhao, Y.X., Gao, B.Y., Shon, H.K., Kim, J.-., and Yue, Q.Y. 2011. Effect of shear force, solution pH and breakage period on characteristics of flocs formed by Titanium tetrachloride (TiCl₄) and Polyaluminum chloride (PACl) with surface water treatment. *Journal of Hazardous Materials*, 187(1-3): 495-501.
- Zheng, X., Plume, S., Ernst, M., Croué, J., and Jekel, M. 2012. In-line coagulation prior to UF of treated domestic wastewater – foulants removal, fouling control and phosphorus removal. *Journal of Membrane Science*, 403-404(0): 129-139.

- Zhong, J., Sun, X., and Wang, C. 2003. Treatment of oily wastewater produced from refinery processes using flocculation and ceramic membrane filtration. *Separation and Purification Technology*, 32: 93-98.
- Zhong, J.P., and Clark, D.E. 1993. Interaction between colloidal particles in SiO₂ and TiO₂ sols. *Wechselwirkung Zwischen Kolloidalen Partikeln in SiO₂-Und TiO₂-Solen*, (3): 247.
- Zondervan, E., and Roffel, B. 2007. Evaluation of different cleaning agents used for cleaning ultra filtration membranes fouled by surface water. *Journal of Membrane Science*, 304(1-2): 40-49.
- Zubot, W.A. 2010. Removal of naphthenic acids from oil sands process water using petroleum coke. Master of Sciences Thesis submitted to the Faculty of Graduate Studies and Research, Department of Civil and Environmental Engineering, University of Alberta, Edmonton, Canada.

APPENDIX A

Overall TMP data of all membrane filtration runs

Figure A 1 TMP data of Run 1

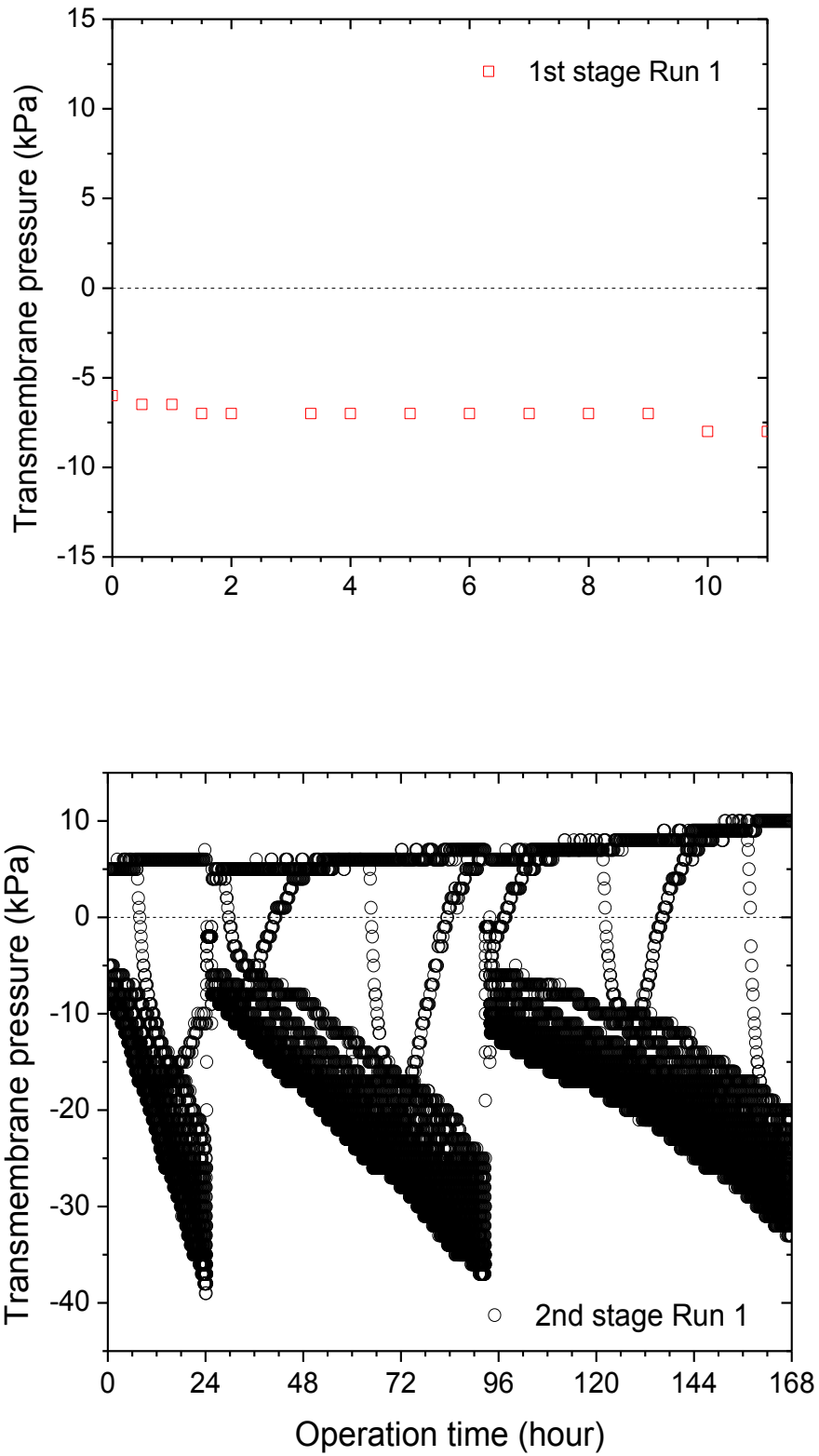


Figure A 2 TMP data of Run 2

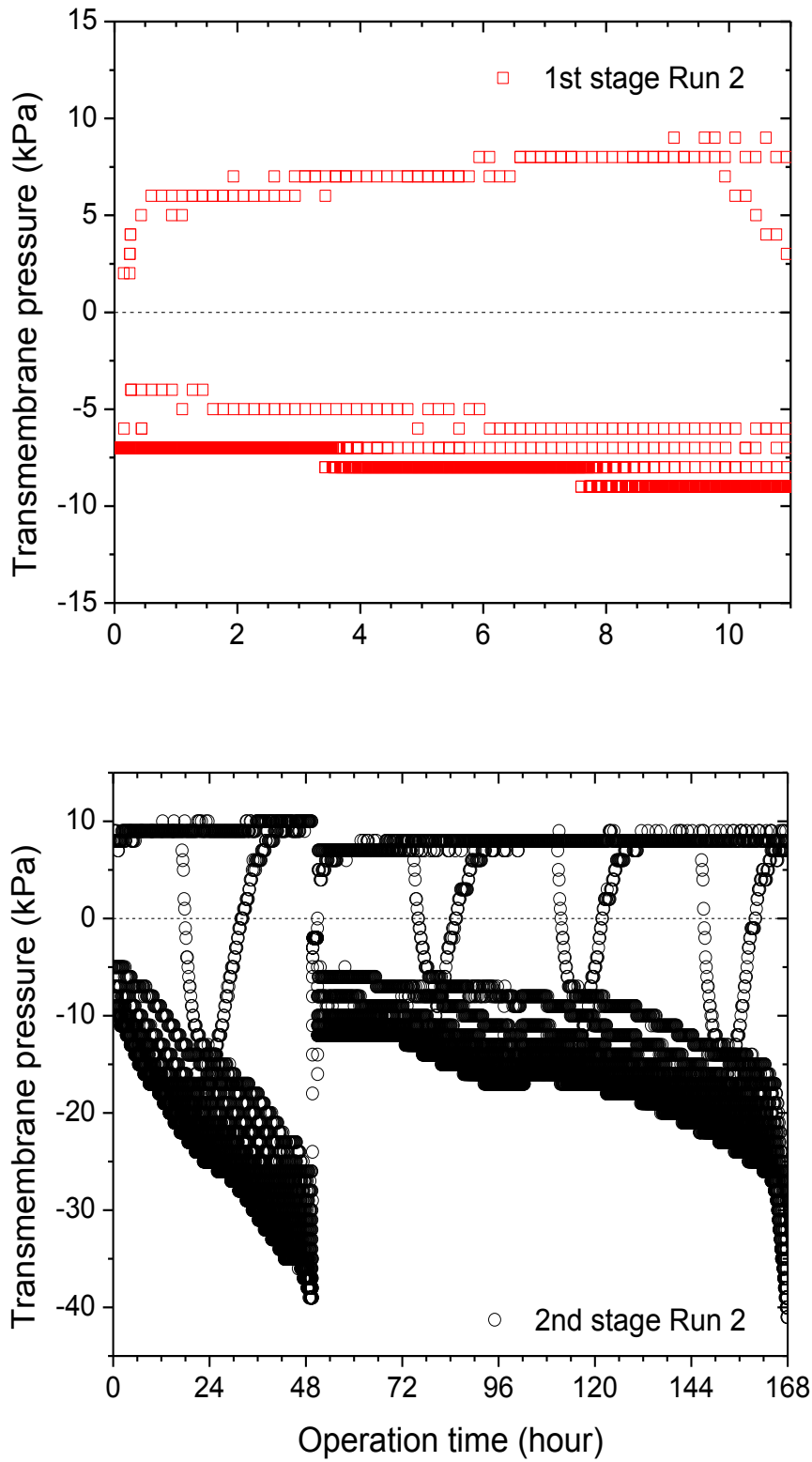


Figure A 3 TMP data of Run 3

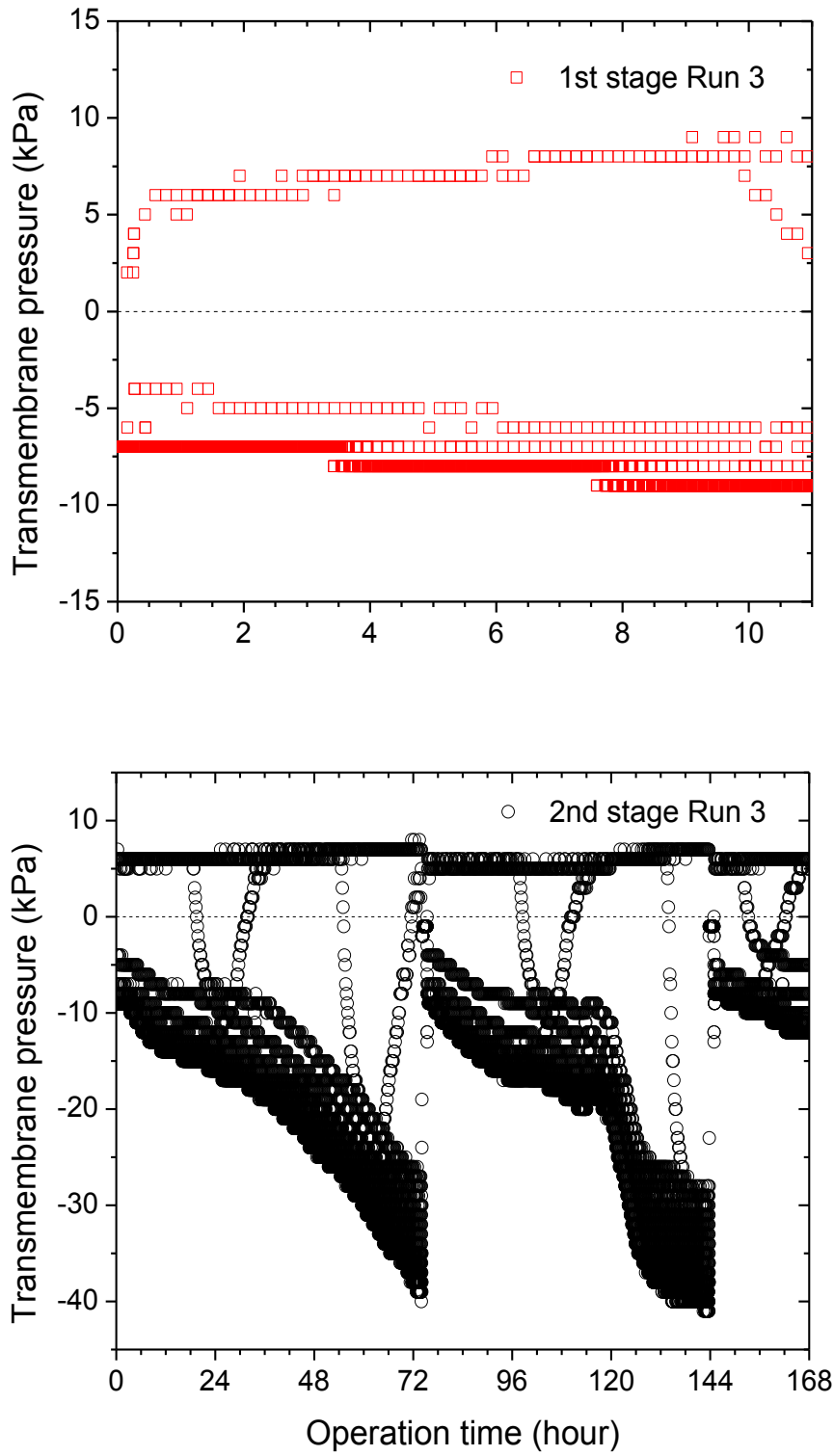


Figure A 4 TMP data of Run 4

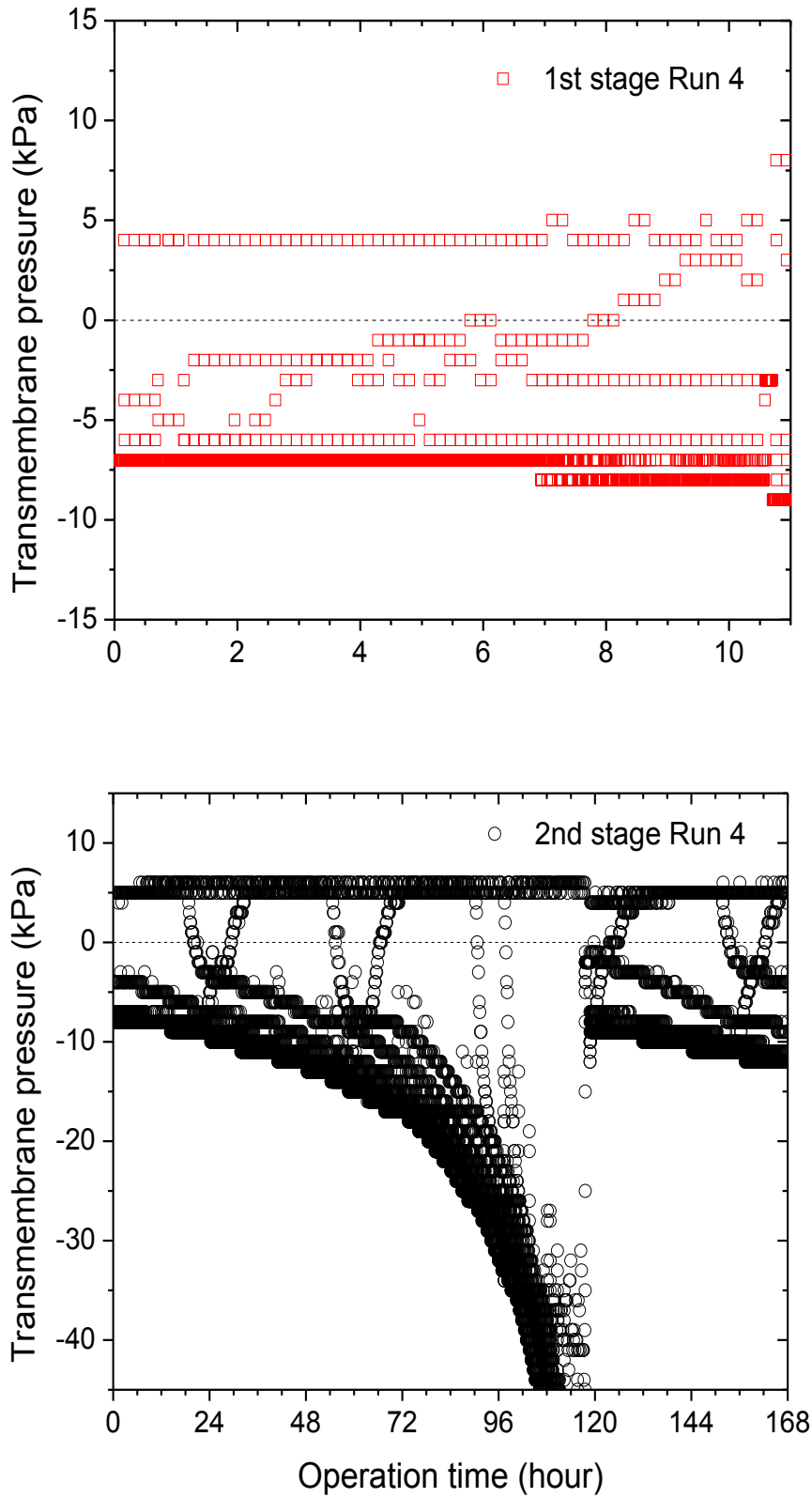


Figure A 5 TMP data of Run 5

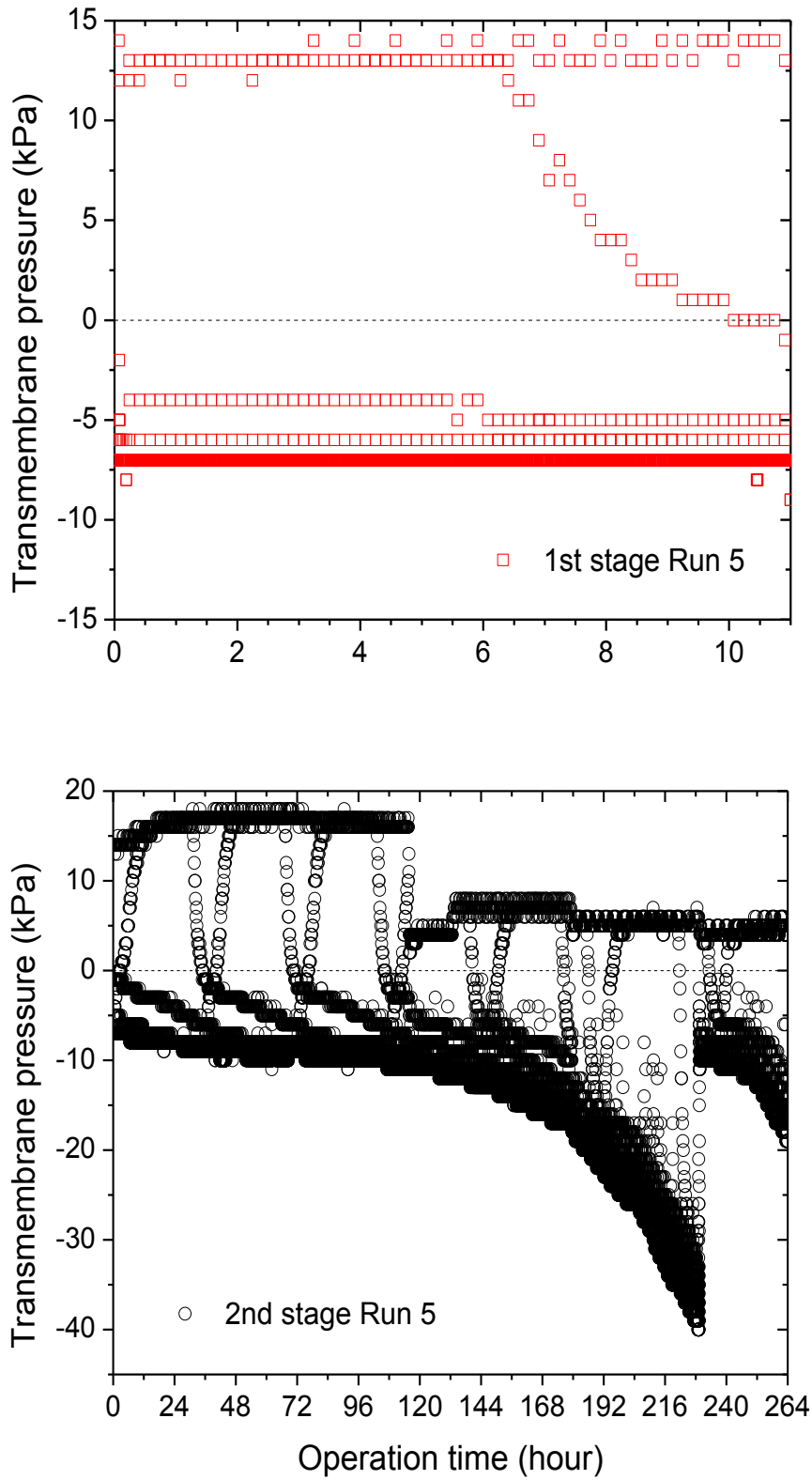


Figure A 6 TMP data of Run 6

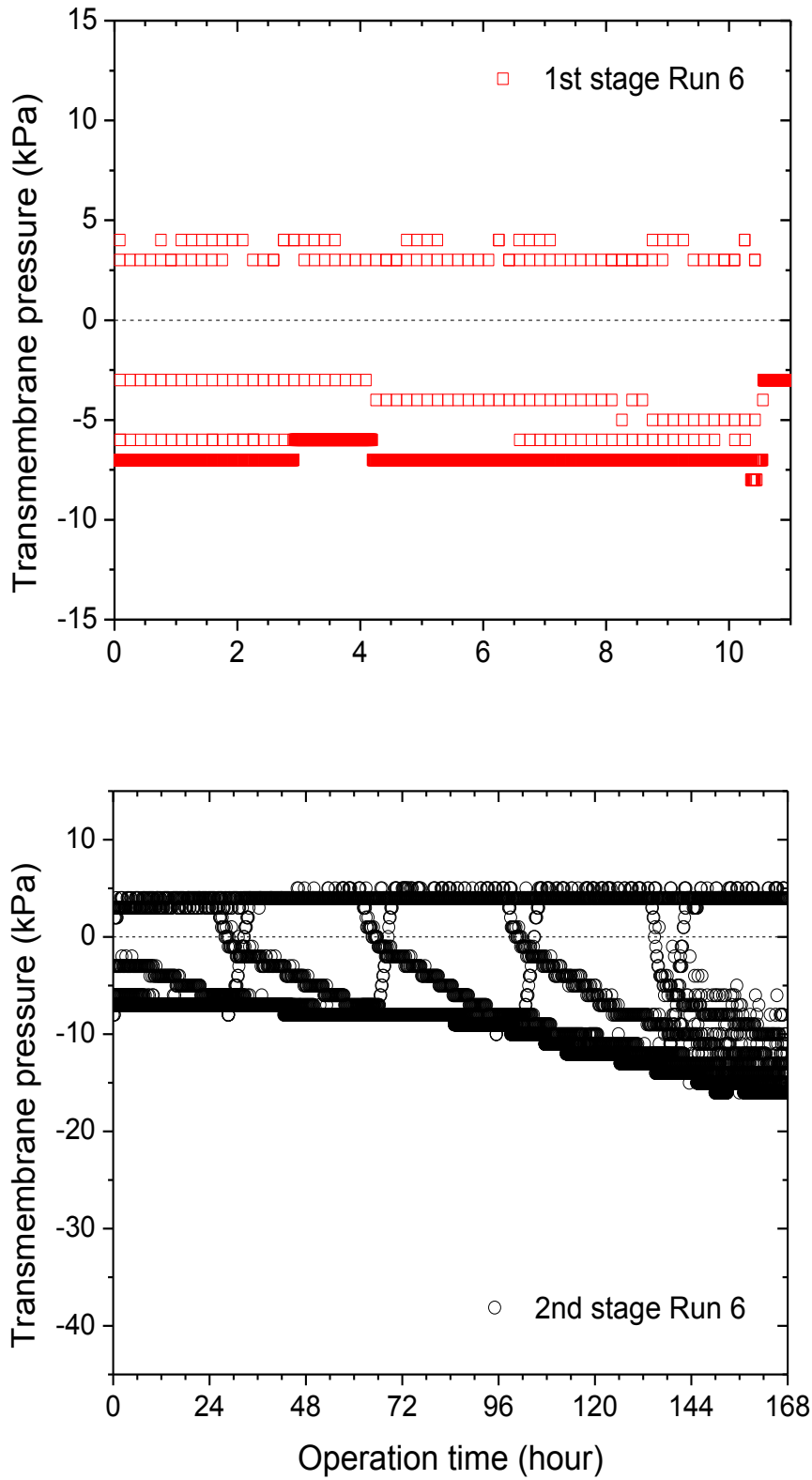


Figure A 7 TMP data of Run 7

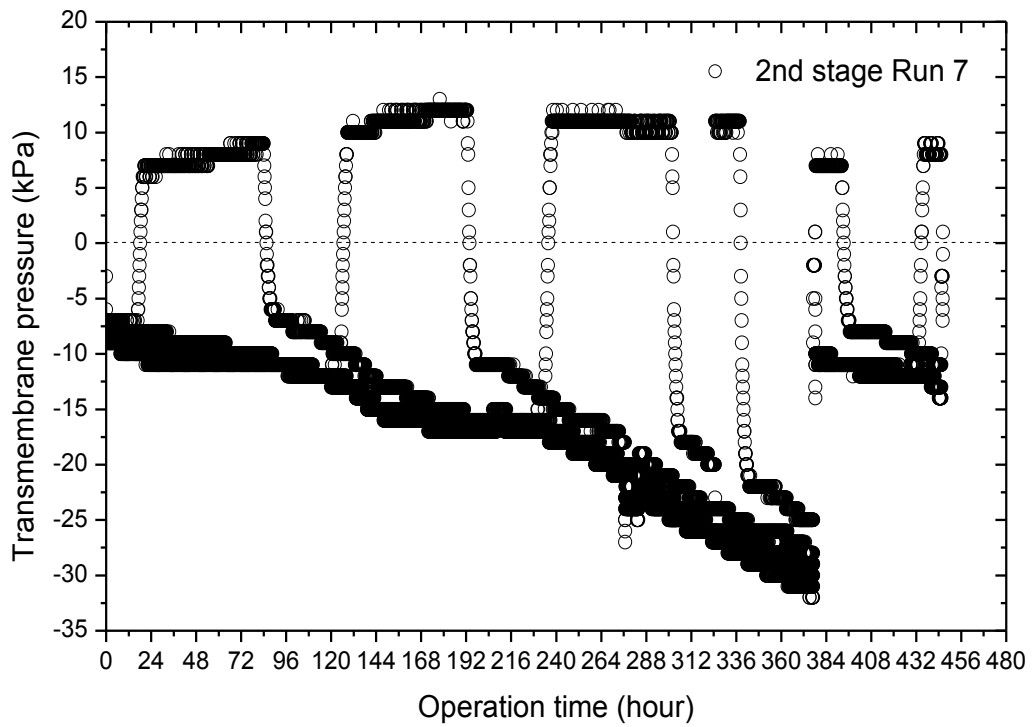
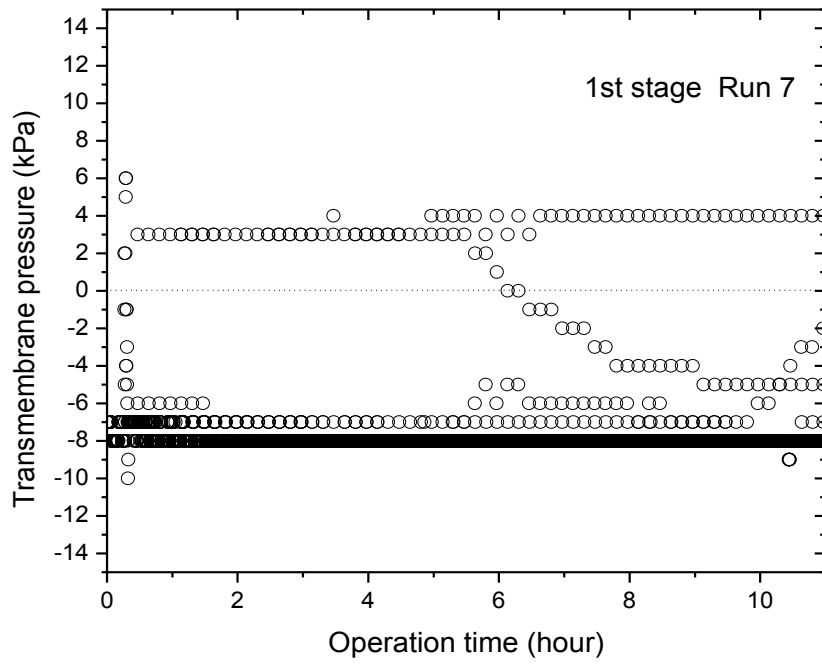
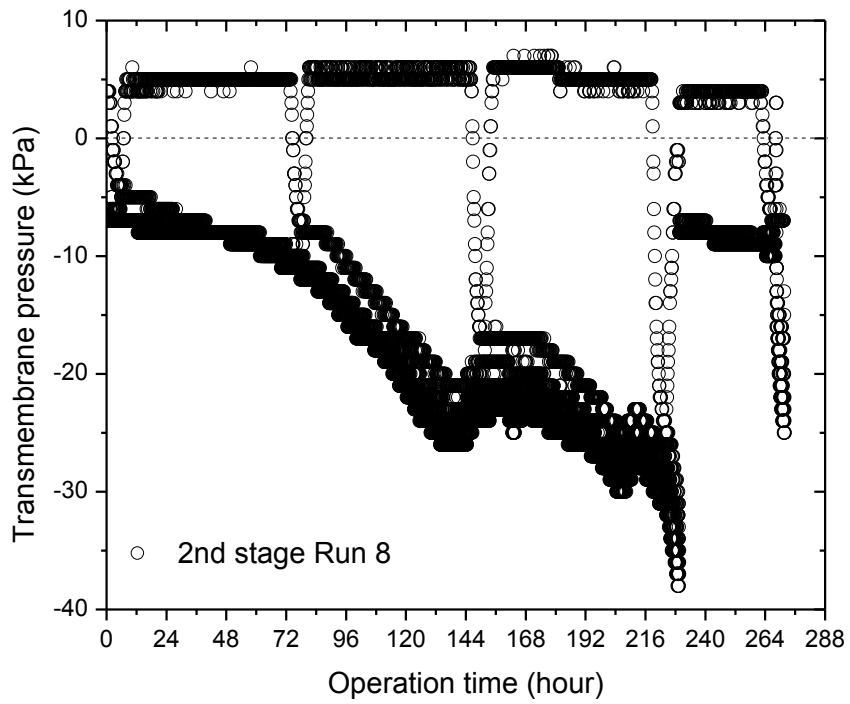
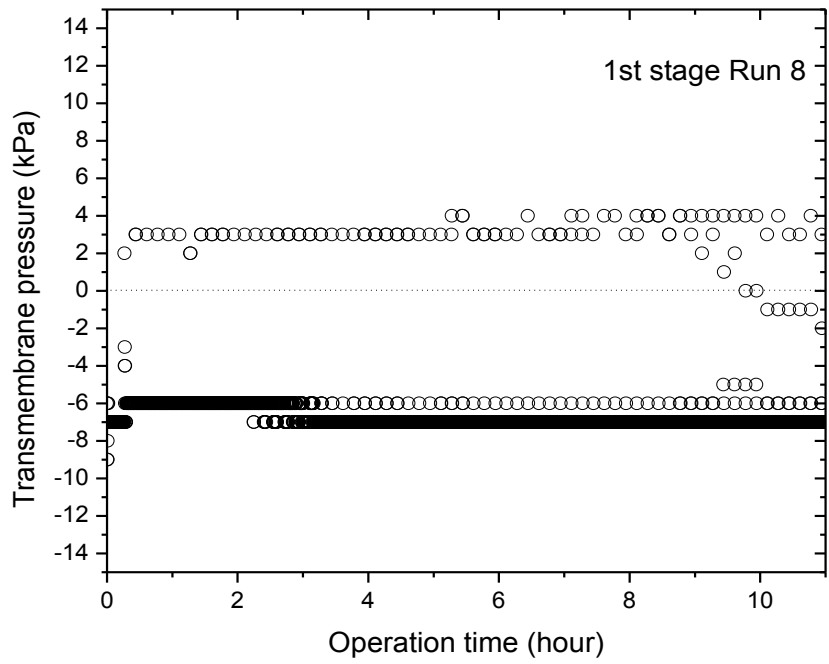


Figure A 8 TMP data of Run 8



APPENDIX B

Physico-chemical properties of OSPW

Table B 1 Physico-chemical properties of OSPW in Run 1

Species	Run #1: Raw OSPW												
	1st stage			2nd stage									
	Raw OSPW	Feed	Permeate Final 11h	Feed	Permeate 24 h	Permeate 48 h	Permeate 72 h	Permeate 96 h	Permeate 120 h	Permeate 144 h	Feed 168 h	M Tank 168 h	Permeate 168 h
pH	7.32	7.32	8.01	8.02	7.93	7.91	7.91	7.55	7.57	7.55	7.53	7.33	7.39
Conductivity, µS/cm	3576.67	3576.67	3523.00	3584.67	3290.33	3587.67	3637.67	3653.33	3676.67	3786.33	3757.67	3789.00	3517.67
Turbidity, NTU	25.33	25.33	0.96	67.43	0.68	0.71	0.77	0.62	0.69	0.69	49.40	6.36	0.68
Total organic carbon (TOC), mg/L	41.40		36.23	44.71	35.99	35.99	37.16	36.71	35.57	37.37	42.10		36.11
Chemical oxygen demand (COD), mg/L	124.00		112.33								154.00		114.33
Total suspended solids (TSS), mg/L	22.17		1.00								89.04		1.50
Total dissolved solids (TDS), mg/L	1872.50		1853.67								2041.43		2009.56
Extractable organic fraction, mg/L	29.44		29.86								31.74		29.74
Silt density index (SDI)	6.22		1.89								n/a		1.52
D50	737.10		573.70								1527.60		833.50
Magnesium, mg/L	120.00		11.80								13.30		12.10
Calcium, mg/L	25.50		25.20								27.00		24.60
Iron, mg/L	0.21		n/d								0.35		n/d
Manganese, mg/L	0.08		0.02								0.11		0.07
Silicon, mg/L	5.01		4.96								5.58		4.99
Fluoride, mg/L	2.01		2.21								2.99		2.17
Chloride, mg/L	1869.20		1765.10								2004.10		1812.50
Bromide, mg/L	n/d		n/d								n/d		n/d
Phosphate, mg/L	n/d		n/d								n/d		n/d
Sulfate, mg/L	77.96		78.15								81.26		80.11
Nitrate, mg/L	n/d		n/d								n/d		n/d
Sodium, mg/L	715.30		702.90								784.30		768.10
Potassium, mg/L	13.00		11.00								14.60		13.20
Naphthenic acids, mg/L	6.35		6.14								6.08		6.57

n/d: not detected

Table B 2 Physico-chemical properties of OSPW in Run 2

Species	Run #2: PAC 20 mg/L coagulated OSPW												
	1st stage			2nd stage									
	Raw OSPW	Feed	Permeate Final 11h	Feed	Permeate 24 h	Permeate 48 h	Permeate 72 h	Permeate 96 h	Permeate 120 h	Permeate 144 h	Feed 168 h	M Tank 168 h	Permeate 168 h
pH	6.01	6.36	7.28	7.54	7.50	7.58	7.52	7.47	7.41	7.64	7.81	7.76	7.79
Conductivity, µS/cm	3440.5	3407.0	3284.0	3423.0	3531.0	3496.0	3515.5	3704.0	3521.0	3589.0	3481.5	3513.0	3536.0
Turbidity, NTU	24.05	25.50	1.06	80.77	1.09	1.02	0.97	0.96	0.84	0.89	80.25	54.00	0.90
Total organic carbon (TOC), mg/L	40.0		34.4	46.6	39.3	37.0	38.9	37.8	38.5	37.1	54.4		35.8
Chemical oxygen demand (COD), mg/L	144.6		131.3								305.0		133.5
Total suspended solids (TSS), mg/L	16.1		0.0								435.0		0.0
Total dissolved solids (TDS), mg/L	1900.6		1871.4								2091.2		1947.9
Extractable organic fraction, mg/L	36.7		37.4								39.7		37.3
Silt density index (SDI)	6.73		2.01								n/a		1.44
D50	457.5		378.7								1192.0		425.0
Magnesium, mg/L	12.6		11.2								13.8		13.1
Calcium, mg/L	26.0		29.7								35.2		31.9
Iron, mg/L	0.12		n/d								0.33		n/d
Manganese, mg/L	0.063		0.061								0.068		0.063
Silicon, mg/L	4.87		4.03								6.54		4.06
Fluoride, mg/L	2.08		2.13								2.54		2.39
Chloride, mg/L	1992		1956								2090		2063
Bromide, mg/L	n/d		n/d								n/d		n/d
Phosphate, mg/L	n/d		n/d								n/d		n/d
Sulfate, mg/L	75.33		76.88								84.67		81.64
Nitrate, mg/L	n/d		n/d								n/d		n/d
Sodium, mg/L	687.0		656.0								694.0		695.0
Potassium, mg/L	14.8		11.9								13.9		12.7
Oil contents, mg/L	4.0												
Naphthenic acids, mg/L	8.28		7.92								8.44		8.16

n/d: not detected

Table B 3 Physico-chemical properties of OSPW in Run 3

Species	Run #3: ALUM 10 mg/L coagulated OSPW												
	1st stage			2nd stage									
	Raw OSPW	Feed	Permeate Final 11h	Feed	Permeate 24 h	Permeate 48 h	Permeate 72 h	Permeate 96 h	Permeate 120 h	Permeate 144 h	Feed 168 h	M Tank 168 h	Permeate 168 h
pH	7.16	6.81	7.30	7.29	7.49	7.58	7.41	7.49	7.39	7.46	7.37	7.27	7.36
Conductivity, µS/cm	3825.5	3510.7	3307.7	3519.0	3445.0	3451.0	3618.0	3669.0	3651.0	3747.0	3707.5	3623.0	3760.5
Turbidity, NTU	29.50	27.95	0.75	56.13	0.79	0.75	0.84	0.71	0.80	0.84	217.67	27.00	0.92
Total organic carbon (TOC), mg/L	42.2		39.2	37.5	42.5	38.6	40.9	40.2	42.8	40.0	46.8		39.2
Chemical oxygen demand (COD), mg/L	145.3		134.7								267.0		139.0
Total suspended solids (TSS), mg/L	19.2		n/d								227.5		n/d
Total dissolved solids (TDS), mg/L	1933.6		1889.0								2130.6		2130.6
Extractable organic fraction, mg/L	33.4		33.0								34.3		34.2
Silt density index (SDI)	6.36		1.85								n/a		1.35
D50	679.2		653.6								2184.0		557.0
Magnesium, mg/L	13.1		12.5								13.9		12.8
Calcium, mg/L	26.1		25.4								33.9		32.4
Iron, mg/L	0.20		n/d								0.19		n/d
Manganese, mg/L	0.085		0.089								0.094		0.083
Silicon, mg/L	5.03		5.10								6.99		5.84
Fluoride, mg/L	1.75		1.49								2.13		2.10
Chloride, mg/L	924.7		884.3								984.0		975.7
Bromide, mg/L	n/d		n/d								n/d		n/d
Phosphate, mg/L	n/d		n/d								n/d		n/d
Sulfate, mg/L	39.02		38.89								44.39		42.95
Nitrate, mg/L	n/d		n/d								n/d		n/d
Sodium, mg/L	689.3		677.4								690.1		690.4
Potassium, mg/L	12.6		12.3								13.8		13.1
Naphthenic acids, mg/L	7.80		7.90								8.06		8.54

n/d: not detected

Table B 4 Physico-chemical properties of OSPW in Run 4

Species	Run #4: ALUM 30 mg/L coagulated OSPW												
	1st stage			2nd stage									
	Raw OSPW	Feed	Permeate Final 11h	Feed	Permeate 24 h	Permeate 48 h	Permeate 72 h	Permeate 96 h	Permeate 120 h	Permeate 144 h	Feed 168 h	M Tank 168 h	Permeate 168 h
pH	7.39	6.86	7.32	7.57	7.43	7.35	7.22	7.33	7.19	7.14	7.18	7.12	7.14
Conductivity, µS/cm	3492.3	3445.0	3497.3	3491.0	3446.7	3515.3	3611.0	3391.0	3641.0	3739.7	3601.0	3600.7	3629.7
Turbidity, NTU	24.63	26.57	0.79	69.80	0.80	0.81	0.90	0.72	0.76	0.97	58.85	17.70	0.63
Total organic carbon (TOC), mg/L	41.7		35.2	43.9	35.1	37.5	37.7	36.9	36.4	34.4	41.3		34.9
Chemical oxygen demand (COD), mg/L	138.7		125.3								267.0		126.7
Total suspended solids (TSS), mg/L	21.2		1.0								251.7		0.0
Total dissolved solids (TDS), mg/L	1916.9		1843.8								2027.4		1981.0
Extractable organic fraction, mg/L	33.9		33.2								34.8		34.2
Silt density index (SDI)	6.15		1.89								n/a		1.30
D50	633.1		482.8								987.6		617.1
Magnesium, mg/L	11.7		11.8								13.1		11.9
Calcium, mg/L	25.1		23.9								25.8		24.0
Iron, mg/L	0.21		n/d								n/d		n/d
Manganese, mg/L	0.069		n/d								0.081		n/d
Silicon, mg/L	5.92		4.67								6.08		4.93
Fluoride, mg/L	1.98		1.21								2.12		1.93
Chloride, mg/L	979.1		938.7								1030.0		1023.2
Bromide, mg/L	n/d		n/d								n/d		n/d
Phosphate, mg/L	n/d		n/d								n/d		n/d
Sulfate, mg/L	60.23		52.64								56.83		55.88
Nitrate, mg/L	0.84		n/d								2.79		0.68
Sodium, mg/L	709.4		682.9								710.4		691.3
Potassium, mg/L	12.5		12.0								13.1		12.4
Naphthenic acids, mg/L	8.55		8.19								7.98		7.63

n/d: not detected

Table B 5 Physico-chemical properties of OSPW in Run 5

Species	Run #5: ALUM 10 mg/L coagulated OSPW at pH 10															
	1st stage			2nd stage												
	Raw OSPW	Feed	Permeate Final 11h	Feed	Permeate 24 h	Permeate 48 h	Permeate 72 h	Permeate 96 h	Permeate 120 h	Permeate 144 h	Permeate 168 h	Permeate 192 h	Permeate 216 h	Feed 240 h	M Tank 240 h	Permeate 240 h
pH	6.34	9.96	9.52	9.39	8.95	8.86	8.77	8.83	9.15	9.19	9.06	9.23	9.17	9.22	9.16	9.27
Conductivity, µS/cm	3647.67	3762.67	3526.00	3739.67	3516.00	3205.00	3655.33	3792.00	3426.00	3711.33	4201.50	4340.33	4365.33	4582.33	4627.00	4557.67
Turbidity, NTU	26.23	25.45	0.92	40.63	0.73	0.81	0.80	0.62	0.72	0.62	0.96	0.75	0.73	73.07	20.47	0.61
Total organic carbon (TOC), mg/L	41.40	n/d	38.45	40.81	37.62	39.27	36.14	36.25	36.09	39.52	35.62	38.27	36.41	42.64	n/d	36.93
Chemical oxygen demand (COD), mg/L	128.33	n/d	122.00	n/d	n/d	n/d	n/d	n/d	n/d	n/d	n/d	n/d	n/d	325.00	n/d	121.50
Total suspended solids (TSS), mg/L	22.00	n/d	1.33	n/d	n/d	n/d	n/d	n/d	n/d	n/d	n/d	n/d	n/d	530.83	n/d	0.67
Total dissolved solids (TDS), mg/L	1878.00	n/d	1905.71	n/d	n/d	n/d	n/d	n/d	n/d	n/d	n/d	n/d	n/d	2508.21	n/d	2480.48
Extractable organic fraction, mg/L	30.60	n/d	30.18	n/d	n/d	n/d	n/d	n/d	n/d	n/d	n/d	n/d	n/d	33.32	n/d	32.37
Silt density index (SDI)	5.92	n/d	1.98	n/d	n/d	n/d	n/d	n/d	n/d	n/d	n/d	n/d	n/d	n/a	n/d	1.29
D50	852.50	n/d	659.30	n/d	n/d	n/d	n/d	n/d	n/d	n/d	n/d	n/d	n/d	4091.00	n/d	484.40
Magnesium, mg/L	13.60	n/d	12.90	n/d	n/d	n/d	n/d	n/d	n/d	n/d	n/d	n/d	n/d	14.80	n/d	13.90
Calcium, mg/L	27.80	n/d	26.70	n/d	n/d	n/d	n/d	n/d	n/d	n/d	n/d	n/d	n/d	29.30	n/d	28.10
Iron, mg/L	0.36	n/d	0.28	n/d	n/d	n/d	n/d	n/d	n/d	n/d	n/d	n/d	n/d	0.53	n/d	0.41
Manganese, mg/L	n/d	n/d	n/d	n/d	n/d	n/d	n/d	n/d	n/d	n/d	n/d	n/d	n/d	n/d	n/d	n/d
Silicon, mg/L	6.93	n/d	6.55	n/d	n/d	n/d	n/d	n/d	n/d	n/d	n/d	n/d	n/d	7.85	n/d	7.12
Fluoride, mg/L	1.50	n/d	1.59	n/d	n/d	n/d	n/d	n/d	n/d	n/d	n/d	n/d	n/d	3.59	n/d	n/d
Chloride, mg/L	979.90	n/d	973.20	n/d	n/d	n/d	n/d	n/d	n/d	n/d	n/d	n/d	n/d	1055.20	n/d	n/d
Bromide, mg/L	n/d	n/d	n/d	n/d	n/d	n/d	n/d	n/d	n/d	n/d	n/d	n/d	n/d	n/d	n/d	69.68
Phosphate, mg/L	n/d	n/d	n/d	n/d	n/d	n/d	n/d	n/d	n/d	n/d	n/d	n/d	n/d	n/d	n/d	n/d
Sulfate, mg/L	53.47	n/d	49.97	n/d	n/d	n/d	n/d	n/d	n/d	n/d	n/d	n/d	n/d	70.90	n/d	69.68
Nitrate, mg/L	n/d	n/d	n/d	n/d	n/d	n/d	n/d	n/d	n/d	n/d	n/d	n/d	n/d	n/d	n/d	n/d
Sodium, mg/L	734.60	n/d	722.80	n/d	n/d	n/d	n/d	n/d	n/d	n/d	n/d	n/d	n/d	743.70	n/d	739.10
Potassium, mg/L	13.90	n/d	12.70	n/d	n/d	n/d	n/d	n/d	n/d	n/d	n/d	n/d	n/d	14.40	n/d	13.80
Naphthenic acids, mg/L	6.31	n/d	6.02	n/d	n/d	n/d	n/d	n/d	n/d	n/d	n/d	n/d	n/d	7.30	n/d	7.27

n/d: not detected

Table B 6 Physico-chemical properties of OSPW in Run 6

Species	Run #5: ALUM 10 mg/L coagulated OSPW at pH 10															
	1st stage			2nd stage												
	Raw OSPW	Feed	Permeate Final 11h	Feed	Permeate 24 h	Permeate 48 h	Permeate 72 h	Permeate 96 h	Permeate 120 h	Permeate 144 h	Permeate 168 h	Permeate 192 h	Permeate 216 h	Feed 240 h	M Tank 240 h	Permeate 240 h
pH	6.34	9.96	9.52	9.39	8.95	8.86	8.77	8.83	9.15	9.19	9.06	9.23	9.17	9.22	9.16	9.27
Conductivity, µS/cm	3647.67	3762.67	3526.00	3739.67	3516.00	3205.00	3655.33	3792.00	3426.00	3711.33	4201.50	4340.33	4365.33	4582.33	4627.00	4557.67
Turbidity, NTU	26.23	25.45	0.92	40.63	0.73	0.81	0.80	0.62	0.72	0.62	0.96	0.75	0.73	73.07	20.47	0.61
Total organic carbon (TOC), mg/L	41.40	n/d	38.45	40.81	37.62	39.27	36.14	36.25	36.09	39.52	35.62	38.27	36.41	42.64	n/d	36.93
Chemical oxygen demand (COD), mg/L	128.33	n/d	122.00	n/d	n/d	n/d	n/d	n/d	n/d	n/d	n/d	n/d	n/d	325.00	n/d	121.50
Total suspended solids (TSS), mg/L	22.00	n/d	1.33	n/d	n/d	n/d	n/d	n/d	n/d	n/d	n/d	n/d	n/d	530.83	n/d	0.67
Total dissolved solids (TDS), mg/L	1898.78	n/d	1905.71	n/d	n/d	n/d	n/d	n/d	n/d	n/d	n/d	n/d	n/d	2508.21	n/d	2480.48
Extractable organic fraction, mg/L	30.60	n/d	30.18	n/d	n/d	n/d	n/d	n/d	n/d	n/d	n/d	n/d	n/d	33.32	n/d	32.37
Silt density index (SDI)	5.92	n/d	1.98	n/d	n/d	n/d	n/d	n/d	n/d	n/d	n/d	n/d	n/d	n/a	n/d	1.29
D50	852.50	n/d	659.30	n/d	n/d	n/d	n/d	n/d	n/d	n/d	n/d	n/d	n/d	4091.00	n/d	484.40
Magnesium, mg/L	13.60	n/d	12.90	n/d	n/d	n/d	n/d	n/d	n/d	n/d	n/d	n/d	n/d	14.80	n/d	13.90
Calcium, mg/L	27.80	n/d	26.70	n/d	n/d	n/d	n/d	n/d	n/d	n/d	n/d	n/d	n/d	29.30	n/d	28.10
Iron, mg/L	0.36	n/d	0.28	n/d	n/d	n/d	n/d	n/d	n/d	n/d	n/d	n/d	n/d	0.53	n/d	0.41
Manganese, mg/L	n/d	n/d	n/d	n/d	n/d	n/d	n/d	n/d	n/d	n/d	n/d	n/d	n/d	n/d	n/d	n/d
Silicon, mg/L	6.93	n/d	6.55	n/d	n/d	n/d	n/d	n/d	n/d	n/d	n/d	n/d	n/d	7.85	n/d	7.12
Fluoride, mg/L	1.50	n/d	1.59	n/d	n/d	n/d	n/d	n/d	n/d	n/d	n/d	n/d	n/d	3.59	n/d	n/d
Chloride, mg/L	979.90	n/d	973.20	n/d	n/d	n/d	n/d	n/d	n/d	n/d	n/d	n/d	n/d	1055.20	n/d	n/d
Bromide, mg/L	n/d	n/d	n/d	n/d	n/d	n/d	n/d	n/d	n/d	n/d	n/d	n/d	n/d	n/d	n/d	69.68
Phosphate, mg/L	n/d	n/d	n/d	n/d	n/d	n/d	n/d	n/d	n/d	n/d	n/d	n/d	n/d	n/d	n/d	n/d
Sulfate, mg/L	53.47	n/d	49.97	n/d	n/d	n/d	n/d	n/d	n/d	n/d	n/d	n/d	n/d	70.90	n/d	69.68
Nitrate, mg/L	n/d	n/d	n/d	n/d	n/d	n/d	n/d	n/d	n/d	n/d	n/d	n/d	n/d	n/d	n/d	n/d
Sodium, mg/L	734.60	n/d	722.80	n/d	n/d	n/d	n/d	n/d	n/d	n/d	n/d	n/d	n/d	743.70	n/d	739.10
Potassium, mg/L	13.90	n/d	12.70	n/d	n/d	n/d	n/d	n/d	n/d	n/d	n/d	n/d	n/d	14.40	n/d	13.80
Naphthenic acids, mg/L	6.31	n/d	6.02	n/d	n/d	n/d	n/d	n/d	n/d	n/d	n/d	n/d	n/d	7.30	n/d	7.27

n/d: not detected

Table B 7 Physico-chemical properties of OSPW in Run 7

Species	Silica modified membrane with alum 10 mg/L coagulated OSPW													
	1st stage			2nd stage										
	Raw OSPW	Feed	Permeate Final 11h	Feed	Permeate 96 h	Permeate 120 h	Permeate 192 h	Permeate 216 h	Permeate 288 h	Permeate 360 h	Permeate 384 h	Permeate 408 h	Feed 432 h	Permeate 432 h
pH	7.76	7.72	7.80	8.00	7.82	7.71	7.44	7.31	7.29	7.50	7.45	7.38	7.23	7.14
Conductivity, µS/cm	3.44	3.37	3.35	2.92	3.59	3.65	3.68	3.71	3.82	3.60	3.62	3.54	4.02	4.10
Turbidity, NTU	28.50	29.00	0.90	90.70	0.74	0.75	0.69	0.70	0.78	0.78	0.80	0.71	198.00	0.76
Total organic carbon (TOC), mg/L	38.20		36.31										48.29	35.43
Chemical oxygen demand (COD),	124.00		118.00										168.00	117.00
Total suspended solids (TSS), mg/L	22.67		0.00										66.19	0.00
Total dissolved solids (TDS), mg/L	1902.10		1958.57										2220.50	2168.60
Extractable organic fraction, mg/L	31.49		33.10										32.29	34.30
Silt density index (SDI)	6.20		1.96										n/d	1.41
D50	863.00		580.60										1378.63	833.40
Magnesium, mg/L	11.70		11.90										13.40	13.30
Calcium, mg/L	27.60		29.80										31.30	32.10
Iron, mg/L	0.14		0.01										0.03	n/d
Manganese, mg/L	0.06		0.06										0.08	0.08
Silicon, mg/L	5.75		5.90										5.48	6.41
Fluoride, mg/L	1.73		1.69										2.09	1.96
Chloride, mg/L	998.10		997.50										1113.90	1123.40
Bromide, mg/L	n/d		0.64										n/d	0.68
Phosphate, mg/L	n/d		n/d										n/d	n/d
Sulfate, mg/L	70.31		64.59										73.86	69.04
Nitrate, mg/L	4.76		n/d										4.67	4.52
Sodium, mg/L	639.00		639.00										725.00	721.00
Potassium, mg/L	12.50		12.10										14.50	14.20
Oil contents, mg/L	4.00		3.80											2.70
Naphthenic acids, mg/L	6.12		6.30										5.30	5.10

n/d: not detected

Table B 8 Physico-chemical properties of OSPW in Run 8

Species	Titania modified membrane with alum 10 mg/L coagulated OSPW												
	1st stage			2nd stage									
	Raw OSPW	Feed	Permeate Final 11h	Feed	Permeate 24 h	Permeate 48 h	Permeate 72 h	Permeate 96 h	Permeate 120 h	Permeate 144 h	Permeate 168 h	Feed 192 h	Permeate 192 h
pH	7.74	7.82	7.87	8.03	7.99	7.86	7.89	7.71	7.69	7.55	7.46	6.86	7.56
Conductivity, µS/cm	3.536	3.502	3.364	3.473	3.581	3.550	3.823	3.718	3.787	3.914	3.825	3.962	3.687
Turbidity, NTU	32.50	29.3	0.90	83.70	0.99	0.78	0.75	0.76	0.68	0.70	0.78	172.40	0.72
Total organic carbon (TOC), mg/L	40.90		36.06									52.35	36.82
Chemical oxygen demand (COD), mg/L	127.00		112.67									199.00	116.67
Total suspended solids (TSS), mg/L	21.78		0.00									197.78	0.00
Total dissolved solids (TDS), mg/L	1920.37		1890.95									2377.46	2289.05
Extractable organic fraction, mg/L	39.54		37.85									37.13	38.70
Silt density index (SDI)	6.08		1.98									n/d	1.90
D50	833.3		619.8									1262.33333	810.25
Magnesium, mg/L	11.6		11.60									14.00	14.00
Calcium, mg/L	26.5		28.00									33.00	28.00
Iron, mg/L	0.263		n/d									n/d	n/d
Manganese, mg/L	0.0628		0.59									0.08	0.75
Silicon, mg/L	7.21		5.22									4.92	5.22
Fluoride, mg/L	1.89		1.75									2.56	2.03
Chloride, mg/L	1035.20		1026.14									1242.60	1188.70
Bromide, mg/L	n/d		0.80									n/d	n/d
Phosphate, mg/L	n/d		n/d									n/d	n/d
Sulfate, mg/L	65.65		73.64									89.12	89.70
Nitrate, mg/L	n/d		n/d									5.11	4.65
Sodium, mg/L	625		611.00									751.00	750.00
Potassium, mg/L	12.6		12.00									14.90	12.00
Oil contents, mg/L	4		3.60										2.90
Naphthenic acids, mg/L	6.00		6.15									5.90	5.80

n/d: not detected